Simultaneous Wireless Information and Power Transfer in Full-Duplex Communication Systems

Alexander Akpofure Okandeji

A dissertation submitted in partial fulfillment

of the requirements for the degree of

Doctor of Philosophy

of

University College London.

Department of Electronic and Electrical Engineering

University College London

July 26, 2017

I, Alexander Akpofure Okandeji, confirm that the work presented in this thesis is my own. Where information has been derived from other sources, I confirm that this has been indicated in the work.

Abstract

As wireless devices are mostly constrained by their inability to operate independently infinitely away from centralised power sources, radio frequency (RF) energy harvesting (EH) has been identified as a promising technique for future wireless devices. For this reason, this thesis introduces a novelty in RF EH full-duplex (FD) wireless communication systems. Specifically, this thesis investigate the potentials of simultaneous wireless information and power transfer (SWIPT) in FD communication systems.

This thesis firstly focuses on optimal transmit strategies, rate maximization and power minimizing approach for SWIPT in FD systems. Using the rate-split method, difference of convex programming, semi-definite programming technique and one-dimensional search, we reformulate complex optimization problems to yield problem formulations that can be efficiently solved, thus we develop rate maximization algorithm for SWIPT in a point-to-point FD system, SWIPT in FD multiple-input multiple-output (MIMO) two-way relay system and power minimization approach for SWIPT in a multiuser MIMO FD system.

This thesis also presents research work carried out with the aim of maximising the secrecy sum-rate for SWIPT in FD systems. In this context, we employ the use of an amplify and forward (AF) relay to inject artificial noise (AN) in order to confuse the eavesdropper. Thus, we address the optimal joint design of the beamforming matrix and AN covariance matrix at the relay, and the transmit power at the sources. Comprehensively, we present extensive theoretical and computer simulations to corroborate the need for joint optimization.

Acknowledgements

This thesis represents the contribution of several remarkable individuals for which I would love to show appreciation.

First, I would like to thank my primary supervisor Professor Kit Wong, he was there for me all through my research years at UCL. Although he was very tough with me at the beginning, he stood by me to the very end. His toughness brought out the best in me. I am forever indebted by your personal and professional support through out my research years. Being your PhD student has been a privilege, you are the best. My sincere appreciation goes to Dr. Muhammad Ruhul Amin Khandaker, a true friend and co-researcher, who stood by me when the going was very tough.

I would like to thank my research group members and UCL colleagues for the technical discussions and support during my PhD. I would like to acknowledge Prof. Izzat, Prof. Jonathon Chambers, Prof. Sangarapillai Lambotharan, Dr. Kenneth Tong, Dr. Lifeng Wang, Dr. Arman, Yongxu Zhu, Jialing Lao and Raoul Guizon for their support and encouragements for the entire period of my research. Our highly intellectual group meetings and constructive criticism contributed immensely to our research output. I would also like to show my gratitude to my mum, Christiana Okandeji, my siblings; Dr. Michael, Peter and Irene for their love, prayers and support throughout my research years.

Finally, this thesis is dedicated to the memory of my late father, Roland Amone Okandeji. My hero, although you didn't live to see me become a Dr., achieving this goal would have been impossible without your devoted support.

Contents

List of Figures

List of Abbreviations

- AC: Analog cancellation
- ADC: Analog-to-digital converter
- AF: Amplify and forward relay
- AWGN: Additive white Gaussian noise
- AN: Artificial noise
- BS: Base station
- CSI: Channel state information
- CSCG: Circularly symmetric gaussian random variable
- CVX: Convex programming
- DC: Digital cancellation
- DCP: Difference of convex programming
- DPS: Dynamic power splitting
- EH: Energy harvesting
- FD: Full-duplex
- FRBV: Fixed received beamforming vector
- HD: Half-duplex
- i.d.d: Independent and identically distributed
- ID: Information decoder
- IR: Information receiver
- JBPS: Joint beamforming and receiver power splitting

- LOS: Line of sight
- LPF: Low pass filter
- MISO: Multiple-input single-output
- MIMO: Multiple-input multiple-output
- MS: Mobile station
- OPS: Optimal power splitting
- PHY: Physical layer security
- PS: Power splitter
- QoS: Quality of service
- RF: Radio frequency
- RSI: Residual self-interference
- SDR: Semidefinite relaxation
- SI: Self-interference
- SIC: Self-interference cancellation
- SINR: Signal-to-interference plus noise ratio
- SNR: Signal-to-noise ratio
- SWIPT: Simultaneous wireless information and power transfer
- TSR: Time switched relaying
- UPS: Uniform power splitting
- WIT: Wireless information transfer
- WPT: Wireless power transfer
- ZF: Zeroforcing

Chapter 1

Introduction

The exponential growth in the demand for high data rate in wireless communication networks has led to a tremendous need for energy. However, the increased rate at which energy is consumed not only causes an increase in the operating cost of wireless communication systems, but also raises serious environmental concerns. Generally, conventional energy-constrained wireless networks such as sensor nodes are typically powered by fixed energy supplies that have limited operation time e.g., batteries. Although the lifetime of such networks can be extended by replacing or recharging the batteries, the replacement or recharging process incurs high cost, it can be inconvenient, hazardous or sometimes impossible. The lifetime of such network can therefore be regarded as an important performance indicator. Consequently, a more convenient, safer and cheaper alternative is thus to harvest energy from the environment which can provide unlimited energy supplies to wireless devices. Powering mobile devices by harvesting energy from ambient sources such as solar, wind, and kinetic activities make wireless networks not only environmentally friendly but also self-sustaining. Recently, harvesting energy from the environment has been identified as an attractive solution as it can prolong the lifetime of wireless sensor networks since energy harvesting (EH) networks potentially have an unlimited energy supply from the environment. Among the existing renewable energy sources such as solar and wind, radio frequency (RF) radiated by ambient transmitters can be a viable new source for wireless EH. Since radio signals that

convey information can also be used as a vehicle for transporting energy, an interesting new research namely simultaneous wireless information and power transfer (SWIPT) is currently being explored [1], [2]. Specifically, different from the various conventional energy sources such as wind, solar, piezoelectric and hydroelectric, RF SWIPT can provide reliable supply of energy to solve the energy scarcity problem of wireless applications such as wireless sensor networks [3], and wireless body sensor networks [4]. Thus, RF SWIPT allows for the proper utilization of interference signals for EH. Authors in [1] and [2] studied the fundamental performance limits of wireless information and power transfer in communication systems under different channel set-up based on the assumption that the receiver circuit is capable of simultaneously decoding information and harvesting energy from the same received signal, which is not yet realizable due to practical circuit limitations [5].

Despite the recent interest in SWIPT, there remains two key challenges for practical implementation. Firstly, it is assumed in [1], [2] that the receiver is able to extract power simultaneously from the received information signal. However, this assumption does not hold in practice, as practical circuits for harvesting energy from radio signals are not yet able to decode information directly. Hence, the results in [1], [2] only provided optimistic bounds. Consequently, to coordinate SWIPT at the receiver side, two power splitting schemes were proposed namely [5]: *time switching* which is divided into; (i) Uniform power splitting (UPS), where equal power is split between the information decoder (ID) and energy decoder (ii) On-Off power splitting (OOPS) scheme where, depending on system conditions, the receiving node can switch between ID or EH modes; and *power splitting*; Optimal power splitting (OPS) scheme where the receive power split between the ID and energy decoder is governed by a device which coordinates the optimal processes of information decoding and EH thus allows for optimum system performance [5].
Secondly, information and energy receivers in practice operate with different power sensitivity (e.g., -10dBm for energy receivers versus -60dBm for information receivers). Thus, for a system that involves both wireless information transfer (WIT) and wireless power transfer (WPT), the receiver should be optimised for WPT [6].

Existing system set-up for SWIPT considered point-to-point half-duplex (HD) systems, HD multiple-input single-output (MISO) systems, HD multiple-input multiple-output (MIMO) systems [7]- [20], while [21]- [27] considered SWIPT in full-duplex (FD) systems without the OPS scheme. However, in future practical SWIPT systems, full-duplexity along with the OPS scheme should be explored as it offers higher spectral efficiency when compared to its HD counterpart, and also guarantees optimal system performance with information decoding and energy harvesting.

Recently, the exponential increase in mobile devices as well as the escalating high data rate requirements have resulted in spectrum scarcity efficiency problem. Full-duplex communications which is a promising technique to tackle the spectrum scarcity efficiency problem has attracted a lot of interest due to its ability to increase throughput, eliminate hidden terminals, improvements in the network layer and its unique ability to eliminate duplexing filter [28]. Full-duplex radio technology, where devices transmit and receive signals simultaneously at the same frequency is the new breakthrough in wireless communication system. Consequently, as this simultaneous transmission and reception of radio signals happen at the same time and at the same frequency, FD theoretically doubles the spectral efficiency.

A full-duplex radio is defined as a radio frequency transceiver that can transmit and receive signals at the same time and frequency [28]. Currently deployed EH systems are HD, which transmit and receive signals in two separate channels. A FD radio however, can have twice as high spectral efficiency as a half-duplex radio. The main limitation impacting full-duplex transmission is the strong self-interference (SI) signal imposed by the transmit antenna on the receive antenna within the same transceiver. Thus, for full-duplex system to achieve its maximum efficiency, the SI signal has to be significantly suppressed to the receiver's noise floor. For example, in WiFi systems, the transmit power can go up to 20 dBm and the typical receiver's noise floor could be at -90 dBm, this implies that a total of 110 dBm self-interference cancellation (SIC) is required for proper operation of the full-duplex system. Consequently, in a case where the achieved amount of SIC does not reach

the receiver noise floor, the residual self-interference (RSI) power will degrade the system's signal to noise ratio (SNR) and therefore negatively impacts the system throughput.

Recently, several publications [29]- [32] have considered the problem of SIC in full-duplex systems by investigating different system architectures and SIC techniques to mitigate the self-interference signal. Typically, SIC techniques are divided into two main categories namely: passive suppression and active cancellation. In passive cancellation, the self-interference signal is suppressed in the propagation domain before it is processed by the receiver circuitry [33]. However, in active cancellation (e.g. digital cancellation) technique [29], the self-interference signal is mitigated by subtracting a processed copy of the transmitted signal from the received signal. Due to error in channel estimation, digital SIC technique does not completely nullify the self-interference thus leading to RSI which can negatively affect the performance of FD systems.

1.1 Aim and motivation

Conventionally, wireless communication nodes transmit and receive signals over orthogonal frequency or time resources. This traditional way of information transmission termed HD mode has been identified to inefficiently utilise the limited available spectral resource [29]. Recently, advancement in technology which has enabled services with high data requirements, high speed internet access, has led to an increasing need for optimal usage of the limited spectral resource. Full-duplex technology which allows simultaneous transmission and reception of radio signal at the same time and frequency has been identified to double throughput hence, increasing spectral efficiency [34]. However, the practicability of FD technology is dependent upon the successful cancellation of the generated SI. Recent advances in SI cancellation techniques suggest that if SI can be significantly cancelled, radio will work in FD. Consequently, result obtained at Stanford University on the design and implementation of the first FD WiFi radio capable of simultaneously transmit-

ting and receiving information on the same signal using WiFi 802.11a show that for practical development scenario, the throughput of the wireless network is doubled [34], an indication that SI can be sufficiently cancelled. FD is thus a promising technology capable of tackling spectral inefficiency in wireless communications.

Meanwhile, to solve the problem of wireless nodes, currently faced with the challenge of limited power supply, wireless power transfer has been identified as a promising technology which aims to provide convenient energy supplies to wireless network [1]. Since the signal that carries information can be used as a vehicle to carry energy, simultaneous wireless information and power transfer has recently been explored. Recent works, have however considered SWIPT in HD systems, and SWIPT in FD systems without the OPS scheme, it is therefore important to develop novel algorithm which investigates the potentials of integrating SWIPT in FD systems with the OPS scheme. Hence, this thesis documents work done on SWIPT in FD systems considering different wireless network architecture.

Furthermore, the conventional wireless networks are vulnerable to security threats. In this context, unintended receivers have the potential to eavesdrop information dedicated to legitimate receivers. Hence, valuable information such as bank details can be intercepted thereby creating an unreliable wireless network. To address this security threat in FD SWIPT systems, this thesis documents novel work done to investigate secrecy in FD SWIPT systems. In particular, we develop secrecy sum-rate maximization algorithm for SWIPT in FD MIMO relay system.

1.2 Main Contributions

In this thesis, SWIPT in FD communication systems subject to transmit power and receive power splitter constraints is considered. The major difference between the proposed method and the existing method is that while several existing model considered SWIPT set-up in HD, and FD systems using various time switching schemes [5]- [20], this thesis investigate SWIPT in FD communication systems using the OPS scheme where the receive power splitter coefficient at optimality, al-

lows simultaneous information and power transfer in FD systems. Subsequently, to achieve FD, digital SIC technique is explored to mitigate the self-Interference. The contributions of this thesis are summarized below:

- The first contribution of this work is the design of an optimal transmit strategy and rate-maximization algorithm for SWIPT in a point-to-point FD communication system. Using the rate-split method, we develop the rate-maximization algorithm that jointly optimises the transmit power and the receive signal power splitter coefficient.

- The second contribution of this work investigates SWIPT in FD MIMO amplify and forward (AF) two-way relay communication system. Using the difference of convex programming and one-dimension search, we develop the rate-maximization algorithm for SWIPT in FD MIMO AF two-way relay system.

- Thirdly, we investigate SWIPT in a multi-user MIMO FD system and addressed the optimal joint design of the power splitter (PS) ratio and the transmit power at the mobile stations (MSs), and the beamforming vector at the base station (BS).

- The fourth contribution investigates the secrecy sum-rate maximization approach for SWIPT in FD systems. In particular, we consider SWIPT in a three node MIMO relay network with source nodes exchanging confidential information enabled by a FD relay node in the presence of an eavesdropper. The problem of secrecy sum-rate maximization for SWIPT in MIMO FD relay is addressed while guaranteeing the receive signal to interference plus noise ratio (SINR) at the legitimate source nodes is greater than or equal to a given threshold, and the SINR of the eavesdropper is less than or equal to a specified threshold.

1.3 Thesis Organisation

Subsequent to the introductory chapter, this thesis is organised as described below: Chapter 2 introduces full-duplex systems, point-to-point FD systems and MIMO relay systems. In particular, this chapter presents a review of full-duplex technology with emphasis on existing SIC mechanism.

Chapter 3 introduces energy harvesting systems. Specifically, this chapter presents a review of EH technologies with emphasis on RF energy harvesting technology. Also, a review of the receiver architecture of energy harvesting systems is presented in this chapter.

Chapter 4 presents SWIPT in a point-to-point FD communication system. In particular, the problem of joint optimization of system parameters to ensure sum-rate maximization via optimal transmission strategy for wireless information and power transfer in a point-to-point FD system is addressed.

Chapter 5 presents the joint beamforming optimization for SWIPT in a MIMO FD AF two-way relay channel and the rate-maximization algorithm. In particular, SWIPT in a three-node MIMO relay system is considered where bi-directional information exchange between two source nodes is made possible via the energy harvested by the relay node.

In chapter 6, this thesis investigate SWIPT in a virtual MIMO system. In particular, a multi-user MIMO FD system for SWIPT in which a multi-antenna base station simultaneously transmit wireless information and power to a set of single antenna mobile stations using power splitters is investigated. This chapter addresses the joint design of the receive PS ratio and the transmit power at the mobile station as well as the beamforming matrix at the base station subject to SINR and harvested power constraints.

Chapter 7 investigates secrecy sum-rate maximization approach for FD SWIPT systems. Specifically, a three node MIMO relay FD system is investigated. Thus, a scenario where two source nodes exchange confidential information via a relay node in

the presence of an eavesdropper is investigated. In particular, the secrecy sum-rate maximization problem subject to the SINR of the source nodes and the eavesdropper as well as transmit power, and harvested energy constraints is considered.

We conclude this thesis in Chapter 8 with a summary of the research and the description of future work.

Finally, mathematical proofs developed throughout this thesis are described in Appendices A-B.

1.4 Publications

The research work in this thesis has led to the following peer-reviewed publications:

1. **A. A. Okandeji**, M. R. A. Khandaker, K-K. Wong, G. Zheng, Y. Zhang, and Z. Zheng "SWIPT in MISO full-duplex systems," accepted in *Journal of Communications and Networks*.

2. **A. A. Okandeji**, M. R. A. Khandaker, and K-K. Wong "Wireless information and power transfer in full-duplex communication systems," in *proc. IEEE International Conference on Communication*, May 23 - May 27 2016, Kuala Lumpur, Malaysia.

3. **A. A. Okandeji**, M. R. A. Khandaker, and K-K. Wong "Two-way beamforming optimization for full-duplex SWIPT systems," in *proc. special session on full-duplex radio, European Signal Processing Conference*, 29 Aug. - 02 Sep. 2016, Budapest, Hungary.

4. **A. A. Okandeji**, M. R. A. Khandaker, K-K. Wong, and Z. Zheng "Joint transmit power and relay two-way beamforming optimization for energy-harvesting full-duplex communications," in *proc. The first international workshop on full-duplex wireless communications*, Globecom, Washington, USA, Dec. 2016.

5. **A. A. Okandeji**, M. R. A. Khandaker, K-K. Wong, G. Zheng, Y. Zhang, and

Z. Zheng "Secure Full-Duplex Two-way Relaying for SWIPT," Submitted to *IEEE Wireless Communication Letters*.

Chapter 2

Full-Duplex systems

2.1 Full-Duplex technology

In this chapter, a review of the existing FD wireless communication system architectures is provided. In particular, our aim is to understand full-duplexity in the existing architectures thus, enhancing successful integration of EH. Full-duplexity in radio communication is a novel pattern in the field of wireless communications [35]- [37]. It basically involves the transmission and reception of signals simultaneously at the same time on the same frequency. The exponential development of wireless communication has led to spectral resource gradually becoming a limiting factor. It is observed that a higher spectral efficiency in wireless communication is needed in order to save cost and to maximise the use of available resources. Thus, FD emerges as a technique which can be used to achieve optimal utilization of the limited available spectral resource [29].

From a theoretical point of view, FD can double the spectral efficiency of a wireless communication system. However, an improved spectral efficiency is preceded by successful self-interference cancellation [29]. The key challenge in realising a full-duplex system is the self-interference signal which can be up to 100 dB stronger than the desired received signal; due to the proximity between the transmit and receive antenna at the FD node. Hence, signal reception becomes impossible unless SI is significantly reduced. Thus, for FD systems to achieve maximum spectral effi-

ciency, SI must be significantly suppressed to the receiver's noise floor. It is shown in [29] that if the SI within a node can be successfully mitigated, the radios can work in FD.

2.2 Existing method of self-interference cancellation in FD systems

Recently, work done in [30]- [31] have considered the problem of SIC in FD systems by investigating different wireless communication system architectures and self-interference cancellation technique to mitigate the self-interference signal. A commonly used technique to tackle SI problem is to subtract a copy of a node's own transmit signal from the received signal [32].

Conventionally, self-interference cancellation techniques are divided into two main categories: passive cancellation, and active cancellation techniques [29]. Active cancellation technique could be divided into digital and analogue cancellation techniques based on the signal domain (digital-domain or analog-domain) where the self-interference signal is subtracted. Digital cancellation (DC) is an active cancellation mechanism in which the knowledge of a node's own transmit signal is used to cancel the interfering signal while analog cancellation (AC) is an active cancellation mechanism which sends a cancelling signal through another radio chain and adds it to the signal at the receiving antenna [29]. In contrast, passive SI cancellation refers to any technique that can electromagnetically isolate the transmit and receive antennas. An example of passive cancellation technique includes SI cancellation based on specific antenna placement. In particular, this passive technique requires two transmit antennas to be spaced apart from a receiving antenna at distances d and $d + \frac{\lambda}{2}$, respectively. Specifically, this spacing enables the signal from the two transmit antennas to superpose a null at the receive antenna location. This method is however only useful in a narrow band scenario and will fail in case of broadband signals.

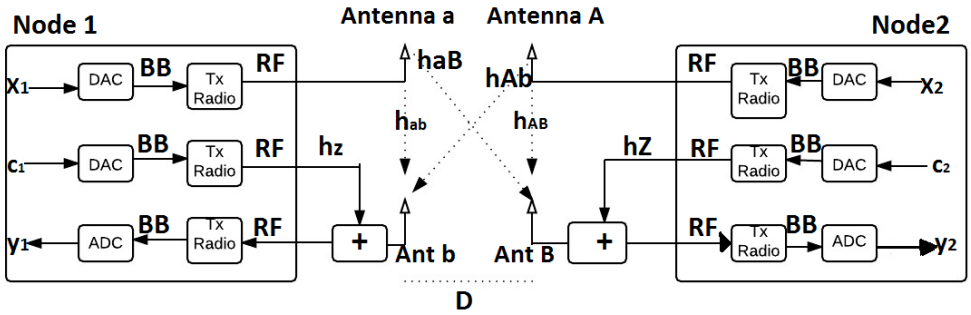

Figure 2.1: *SI cancellation model.*

2.3 Mechanisms for self-interference cancellation

It is worth nothing that the RF signal model of the full-duplex system considered in this thesis is shown in Fig.2.1. x_1 is used to denote the signal transmitted from node 1 (N1), h_{aB} denotes the wireless channel from antenna a to antenna B, and h_{ab} represents the wireless channel from antenna a to antenna b. Similarly, x_2 denote the signal transmitted from node 2 (N2), the wireless channel from antenna A to antenna b is represented as h_{Ab} while h_{AB} denotes the wireless channel from antenna A to antenna B. Furthermore, d represents the distance between interfering antennas (same node antennas) and D represents the distance between the nodes. Also, the noisy estimate h_{ab} and h_{AB} is, respectively, represented by $\hat{h}_{\text{ab}}$ and $\hat{h}_{AB}$. The idea of SI cancellation to achieve FD communication considered in this thesis is based on the SI cancellation technique described in [29]. Authors of [29] presented a measurement based characterization of different self-interference cancellation mechanisms. Consequently, a summary of the existing SI cancellation techniques is provided below.

2.3.1 Antenna separation and digital cancellation (ASDC)

Suppose it is required to achieve SI cancellation by antenna separation and digital cancellation. The self-interfering signal at N1 is represented as $h_{\text{ab}}x_1$ and the self-interfering signal at N2 is represented as $h_{AB}x_2$. In practical circuits, N1 and N2 can estimate h_{ab} and h_{AB}, respectively, via the transmission of dedicated training symbols, and can make use of these estimates in the digital domain to cancel the

interference by subtracting $\hat{h}_{\text{ab}}x_1$ at N1 and $\hat{h}_{AB}x_2$ at N2 from the received signal. Consequently, after the application of antenna separation and digital cancellation (ASDC), the interfering signal at N1 is given as $(h_{\text{ab}} - \hat{h}_{\text{ab}})x_1$ and the interfering signal at N2 is given as $(h_{AB} - \hat{h}_{AB})x_2$. Note that due to the channel error in the estimation of h_{ab} and h_{AB}, perfect cancellation is not possible. Thus, the power of the interfering signal at N1 and N2 after ASDC is represented as $P^{\text{N1}}_{\text{ASDC}} = \mathbb{E}[|(h_{ab} - \hat{h}_{ab})x_1|^2]$ and $P^{\text{N2}}_{\text{ASDC}} = \mathbb{E}[|(h_{AB} - \hat{h}_{AB})x_2|^2]$, respectively [29].

2.3.2 Antenna separation and analog cancellation (ASAC)

The analog SIC for N1 involves the node sending the canceller signal c_1 through an additional transmitter radio which converts the signal to RF and further adds the output of the radio to the received signal. In particular, to cancel the self-inference at N1, the canceller signal must be equal to $c_1 = -(\hat{h}_{\text{ab}}/\hat{h}_z)x_1$, where h_z denotes the magnitude and phase applied by N1's transmitter RF chain to signal c_1. However, due to the presence of additive noise and other distortions in the system, N1 cannot have a perfect channel estimate of h_{ab} and h_z. Consequently, the analog canceller cannot completely cancel the SI. Suppose the noisy estimate of h_z is represented by $\hat{h}_z$. Thus, the interfering signal at N1 after antenna separation and analog cancellation (ASAC) is given as $(h_{\text{ab}} - h_z\hat{h}_{\text{ab}}/\hat{h}_z)x_1$. The power of the interfering signal at N1 after ASAC is given by $P^{\text{N1}}_{\text{ASAC}} = \mathbb{E}[|(h_{\text{ab}} - h_z\hat{h}_{\text{ab}}/\hat{h}_z)x_1|^2]$. Similarly, suppose $c_2 = -(\hat{h}_{AB}/\hat{h}_Z)x_2$ denotes the canceller signal, where h_Z is the magnitude and phase applied by N2's transmitter RF chain to signal c_2. The self interfering signal at N2 after ASAC is given as $(h_{AB} - h_Z\hat{h}_{AB}/\hat{h}_Z)x_2$ where $\hat{h}_Z$ is the noisy estimate of h_Z. The power of the interfering signal at N2 after ASAC is given by $P^{\text{N2}}_{\text{ASAC}} = \mathbb{E}[|(h_{AB} - h_Z\hat{h}_{AB}/\hat{h}_Z)x_2|^2]$ [29].

2.3.3 Antenna separation, analog and digital cancellation (ASADC)

Generally, due to the presence of noise in the estimate of the signals required for cancellation, the ASAC mechanism cannot completely cancel the self-interference. Hence, to achieve larger cancellation of SI signal, digital cancellation is applied after ASAC. To proceed, suppose $h_{\mathrm{ASAC}}^{\mathrm{N1}} = h_{\mathrm{ab}} - h_z\hat{h}_{\mathrm{ab}}/\hat{h}_z$ and $h_{\mathrm{ASAC}}^{\mathrm{N2}} = h_{AB} - h_Z\hat{h}_{AB}/\hat{h}_Z$ is the equivalent self-interfering channel after ASAC at N1 and N2, respectively. Specifically, digital cancellation after ASAC involves estimating $h_{\mathrm{ASAC}}^{\mathrm{N1}}$ and $h_{\mathrm{ASAC}}^{\mathrm{N2}}$, and using these estimates to cancel the interfering signal in the digital domain. Suppose the noisy estimates of h_{ASAC}^{N1} and h_{ASAC}^{N2} is represented as $\hat{h}_{\mathrm{ASAC}}^{N1}$ and $\hat{h}_{ASAC}^{N2}$, respectively. Thus, the self-interfering signal after antenna separation, analog and digital cancellation (ASADC) at N1 is given by $(h_{ASAC}^{N1} - \hat{h}_{ASAC}^{N1})x_1$ and the self-interfering after ASADC at N2 can be written as $(h_{\mathrm{ASAC}}^{N2} - \hat{h}_{\mathrm{ASAC}}^{N2})x_1$. The power of the self interfering signal at N1 after ASADC is given as $P_{\mathrm{ASADC}}^{\mathrm{N1}} = \mathbb{E}[|(h_{\mathrm{ASAC}}^{\mathrm{N1}} - \hat{h}_{\mathrm{ASAC}}^{\mathrm{N1}})x_1|^2]$ while the power of the self-interfering signal at N2 can be written as $P_{\mathrm{ASADC}}^{N2} = \mathbb{E}[|(h_{\mathrm{ASAC}}^{\mathrm{N2}} - \hat{h}_{\mathrm{ASAC}}^{\mathrm{N2}})x_2|^2]$ [29]. The results obtained in [29] show that FD systems are feasible and can achieve rates larger than the HD counterpart.

2.4 Point-to-point full-duplex systems

In this section, the system model for a bidirectional FD point-to-point system is described. As shown in Fig. 2.2, it consist of two nodes namely node 1 and node 2 with each having identical transmitter-receiver pair for transmission and reception of radio signals, respectively. Each node is assumed to operate in full-duplex, where the transmission and reception of radio signals are done simultaneously. Effectively, the simultaneous transmission and reception of radio signals at each node generates the self-interference signal. The interfering signal is thus received together with the desired signal. It is worth noting that the self-interference signal is known to have a destructive effect on achievable rate which invariably give rise to spectrum inef-

ficiency. From Fig. 2.2, the received signal at node 1 and node 2 can, respectively, be written as

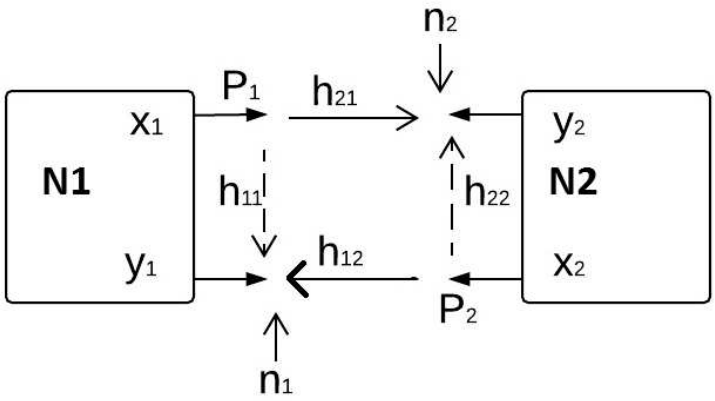

Figure 2.2: *Point-to-point FD system*

$$y_1 = h_{12}P_2x_2 + h_{11}I_1x_1 + n_1, \tag{2.1}$$

$$y_2 = h_{21}P_1x_1 + h_{22}I_2x_2 + n_2, \tag{2.2}$$

where $P_i, i \in (1,2)$ and $I_i, i \in (1,2)$ are the transmit power and RSI power at the nodes, respectively. Also, the normalised transmitted signal at node 1 and node 2 is represented as x_1 and x_2, respectively, where $\mathbb{E}[x_2x_2^H] = \mathbb{E}[x_1x_1^H] = 1$. Furthermore, h_{11} and h_{22} represent the SI channel of the 1st and 2nd nodes, respectively, n is the Additive White Gaussian noise (AWGN). Previous study on point-to-point FD systems have modelled SI in different ways. The authors in [38] modelled SI as a Rician fading channel and showed that active SIC has better performance in terms of its outage probability than passive cancellation. In this thesis, we model the SI channel for simplicity as a Gaussian channel. For the model in Fig. 2.2 to work in FD, I must be significantly reduced. An advance signal processing technique to cancel self-interference was designed in [36]. This design uses a combination of radio frequency and baseband techniques to achieve full-duplex with minimal effect on the reliability of the FD link.

2.5 MIMO relay full-duplex systems

The demand for high data rate over long distances has been the motivation behind the development of MIMO systems. MIMO techniques in general, support enhanced data throughput under conditions of interference, signal fading and multipath. Theoretically, shannon capacity is given as

$$\text{Capacity} = \text{BW}\log_2(1+\text{SNR}), \tag{2.3}$$

where BW = bandwidth and SNR = signal-to-noise ratio. As shown in equation (2.3), an increase in the channel's SNR causes a marginal increase in the channel throughput. Hence, the traditional way to achieve a higher data rate is by increasing the signal bandwidth. Unfortunately, increasing the signal bandwidth by increasing the symbol rate of a modulated carrier, increases the susceptibility to multipath fading. Thus, a direct solution to tackle the challenge of multipath fading is the use of multiple antennas. Essentially, the use of multiple antennas give rise to multiple signal paths used to gain knowledge of the communication channel. MIMO uses the spatial dimension of a communication link to achieve higher data rates than the traditional single-input single-output (SISO) channels.

Meanwhile, cooperative relaying which in general, is used as a technique to exploit spatial diversity to combat fading has gained much attention in recent years [39]. Due to the broadcast nature of wireless transmissions, cooperative communications enables neighbouring network nodes to share resources and cooperate to send information to an intended node in order to improve system performance, expand coverage and robustness of the wireless network. Practical cooperative relaying protocols has recently been investigated [39]- [40] and several relaying protocols have been proposed. Specifically, the regenerative relaying (decode and forward relaying) and the non-regenerative relaying (amplify and forward relaying) have been studied [41]. In decode and forward relaying, the source symbol is decoded at the relay and the re-encoded symbol is forwarded to the destination. In contrast, in amplify and forward relaying, the received signal at the relay is amplified by a

factor and then forwarded to the destination. One of the central factors considered in the design of relay communications is the choice between full-duplex and half-duplex relaying modes. The key baseline assumption in user cooperation is to apply HD mode [41], where orthogonal time slots are allocated for reception and transmission at the relay. However, in practical communication scenarios, data flows in both directions. Thus, applying FD technique into relay communication, the relay can receive and retransmit signal simultaneously and thus improves the spectral efficiency.

Technically, simultaneous transmission and reception of signals in FD mode is not considered feasible for compact single-antenna relays because any practical application would suffer a significant level of self-interference [42]. Thus, in MIMO relay system, the relay is equipped with multiple-antennas. As with the point-to-point FD system, full-duplex MIMO relay system are also faced with the challenges of self-interference. Existing self-interference cancellation technique (digital cancellation, analogue cancellation) has been adopted to mitigate the generated SI [43], to ensure spectrum efficiency. To summarize, the system model for a bidirectional full-duplex MIMO relay system is described as a three-node MIMO relay network consisting of two sources and a MIMO relay. The sources operating in FD want to exchange information from each other but due to fading and shadowing effect, their is no direct link between these sources hence, they must totally rely on the relay to achieve this exchange. A practical model is presented in chapter 5 and the design of the optimal transmit strategy of the relay which maximises the system throughput is proposed.

2.6 MISO full-duplex systems

Conventionally, wireless communication systems use single antenna at the source and destination nodes. However, obstructions caused by buildings along the communication path can result to multipath problems, causing the radio signal to reach the destination nodes in two or more paths. Consequently, multipath resulting from

multiple signal arrival, causes multiple interference including destructive interference such as fading. For this reason, digital communication systems adopts the use of multiple antennas to avoid multipath induced errors, thereby ensuring the transmission of multiple signals, one for each antenna, at the source to mitigate the effect of multipath wave propagation thus, increasing the quality of communications. MISO technology is therefore a promising technology with a widespread application in wireless local area networks, metropolitan area networks and mobile communications. The use of multiple antenna array in general, can successfully tackle the challenge of multipath fading and interference. Thus, the MISO set-up outperforms their single-antenna counterpart. However, the enhanced performance achieved by the MISO set-up is dependent upon the channel state information (CSI) available at the transmitter. Specifically, for a MISO set-up with perfect CSI in a spatially uncorrelated Rayleigh-fading environment, it is known that the gain in throughput as a result of transmit optimization is represented mathematically as $\log_2(n)$, where n denotes the number of transmitter antennas [44]. In particular, the MISO set-up use the knowledge of the CSI available at the transmitter to increase the mutual information by transmitting with a signal covariance that maximises the SNR at the receiver [44].

As stated earlier in this chapter, FD increases spectral efficiency only if the generated SI can be successfully cancelled. Multi-user MIMO FD communications are however much more complex to deal with as the generated interference are of two folds. The SI due to the receiving antenna of intended nodes as well as interfering signal from neighbouring nodes. Generally, the exponential growth in wireless traffic necessitates a need for proper interference management to ensure the required quality of service is delivered. For a multi-user MIMO FD set-up, where each user has access to its perfect CSI, and the BS has only statistical CSI of all the users, it is important to ensure the resulting SI is significantly cancelled to ensure the quality of service requirements is maintained. To this end, this thesis documents the novel integration of SWIPT into FD multi-user MIMO set-up. In particular, the problem of the joint optimization of system parameters to ensure individual user's quality of

service requirements is achieved is investigated.

2.7 Secure wireless communication systems

Generally, there is an uncontrolled growth in the integration of wireless technology into our everyday life. To name a few, for example, radio propagation in cellular mobile networks, smart grid and smart cities are examples of this integration. Due to the broadcast nature of radio propagation in wireless communication networks, the secrecy of information transmitted through these networks remains a critical issue. Conventionally, cryptographic techniques have been used to address security threats in wireless networks. Specifically, cryptographic security technique using secret keys assumes that eavesdroppers in general, have limited computational resources. However, an increase in computational power as well as difficulties and vulnerabilities associated with key distribution and managements suggest that cryptography is insufficient to provide the desired level of security. To address this issue, pioneering work known as the wiretap channel in [45] demonstrated from an information theoretic view point, the feasibility of perfect secrecy when the physical characteristics of wireless channels are used. Recently, workdone in [46]- [48] suggest that adding controlled interference or artificial noise (AN) to degrade the decoding capability of the eavesdroppers could serve as an efficient way to increase secrecy in wireless networks. In this context, the AN designed to harm the eavesdropper but not the legitimate receiver is embeded into the transmitted signal from a transmitting node with multiple antennas. Alternatively, when the transmitter is restricted to the use of a single antenna, cooperative jamming approach which incorporates the use of external relay to send jamming signal to degrade the eavesdroppers channel has also been employed [49]- [53]. However, the cooperative jamming approach mainly rely on external helpers, thus it suffers from issues related to helper mobility, synchronization and trustworthiness [54]. Furthermore, the iJam scheme in which a receiver acts as a jammer by randomly jamming one of the transmitted copies in each sample time was proposed in [55]. The inability of the eavesdropper to identify a clean sample posses a challenge for decoding the transmitted signal. It is worth

noting that the iJam scheme requires retransmission of the source signal thus, it reduces throughput [55]. To effectively investigate secrecy in SWIPT systems, this thesis documents the successful integration of SWIPT in FD MIMO relay network and physical layer security. In particular, adopting the AN concept of degrading the eavesdroppers channel, the problem of secrecy sum-rate maximization subject to SINR, transmit power as well as harvested energy constraints is investigated in chapter 7.

2.8 Conclusion

To summarise, FD radio technology has the capacity to double spectral efficiency if SI can be suppressed to the noise floor [56]. Irrespective of FD system set-up, either point-to-point, multi-user MIMO FD systems or MIMO relay FD systems, the percentage self-interference cancellation play a major role in the achievable throughput. As the demand for high data rates over long distances in wireless communications increases at an exponential rate, incorporating MIMO relay in FD systems has the potential to double system capacity, increase system efficiency, ensure reliability and extend network coverage. This thesis however takes a step further to integrate EH into the aforementioned system set-up. As the basic assumption of the receiver being able to simultaneously decode information and harvest power is adopted, we provide transmission strategies for FD SWIPT system set-up and show beyond reasonable doubt the need for optimal transmit strategies in order to achieve optimal system performance.

Chapter 3

Energy harvesting systems

3.1 Energy harvesting

Energy harvesting is regarded as an indispensable technology for future wireless systems due to the ability to capture free energy, available without cost from the environment. Energy can be harvested from a number of sources such as vibrations, thermal gradient, sunlight and wind. The adopted energy harvesting source depends on the nature of the application and power requirements of the particular electronic load.

Recently, the development of advanced techniques able to capture, store, and manage amounts of natural energy transforming them into electrical energy has received great interest from both industry and academia because the energy is harvested from renewable sources thus, it significantly reduces the carbon dioxide emission and makes wireless communication environmentally friendly. This property of energy harvesting systems has stimulated researchers to investigate the performance of communication systems employing EH techniques from both theoretical and practical implementation fields [57, 58]. However, due to the random and intermittent nature of the energy arrivals, communications systems powered by EH are not guaranteed to provide reliable and uninterrupted services [58].

3.2 Energy harvesting for wireless communication

In order to eradicate frequent battery replacements for an increasing number of connected devices, to reduce carbon emission and to wipe out the dependence of wireless terminals on the power grid, EH technology is considered as a major component of future wireless networks. Harvesting energy from the environment is capable of extending the lifetime of wireless devices and can provide such device with unlimited mobility, as batteries can be charged without connecting them to the power grid infrastructure. However, despite all its numerous advantages, a bottle neck in designing EH communication systems is the stochastic nature of the energy arrivals which may cause a node powered by EH to run out of energy, degrading the communication performances or continuously harvest energy which might lead to battery overflow and waste of harvested energy.

Consequently, the time varying nature of the available energy motivates the need to design transmission policies that takes into account the random nature of the energy arrival process. To this end, as the power grid is capable of providing persistent power input, the coexistence of EH and grid power supply is considered as a promising technology to solve the problem of simultaneously guaranteeing the users quality of service (QoS) and minimising the power grid energy consumption [59]. Previous research work have focussed on the EH issues. Recently, authors in [60] focussed on the problem of maximising the short-term throughput of EH nodes. The authors in [60] assumed a realistic constraint that an energy harvesting battery must have finite energy storage capacity, thus an optimum transmission policy under the energy storage constraint was developed. In [61], an optimal energy management scheme for energy harvesting systems operating in fading channels with finite capacity rechargeable batteries was investigated. Authors in [61] considered two related optimization problems. The first problem was the maximization of the throughput transmitted by a specified deadline while the second was the maximization of the time delay. It is worth noting that energy harvesting systems are made possible through the deployment of energy harvesting technologies, thus we investigate the existing EH technologies with emphasis on radio frequency energy

harvesting systems which is relevant to this research work.

3.3 Energy harvesting technologies

Energy and its effect on the environment are key issues that have attracted massive interest from researchers all over the globe. Recently, oil and gas are no longer considered as the main source of energy as alternative energy sources that are cheap and environmentally friendly have been discovered. Consequently, the demand of an everlasting cheap source of energy has increased exponentially. Energy harvesting technologies are used to extract energy from ambient sources. Thus, an energy harvesting device converts the extracted energy into electrical energy which is stored in the energy storage device of the sensor. This thesis considers energy harvesting in wireless communication systems, thus a brief insight into the major energy harvesting technologies particularly radio frequency energy harvesting systems is provided.

3.3.1 Solar cells

In harvesting energy from sunlight, solar cells exploit the photovoltaic effect (creation of voltage or electric current in a material upon exposure to light) to convert sunlight into electricity. These materials are usually made of silicon with impurities such that when excited by sunlight, electrons break free from the silicon material in the presence of impurities. The electrons then flow through the silicon surface and create a direct current [62]. Note that in harvesting energy from sunlight via solar cells, the energy transfer mechanism is strongly influenced by the illumination condition such as the angle of incidence of the sunlight on the solar cells which varies with changing weather conditions [62].

Design considerations for existing solar energy harvesting solutions for wireless sensor nodes conceive a simple on/off-threshold charge mechanism relying on a diode connecting the cell with the rechargeable battery [63]. However, a diode based solution is characterised by a fixed electrical working point of the cell and set

by a battery voltage, thus this prevents any adaptation resulting in a disconnect of the cell from the battery whenever the available power is below the set threshold. This function of the diode ensures that no energy is wasted [63].

3.3.2 Vibration based energy harvesting

Electric energy can also be generated from low-level vibrations experienced by a sensor device from its operating environment. Vibration based energy harvesting technology has attracted considerable interest in recent years. By scavenging ambient vibrations and converting them into electric energy, vibration based energy harvesting technology provides a promising way to power low-power consumption sensors. Ambient vibration is found everywhere as long as there are activities related to mechanical oscillations such as those created by mechanical machines, house hold appliances, earthquake and many more. Due to its ubiquitous nature, vibration based energy harvesting is a very popular source of electric energy to power electronic devices especially those intended to be isolated, embedded in buildings and wireless sensor nodes [64].

Energy is harvested either through a micro-generator which contains a permanent magnet with a moving coil or through piezo-electrical material shape change. Ambient vibration sources however, is random and unpredictable which is a critical issue. Thus, a vibration based energy harvesting device is desirable to be able to operate at wider bandwidth in an envelop of frequency range to generate maximum electrical output [64]. To tackle the stochastic nature of the ambient vibration, [64] considered the use of a self-tuning mechanism where the energy harvester can tune its resonant frequency to match the vibration source on which it is mounted, thereby optimising its electrical output. As described in [64], the tuning can be achieved by alternating the parameters of the generator such as the mass, length or the stiffness of the system. A major drawback for this form of energy harvesting is that it depends on the vibration amplitude, and if this is low, it cannot provide energy to be harvested [64].

3.3.3 Radio frequency energy harvesting

Of much relevant to this research is RF energy harvesting. Generally, manufacturers of wireless devices and products have stressed the need for improved technology as wireless devices are constrained by their inability to operate independently infinitely away from centralised power sources. For this reason, there has been a severe restriction on the usefulness of wireless devices as well as their potential range of applications due to the slow advancements of rechargeable battery technology [65]. Future applications need wireless devices to operate for longer durations away from centralised power sources. There have been areas where battery sizes have been reduced such that it becomes easy to carry along with chargeable electronic devices. However, a major drawback of this technology is that the battery charger only carry limited energy thus, it must be charged as soon as it is depleted. Futuristic design will aim to re-structure the mobile system architecture such that energy harvesting antennas are incorporated into the mobile devices.

Currently, many technologies have been developed to overcome the operating power limitations imposed on wireless devices. Radio frequency energy harvesting is a recently developed technology which is able to convert radio waves from ambient air to electrical energy [65]. With a transmission efficiency of 0.4%, above 18.2%, and over 50% at -40dBm, -20dBm and -5dBm input power, respectively [66], RF energy harvesting system which forms the bedrock of this research work is made up of three subsystems namely: a receiving antenna subsystem, a rectifying subsystem and an energy storage subsystem.

3.3.3.1 Receiving antenna subsystem

First, consider the receiving antenna subsystem as shown in Fig. 3.1 which reveals the standard operations at an information receiver with cogent demodulation (assuming that the channel phase shift is perfectly known at the receiver). To proceed, the received RF band signal $y(t)$ is first converted to a complex baseband signal $y_b(t)$ after which it is sampled and digitalized by an analog-to-digital converter (ADC) for

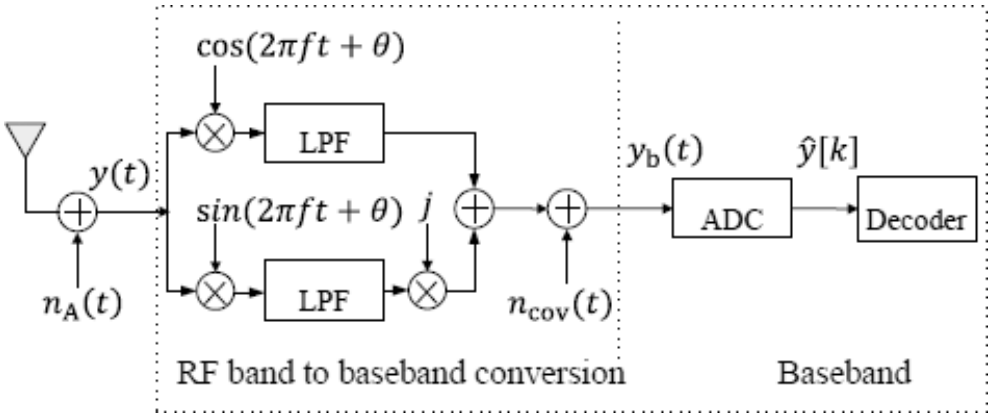

Figure 3.1: *Information receiver.*

further decoding [6]. $n_{cov}(t)$ denotes the noise introduced by the RF band to baseband signal conversion. For simplicity, an ideal ADC with zero noise is assumed. The discrete-time ADC output is thus given by

$$\hat{y}[k] = \sqrt{hP}x[k] + \tilde{n}_A[k] + n_{cov}[k], \tag{3.1}$$

where k = 1,2,..., denotes the symbol index. It follows from (3.1) that the equivalent baseband channel for wireless information is the well known AWGN channel:

$$Y = \sqrt{hP}X + Z, \tag{3.2}$$

where X and Y denote the channel input and output, respectively, and Z $\backsim$ CN$(0, \sigma_A^2 + \sigma_{cov}^2)$ denotes the complex Gaussian noise (assuming independent $\tilde{n}_A(t)$ and $n_{cov}(t)$). When the channel input is distributed as $X \sim \text{CN}(0,1)$, the maximum achievable information rate or the capacity of the AWGN channel is given by [6]

$$R = \log_2\left(1 + \frac{hP}{\sigma_A^2 + \sigma_{cov}^2}\right). \tag{3.3}$$

3.3.3.2 Receiver architecture design for energy harvesting

In this subsection, the practical receiver design for simultaneous wireless information and power transfer is considered. In particular, a general receiver operation

known as dynamic power splitting (DPS) is discussed, from which we consider separated information and energy receiver.

3.3.3.3 Dynamic power splitting

Currently, practical receiver circuits for harvesting energy from radio signals are not yet able to decode the carried information directly i.e., the radio signal used for harvesting energy cannot be reused for decoding information [6]. To counter this potential limitation, authors in [6], proposed a practical dynamic power splitting (DPS) scheme to enable the receiver to harvest energy and decode information from the same received signal at any time t, by dynamically splitting the receive signal into two streams with the power ratio $\rho(t) : 1-\rho(t)$, which are used for harvesting energy and decoding information, respectively, where $0 \leq \rho(t) \leq 1$.
This thesis considers a block-based transmission of duration T with $T = NT_s$, where N denotes the number of transmitted symbol per block and T_s denotes the symbol period. It is assumed that $\rho(t) = \rho_k$ for any symbol interval $t \in [(k-1)T_s, kT_s], k = 1, ..., N$. Furthermore, [6] assumed an ideal power splitter at the receiver which is characterised as having no loss or noise introduced, and that the receiver can perfectly synchronize its operation with that of the transmitter.

During the transmission block time T, the information receiver is assumed to have the capability to operate in two modes namely: off mode for a time duration T_{off} to harvest power, or on mode for a time duration $T_{\text{on}} = T - T_{\text{off}}$ to decode information. In this thesis, we define three special cases of DPS, namely time switching, UPS and OPS as given in [6]. *Time switching*: when the information receiver is switched to its off mode, all signal power is used for energy harvesting. However, when the information receiver operates in the on-mode, all signal power is used for information decoding. Thus, in time switching, the receiver power switches over time between information decoding and energy harvesting i.e., $\rho_k \in (0,1)$. Time switching is also known as on-off power splitting. *UPS*: when equal power is split between the information decoder and the energy harvester i.e., $\rho_k = (\frac{1}{2})$ and *OPS*: when the characteristics system conditions determines the optimal values for ρ.

Optimal power splitting forms a key concept in this research work.

3.3.3.4 Rectifying subsystem

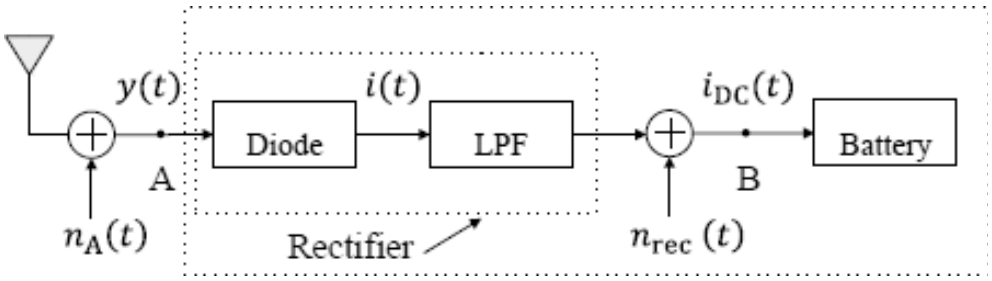

Figure 3.2: *Energy receiver.*

Fig. 3.2 describes the operation of the rectifying subsystem. It typically consist of an energy receiver that converts RF energy directly via a rectenna architecture [6]. In the rectenna, the received RF band signal $y(t)$ is converted to a direct current signal $i_{\mathrm{DC}}(t)$ by a rectifier, which consist of a Schottky diode and a passive low pass filter (LPF). The direct current signal $i_{\mathrm{DC}}(t)$ is then used to charge the battery to store the energy [6]. Particularly, the output current $i(t)$ of the diode is processed by a LPF. The function of the LPF is to remove the high-frequency harmonic components and a direct current signal appears as the output of the rectifier. For simplicity, this thesis assumes that the energy stored in the battery is linearly proportional to $i_{\mathrm{DC}}(t)$ with a conversion efficiency of 1 as described in [67].

3.3.3.5 Energy storage subsystem

Efficient energy management is a crucial component of wireless network design as it helps to achieve increased throughput and network lifetime for battery operated devices that have energy harvesting constraints. It is worth noting that an energy harvesting device converts different forms of environmental energy into electricity supplied to a sensor node. However, since energy is only produced over a limited rate, energy storage mechanisms play an important role to reduce energy consumption in a sensor node. The most common energy storage device in a wireless sensor node is a battery either non- rechargeable or rechargeable. A non-rechargeable battery is often used for devices with very low power consumption such as microsensor

while rechargeable batteries are used widely in sensor node with energy harvesting capabilities. Note that batteries in energy harvesting systems are not used for energy storage only, they are also used to regulate the supply of energy to sensor nodes.

Chapter 4

SWIPT in FD systems

4.1 Wireless information and power transfer in full-duplex communication systems

In this chapter, SWIPT in a point-to-point FD wireless communication systems is investigated. Recently, there has been an upsurge of interest in FD communication due to the fact that full-duplexity can offer higher spectral efficiency compared to its HD counterpart. For this reason, transmit strategies for FD point-to-point system with RSI were studied in [68]. The authors in [68] analysed FD system constraints at optimality and thus developed power adjustment schemes which maximize the system sum-rate in different scenarios. However, the RSI resulting from the concurrent transmission and reception at the same node raises the noise floor and is a dominant factor in the performance of FD communication systems. Hence, considerable efforts have been made in mitigating the effects of RSI in FD systems. In particular, digital self-interference cancellation technique for FD wireless system was studied in [29]. It was shown in [29] that the average amount of SI cancellation achieved for antenna separation and digital cancellation at 20 cm and 40 cm spacing between interfering antennas was 70 dB and 76 dB, respectively, with the RSI modelled as an AWGN with zero-mean and known variance as given in [42].
Furthermore, the authors in [30] presented an experiment-based characterization

of passive suppression and active self-interference cancellation mechanisms in FD wireless communication systems. It was shown in [30] that the average amount of cancellation increases for active cancellation techniques as the received self-interference power increases. Based on extensive experiments, the authors in [30] showed that a total average cancellation of 74 dB can be achieved.

It has been observed that SIC cannot suppress the self-interference down to the noise floor [30], [56]. Thus, a sophisticated digital self-interference cancellation technique was proposed in [56] that eliminates all transmitter impairments, and significantly mitigates the receiver phase noise and nonlinearity effects. The proposed technique in [56] significantly mitigates the SI signal to ~ 3 dB higher than the receiver noise floor, which results in up to $67-76\%$ rate improvement compared to conventional HD systems at 20 dBm transmit power values.

More recently, interest has been focussed on the study of SWIPT in FD systems as it has the potential to improve spectral efficiency and achieve simultaneous transmission of information and power [69]- [70]. The authors of [69] considered an access point operating in FD mode that broadcasts wireless energy to a set of distributed users in the downlink and, at the same time, receives independent information from the users via time-division multiple access in the uplink. In contrast, a scenario is considered in [70] where an energy-constrained FD relay node assists the information transmission from the source to the destination using the energy harvested from the source.

In this chapter, SWIPT in a point-to-point FD wireless communication system for simultaneous bidirectional communication where two nodes equipped with two antennas, one used for signal transmission and the other used for signal reception, communicate in FD mode is investigated. The aim is to maximise the end-to-end sum-rate for SWIPT in FD system while maintaining the energy harvesting threshold at each node by optimizing the receive power splitter and transmit power at each node. Due to insufficient knowledge of the self-interfering channel, the worst-case based model is considered, where the magnitude of the estimation error is bounded. Since the problem is strictly non-convex, an alternating solution is proposed. In

particular, this thesis show that for fixed power splitting ratio, the optimal transmit powers can be obtained by introducing a rate-split scheme between the two nodes, whereas for given transmit power, closed-form expressions for power splitting ratios can be derived. Numerical simulations are carried out to demonstrate the performance of the proposed scheme.

The rest of this chapter is organized as follows. In Section 4.2, the system model of a full-duplex point-to-point communication network with power splitting based energy harvesting nodes is introduced. The proposed joint transmit power and receive PS ratio design algorithm is developed in Section 4.3. Section 4.4 shows the simulation results under various scenarios. A summary of the numerical result is given in Section 4.5.

4.2 System model and problem formulation

Consider FD point-to-point wireless communication system as illustrated in Fig. 4.1. It is assumed that each node houses identical transmitter-receiver pair. Each receiver intends to simultaneously decode information and harvest energy from the received signal. Let us define the received signal at node 1 and node 2 as $y_{2\to1}$ and $y_{1\to2}$, respectively. Let us also denote the transmit and receive antennas at nodes 1 and 2 by (a,b) and (c,d), respectively. Thus, the received signal at node 1 is given by

$$y_{2\to1} = h_{\text{cb}}x_2 + h_{\text{ab}}x_1 + n_{A_1} \tag{4.1}$$

and the received signal at node 2 is

$$y_{1\to2} = h_{\text{ad}}x_1 + h_{\text{cd}}x_2 + n_{A_2}, \tag{4.2}$$

where x_1 denotes the transmitted signal from node 1 to node 2, x_2 denotes the transmitted signal from node 2 to node 1, h_{ad} denotes the wireless channel from node 1 to node 2, h_{cb} denotes the wireless channel from node 2 to node 1, h_{ab} and h_{cd} denote the self-interference channel at node 1 and node 2, respectively. n_{A1} and n_{A2}

are defined as the AWGN with zero mean and unit variance at the receiver antenna at node 1 and node 2, respectively. In this thesis, the general assumption that each

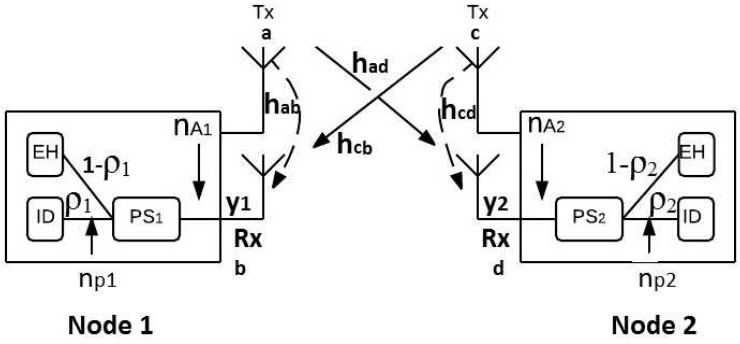

Figure 4.1: *Energy harvesting full-duplex communication system.*

receiver is equipped with a power splitting device which coordinates the processes of information decoding and energy harvesting from the received signal is adopted. For simplicity, it is assumed that the received signal is split such that a $\rho_k, k = 1,2$, portion of the signal power is fed to the ID and the remaining $1-\rho_k$, $k = 1,2$, is fed to the EH at node k. Thus, the signal split to the ID of node 1 and 2 are given, respectively, by

$$y_{2\to1}^{\mathrm{ID}} = \sqrt{\rho_1}(h_{\mathrm{cb}}x_2 + h_{\mathrm{ab}}x_1 + n_{A_1}) + n_{p1}, \tag{4.3a}$$

$$y_{1\to2}^{\mathrm{ID}} = \sqrt{\rho_2}(h_{\mathrm{ad}}x_1 + h_{\mathrm{cd}}x_2 + n_{A_2}) + n_{p2}, \tag{4.3b}$$

where n_{pk}, $k = 1,2$, is the noise introduced by the RF band to baseband signal conversion operation and is defined as $n_{pk} \sim \mathrm{CN}\ (0, \sigma_p^2)$, $k = 1,2$. Also, the signal split to the EH is expressed as

$$y_{1\to2}^{\mathrm{EH}} = \sqrt{1-\rho_2}(h_{\mathrm{ad}}x_1 + h_{\mathrm{cd}}x_2 + n_{A_2}), \tag{4.4a}$$

$$y_{2\to1}^{\mathrm{EH}} = \sqrt{1-\rho_1}(h_{\mathrm{cb}}x_2 + h_{\mathrm{ab}}x_1 + n_{A_1}). \tag{4.4b}$$

The power harvested at the EH of node 1 and node 2 is thus given by

$$Q_{1\to 2} = \alpha(1-\rho_2)(E[|h_{\text{ad}}x_1 + h_{\text{cd}}x_2 + n_{A_2}|^2]), \tag{4.5a}$$

$$Q_{2\to 1} = \alpha(1-\rho_1)(E[|h_{\text{cb}}x_2 + h_{\text{ab}}x_1 + n_{A_1}|^2]), \tag{4.5b}$$

where α denotes the energy conversion efficiency of the EH at each receiver that accounts for the loss in the energy transducer for converting the harvested energy to electrical energy to be stored. In practice, an energy harvesting circuit is equipped at the energy harvesting receiver which is used to convert the received RF power into direct current power. It has been proved that the efficiency of diode-based energy harvesters is non-linear and largely depends on the input power level [71]. Hence, the energy conversion efficiency (α) should be included in optimization expressions. However, for simplicity, it is assumed that $\alpha = 1$.

Let us now define $C_{1\to 2}$ and $C_{2\to 1}$ as the information rate from node $1 \to 2$ and node $2 \to 1$, respectively. Thus, the instantaneous capacity at node 1 and 2 can be written, respectively, as

$$C_{2\to 1} = \log_2\left(1 + \frac{\rho_1|h_{\text{cb}}|^2P_2}{\rho_1(|h_{\text{ab}}|^2P_1 + \sigma_{A_1}^2) + \sigma_{p_1}^2}\right), \tag{4.6a}$$

$$C_{1\to 2} = \log_2\left(1 + \frac{\rho_2|h_{\text{ad}}|^2P_1}{\rho_2(|h_{\text{cd}}|^2P_2 + \sigma_{A_2}^2) + \sigma_{p_2}^2}\right). \tag{4.6b}$$

It is shown later in Section 4.4 through numerical results that if the RSI is not handled properly, it dominates the system performance and prevents from exploiting the benefits of FD by decreasing the information rate. Considering the fact that the RSI can not be eliminated completely, the worst-case performance, based on deterministic model for imperfect self-interfering channels is considered. In particular, it is assumed that the self-interference channels h_{ab} and h_{cd} lie in the neighbourhood of the estimated channels $\hat{h}_{\text{ab}}$ and $\hat{h}_{\text{cd}}$, respectively, available at the nodes. Thus, the actual channels due to imperfect self-interference channel estimate can be written

as

$$h_{\mathrm{ab}} = \hat{h}_{\mathrm{ab}} + \triangle h_{\mathrm{ab}}, \tag{4.7a}$$

$$h_{\mathrm{cd}} = \hat{h}_{\mathrm{cd}} + \triangle h_{\mathrm{cd}}, \tag{4.7b}$$

where $\triangle h_{\mathrm{ab}}$ and $\triangle h_{\mathrm{cd}}$ represents the channel uncertainties which are assumed to be bounded such that

$$|\triangle h_{\mathrm{ab}}| = |h_{\mathrm{ab}} - \hat{h}_{\mathrm{ab}}| \leq \varepsilon_1, \tag{4.8a}$$

$$|\triangle h_{\mathrm{cd}}| = |h_{\mathrm{cd}} - \hat{h}_{\mathrm{cd}}|_2 \leq \varepsilon_2, \tag{4.8b}$$

for some $\varepsilon_1 \geq 0$ and $\varepsilon_2 \geq 0$, where ε_k, $k = 1, 2$, depends on the accuracy of the CSI estimates. To efficiently define the worst-case self-interference level, (4.7a) and (4.7b) are modified using the triangle inequality [72]. It follows from (4.7a) that

$$|h_{\mathrm{ab}}|^2 = |(\hat{h}_{\mathrm{ab}} + \triangle h_{\mathrm{ab}})|^2 \leq |\hat{h}_{\mathrm{ab}}|^2 + |\triangle h_{\mathrm{ab}}|^2 \leq |\hat{h}_{\mathrm{ab}}|^2 + \varepsilon_1^2. \tag{4.9}$$

Note that ε_1 is the minimal knowledge of the upper-bound of the channel error which is sufficient enough to describe the error in the absence of statistical information about the error. Thus, from (4.9), we obtain

$$\max_{|\triangle h_{\mathrm{ab}}| \leq \varepsilon_1} |(\hat{h}_{\mathrm{ab}} + \triangle h_{\mathrm{ab}})|^2 \leq |\hat{h}_{\mathrm{ab}}|^2 + \varepsilon_1^2. \tag{4.10}$$

Similar results can be obtained from (4.8b) as

$$\max_{|\triangle h_{\mathrm{cd}}| \leq \varepsilon_2} |(\hat{h}_{\mathrm{cd}} + \triangle h_{\mathrm{cd}})|^2 \leq |\hat{h}_{\mathrm{cd}}|^2 + \varepsilon_2^2. \tag{4.11}$$

On the other hand, it holds that

$$|(\hat{h}_{\mathrm{ab}} + \triangle h_{\mathrm{ab}})|^2 \geq |\hat{h}_{\mathrm{ab}}|^2 - |\triangle h_{\mathrm{ab}}|^2 \geq |\hat{h}_{\mathrm{ab}}|^2 - \varepsilon_1^2 \tag{4.12}$$

and

$$|(\hat{h}_{\mathrm{cd}} + \triangle h_{\mathrm{cd}})|^2 \geq |\hat{h}_{\mathrm{cd}}|^2 - |\triangle h_{\mathrm{cd}}|^2 \geq |\hat{h}_{\mathrm{cd}}|^2 - \varepsilon_2^2. \tag{4.13}$$

Here, it is assumed that $|\hat{h}_{\mathrm{ab}}| \geq |\triangle h_{\mathrm{ab}}|$ and $|\hat{h}_{\mathrm{cd}}| \geq |\triangle h_{\mathrm{cd}}|$ which essentially means that the errors $|\triangle h_{\mathrm{ab}}|$ and $|\triangle h_{\mathrm{cd}}|$ are sufficiently small. Accordingly,

$$\min_{|\triangle h_{\mathrm{ab}}| \leq \varepsilon_1} |(\hat{h}_{\mathrm{ab}} + \triangle h_{\mathrm{ab}})|^2 \geq |\hat{h}_{\mathrm{ab}}|^2 - \varepsilon_1^2 \tag{4.14}$$

and

$$\min_{|\triangle h_{\mathrm{cd}}| \leq \varepsilon_2} |(\hat{h}_{\mathrm{cd}} + \triangle h_{\mathrm{cd}})|^2 \geq |\hat{h}_{\mathrm{cd}}|^2 - \varepsilon_2^2. \tag{4.15}$$

Substituting the results obtained in (4.14) and (4.15) into (4.5a) and (4.5b), respectively, the minimum power harvested at the EH of node 1 and node 2 is given by

$$\begin{aligned} &\min_{|\triangle h_{\mathrm{ab}}| \leq \varepsilon_1} Q_{2\to 1} \\ &\geq (1-\rho_1)(|h_{\mathrm{cb}}|^2 P_2 + (|\hat{h}_{\mathrm{ab}}|^2 - \varepsilon_1^2)P_1 + \sigma_{A_1}^2), \end{aligned} \tag{4.16a}$$

$$\begin{aligned} &\min_{|\triangle h_{\mathrm{cd}}| \leq \varepsilon_2} Q_{1\to 2} \\ &\geq (1-\rho_2)(|h_{\mathrm{ad}}|^2 P_1 + (|\hat{h}_{\mathrm{cd}}|^2 - \varepsilon_2^2)P_2 + \sigma_{A_2}^2). \end{aligned} \tag{4.16b}$$

The minimum instantaneous capacity at node 1 and 2 can be written, respectively, as

$$\begin{aligned} &\min_{|\triangle h_{\mathrm{ab}}| \leq \varepsilon_1} C_{2\to 1} \\ &\geq \log_2\left(1 + \frac{\rho_1 |h_{\mathrm{cb}}|^2 P_2}{\rho_1((|\hat{h}_{\mathrm{ab}}|^2 + \varepsilon_1^2)P_1 + \sigma_{A_1}^2) + \sigma_{p_1}^2}\right), \end{aligned} \tag{4.17a}$$

$$\begin{aligned} &\min_{|\triangle h_{\mathrm{cd}}| \leq \varepsilon_2} C_{1\to 2} \\ &\geq \log_2\left(1 + \frac{\rho_2 |h_{\mathrm{ad}}|^2 P_1}{\rho_2((|\hat{h}_{\mathrm{cd}}|^2 + \varepsilon_2^2)P_2 + \sigma_{A_2}^2) + \sigma_{p_2}^2}\right). \end{aligned} \tag{4.17b}$$

The sum-rate of information across the communication system is given by

$$\begin{aligned} R_{\text{sum}} &\triangleq C_{2\to1} + C_{1\to2} \\ &= \log_2\left(1 + \frac{\rho_2 |h_{\text{ad}}|^2 P_1}{\rho_2(|\hat{h}_{\text{cd}}|^2 + \varepsilon_2^2)P_2 + \rho_2\sigma_{A_2}^2 + \sigma_{p_2}^2}\right) \\ &+ \log_2\left(1 + \frac{\rho_1 |h_{\text{cb}}|^2 P_2}{\rho_1(|\hat{h}_{\text{ab}}|^2 + \varepsilon_1^2)P_1 + \rho_1\sigma_{A_1}^2 + \sigma_{p_1}^2}\right). \end{aligned} \tag{4.18}$$

In order to maximise the sum-rate of SWIPT in FD systems, the optimal transmit power and receive power splitting problem with transmit power and harvested energy constraints at node 1 and node 2 can be formulated as

$$\max_{\rho_1,\rho_2\in(0,1),P_1,P_2} \quad R_{\text{sum}} \tag{4.19a}$$

$$\text{s.t.} \quad \min_{|\Delta h_{\text{ab}}|\le\varepsilon_1} Q_{2\to1} \ge \bar{Q}_{2\to1}, \tag{4.19b}$$

$$\min_{|\Delta h_{\text{cd}}|\le\varepsilon_2} Q_{1\to2} \ge \bar{Q}_{1\to2}, \tag{4.19c}$$

$$0 \le P_1 \le P_{\max}, \tag{4.19d}$$

$$0 \le P_2 \le P_{\max}, \tag{4.19e}$$

where $\bar{Q}_{1\to2}$ and $\bar{Q}_{2\to1}$ are the minimum amount of harvested energy required to maintain the receivers operation, and $P_{\max}$ is the maximum available transmit power budget at node 1 and node 2, respectively.

4.3 Proposed solution

In this section, the optimum design of the receive power splitter and transmit power for SWIPT in FD communication systems is considered, assuming that the instantaneous CSI is known at the transmitter. Since the problem (4.19) is non-convex, it is very difficult to obtain a closed-form solution that jointly optimizes ρ_1, ρ_2, P_1, and P_2. Hence, to solve this problem, a two-step iterative process is proposed. First, we fix the splitter coefficients, i.e., $\rho_1, \rho_2 \in (0,1)$ and obtain the optimal values for

P_1 and P_2. Then, the optimal P_1^* and P_2^* is used to obtain the optimal ρ_1^* and ρ_2^*.

4.3.1 Transmit power optimization

Algorithm 1 Procedure for solving problem (4.21)

1: Fix ρ_1 and ρ_2 such that ρ_1 , $\rho_2 \in (0,1)$.
2: Set $\eta(0) = 0$.
3: At step k, set $\eta(k) = \eta(k-1) + \Delta\eta$ until $\eta(k) = 1$, where $\Delta\eta$ is the searching step size.
4: Initialize $r_{\text{low}} = 0$, and $r_{up} = r_{\max}$.
5: Repeat
1) Set $r \leftarrow \frac{1}{2}(r_{\text{low}} + r_{\text{up}})$ and calculate β_1, β_2.
2) Obtain P_1, P_2, and R_{sum} for fixed values of ρ_1 and ρ_2 through solving problem (4.21) using CVX.
3) Update r with the bisection search method: If 2) is feasible, set $r_{low} = r$; otherwise, $r_{\text{up}} = r$.
6: Until $r_{\text{up}} - r_{\text{low}} < \varepsilon$, where ε is a small positive number. Thus we get $R_{\text{sum}}(\eta(k))$.
7: $k = k+1$
8: Obtain $R_{\text{sum}}(\eta^o)$ by comparing all $R_{\text{sum}}(\eta(k)), k = 1,2,\cdots$, Corresponding P_1, P_2 are the optimal transmit powers P_1^*, P_2^*.

Upon investigation, it is obvious that even for fixed ρ_1, ρ_2, the problem is still non-convex since the objective function is not a concave function. Hence, to efficiently solve problem (4.19), it is first transformed using the idea of the rate-split method [73], formulated as

$$\max_{P_1,P_2} \quad R_{\text{sum}} \tag{4.20a}$$

$$\text{s.t.} \quad \min_{|\Delta h_{\text{ab}}| \le \varepsilon_1} C_{2\to1} \ge \eta R_{\text{sum}}, \tag{4.20b}$$

$$\min_{|\Delta h_{\text{cd}}| \le \varepsilon_2} C_{1\to2} \ge (1-\eta) R_{\text{sum}}, \tag{4.20c}$$

$$\min_{|\Delta h_{\text{ab}}| \le \varepsilon_1} Q_{2\to1} \ge \bar{Q}_{2\to1}, \tag{4.20d}$$

$$\min_{|\Delta h_{\text{cd}}| \le \varepsilon_2} Q_{1\to2} \ge \bar{Q}_{1\to2}, \tag{4.20e}$$

$$0 \le P_1 \le P_{\max}, \tag{4.20f}$$

$$0 \le P_2 \le P_{\max}, \tag{4.20g}$$

where $\eta \in [0,1]$. For any given η, the first two constraints typically impose a rate-

split between the two nodes i.e., η is a rate-split scheme. If we can solve (4.20) to get $R_{\text{sum}}(\eta)$ for given η, then we can do a one-dimensional search on η to find the maximum $R_{\text{sum}}(\eta^o)$ under the optimal rate-split scheme η^o. To proceed, let us first rewrite the optimization problem (4.20) as

$$\max_{P_1,P_2} \quad r \tag{4.21a}$$

s.t.

$$\rho_2|h_{\text{ad}}|^2P_1 \geq \beta_1\left(\rho_2(|\hat{h}_{\text{cd}}|^2+\varepsilon_2^2)P_2+\rho_2\sigma_{A_2}^2+\sigma_{p_2}^2\right), \tag{4.21b}$$

$$\rho_1|h_{\text{cb}}|^2P_2 \geq \beta_2\left(\rho_1(|\hat{h}_{\text{ab}}|^2+\varepsilon_1^2)P_1+\rho_1\sigma_{A_1}^2+\sigma_{p_1}^2\right), \tag{4.21c}$$

$$(1-\rho_1)(|h_{\text{cb}}|^2P_2+(|\hat{h}_{\text{ab}}|^2-\varepsilon_1^2)P_1+\sigma_{A_1}^2) \geq \bar{Q}_{2\to1}, \tag{4.21d}$$

$$(1-\rho_2)(|h_{\text{ad}}|^2P_1+(|\hat{h}_{\text{cd}}|^2-\varepsilon_2^2)P_2+\sigma_{A_2}^2) \geq \bar{Q}_{1\to2}, \tag{4.21e}$$

$$0 \leq P_1 \leq P_{\max}, \tag{4.21f}$$

$$0 \leq P_2 \leq P_{\max}, \tag{4.21g}$$

where r is the optimal objective value for problem (4.20), $\beta_1 = 2^{\eta r}-1$, and $\beta_2 = 2^{(1-\eta)r}-1$. Problem (4.21) is convex and can be efficiently solved by the disciplined convex programming toolbox like CVX [74]. After solving problem (4.21), the optimal values of the transmit power at node 1 and node 2 denoted as P_1^* and P_2^*, respectively, gives the optimal achievable sum-rate r^o at fixed values of $(\rho_1,\rho_2) \in (0,1)$. Algorithm 1 above summarises the whole procedure of solving problem (4.21). It is obvious that in both initialization and optimization steps, solving for r is the elementary operation in each iteration. CVX package is used to solve the problem and, iteratively update r by using the bisection method. The bounds of the rate search interval are obtained as follows. The lower bound r_{low} of the rate search is obviously 0 while the upper bound $r_{\max}$ is defined as the achievable sum-rate at zero RSI.

4.3.2 Power-splitting ratio optimization

To obtain the optimal value for the received power splitter coefficients ρ_1 and ρ_2, problem (4.19) is reformulated taking into account the optimal transmit powers P_1^* and P_2^* as

$$\max_{\rho_1,\rho_2\in(0,1)} R_{\text{sum}} \quad \text{s.t.} \tag{4.22a}$$

$$Q_{1\to 2} \geq \bar{Q}_{1\to 2}, \tag{4.22b}$$

$$Q_{2\to 1} \geq \bar{Q}_{2\to 1}. \tag{4.22c}$$

Clearly, from equation (4.16) and (4.17), the received power splitter coefficients ρ_1 and ρ_2 are separable with respect to the objective functions and constraints in problem (4.22). Hence, problem (4.22) can be decomposed into two sub-problems, namely,

$$\begin{aligned} &\max_{\rho_1\in(0,1)} C_{2\to 1} \quad \text{s.t.} \\ &\qquad Q_{2\to 1} \geq \bar{Q}_{2\to 1} \end{aligned} \tag{4.23}$$

and

$$\begin{aligned} &\max_{\rho_2\in(0,1)} C_{1\to 2} \quad \text{s.t.} \\ &\qquad Q_{1\to 2} \geq \bar{Q}_{1\to 2} \end{aligned} \tag{4.24}$$

for optimizing ρ_1 and ρ_2, respectively. Let us first analyze the case of optimizing ρ_1. The Lagrangian of problem (4.23) is given as

$$\begin{aligned} &L(\rho_1,\lambda_1) \\ &= \log_2\left(\frac{\rho_1(P_2^*|h_{\text{cb}}|^2+(|\hat{h}_{\text{ab}}|^2+\varepsilon_1^2)P_1^*+\sigma_{A_1}^2)+\sigma_{p_1}^2}{\rho_1((|\hat{h}_{ab}|^2+\varepsilon_1^2)P_1^*+\sigma_{A_1}^2)+\sigma_{p_1}^2}\right) \\ &+ \lambda_1[(1-\rho_1)(|h_{\text{cb}}|^2P_2^*+(|\hat{h}_{\text{ab}}|^2-\varepsilon_1^2)P_1^*+\sigma_{A1}^2) \\ &+ \bar{Q}_{2\to 1}], \end{aligned} \tag{4.25}$$

where $\lambda_1 \geq 0$ is the Lagrangian multiplier associated with the energy harvesting constraint. Obtaining the first order derivative $\frac{\partial L}{\partial \rho_1}$ of (4.25) and after performing some mathematical manipulations, we have

$$\begin{aligned}\frac{\partial L(\rho_1,\lambda_1)}{\partial \rho_1} &= \frac{P_2^*|h_{\mathrm{cb}}|^2\sigma_{p_1}^2}{(\rho_1((|\hat{h}_{\mathrm{ab}}|^2+\varepsilon_1^2)P_1^*+\sigma_{A_1}^2)+\sigma_{p_1}^2)^2} \\ &\quad -\lambda_1(|h_{\mathrm{cb}}|^2P_2+(|\hat{h}_{\mathrm{ab}}|^2-\varepsilon_1^2)P_1+\sigma_{A_1}^2).\end{aligned} \tag{4.26}$$

The Lagrangian dual variable λ_1 is selected such that the energy harvesting constraint in (4.23) is satisfied to equality. After some algebraic manipulation, the following second-order polynomial is obtained from (4.26)

$$a_1\rho_1^2+\rho_1 b_1+c_1=0, \tag{4.27}$$

where $a_1=((|\hat{h}_{\mathrm{ab}}|^2+\varepsilon_1^2)P_1^*+\sigma_{A_1}^2)^2$, $b_1=2a_1\sigma_{p_1}^2$, $c_1=(\sigma_{p_1}^2)^2-\frac{P_2^*|h_{\mathrm{cb}}|^2\sigma_{p_1}^2}{\lambda_1 D_1}$, and $D_1=|h_{\mathrm{cb}}|^2P_2^*+(|\hat{h}_{\mathrm{ab}}|^2+\varepsilon_1^2)P_1^*+\sigma_{A_1}^2$. Since the transmit power must be non-negative, the only acceptable solution of equation (4.27) is given by

$$\rho_1^*=\frac{-b_1+\sqrt{b_1^2-4a_1c_1}}{2a_1}. \tag{4.28}$$

Note that ρ_1^* is an increasing function of the Lagrangian multiplier λ_1 which must be chosen such that

$$\sqrt{b_1^2-4a_1c_1}\geq b_1. \tag{4.29}$$

Equation (4.29) can be further simplified as $4a_1c_1\leq 0$. Since $a_1=((|\hat{h}_{\mathrm{ab}}|^2+\varepsilon_1^2)P_1^*+\sigma_{A_1}^2)^2>0$ always holds in practice, it can be concluded that $c_1\leq 0$. Thus from the definition of c_1, we obtain

$$(\sigma_{p_1}^2)^2-\frac{P_2^*|h_{\mathrm{cb}}|^2\sigma_{p_1}^2}{\lambda_1 D_1}<0. \tag{4.30}$$

From (4.30), the upper bound of λ_1 is defined as

$$\lambda_1 \leq \frac{P_2^* |h_{\mathrm{cb}}|^2 \sigma_{p_1}^2}{\sigma_{P_1}^4 D}.$$

Now we can search for the optimal λ_1 within the following interval

$$\frac{P_2^* |h_{\mathrm{cb}}|^2}{\sigma_{p_1}^2 D} \geq \lambda_1 \geq 0.$$

Similar results can be derived for optimal ρ_2 in problem (4.24) as

$$\rho_2^* = \frac{-b_2 + \sqrt{b_2^2 - 4a_2c_2}}{2a_2}, \tag{4.31}$$

where we define $a_2 = ((|\hat{h}_{\mathrm{cd}}|^2 + \varepsilon_2^2)P_2^* + \sigma_{A_2}^2)^2$, $b_2 = 2a_2\sigma_{p_2}^2$, $c_2 = (\sigma_{p_2}^2)^2 - \frac{P_1^* |h_{\mathrm{ad}}|^2 \sigma_{p_2}^2}{\lambda_2 D_2}$, and $D_2 = |h_{\mathrm{ad}}|^2 P_1^* + (|\hat{h}_{\mathrm{cd}}|^2 + \varepsilon_2^2)P_2^* + \sigma_{A_2}^2$.

4.3.3 Iterative update

Now, the original transmit power and receive power splitter optimization problem (4.19) can be solved by an iterative technique shown in Algorithm 2. Algorithm 2 continually updates the objective function until convergence. Note that the constraints in problem (4.19) are always satisfied in every update as long as the condition on the choice of λ is met.

Algorithm 2 Procedure for solving problem (4.19)

1: Initialise ρ_1 and ρ_2.
2: Repeat
   1) Solve subproblem (4.21) using Algorithm 1 to obtain optimal P_1 and P_2.
   2) Solve subproblems (4.23) and (4.24) to obtain optimal
   ρ_1 and ρ_2.
3: Until convergence.

4.4 Numerical examples

In this section, the performance of the proposed transmit power and received power splitting optimization algorithm for SWIPT in FD communication systems is investigated through numerical simulations. We simulate a flat Rayleigh fading environment where the channel fading coefficients are characterized as complex Gaussian numbers having entries with zero mean and are independent and identically distributed. For simplicity, it is assumed that $\bar{Q}_{1\to 2} = \bar{Q}_{2\to 1} = Q$ and $\rho_1 = \rho_2 = \rho$ unless explicitly mentioned otherwise. All simulations are averaged over 1000 independent channel realizations. In Fig. 4.2, the sum-rate performance of the pro-

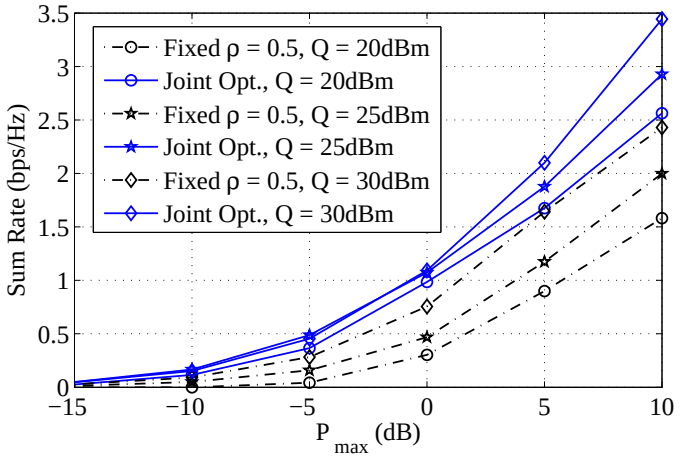

Figure 4.2: *Sum-rate versus* $\mathrm{P}_{\max}$.

posed algorithm versus transmit power budget $\mathrm{P}_{\max}$ (dB) for different values of the harvested energy constraint is investigated. In particular, sum-rate results of the proposed joint transmit power and receive power splitter optimization scheme ('Joint Opt.' in the figures) is compared in Fig. 4.2 with those of the transmit power only optimization scheme (given ρ). For simplicity, it is assumed that 70% of the self-interference power has been cancelled using existing analog and digital cancellation techniques [29]. Interestingly, the proposed joint optimization scheme yields noticeably higher sum-rate compared to the transmit power only optimization which essentially necessitates joint optimization. It can also be observed that an increase in $\mathrm{P}_{\max}$ results to a corresponding increase in the sum-rate rate for both schemes.

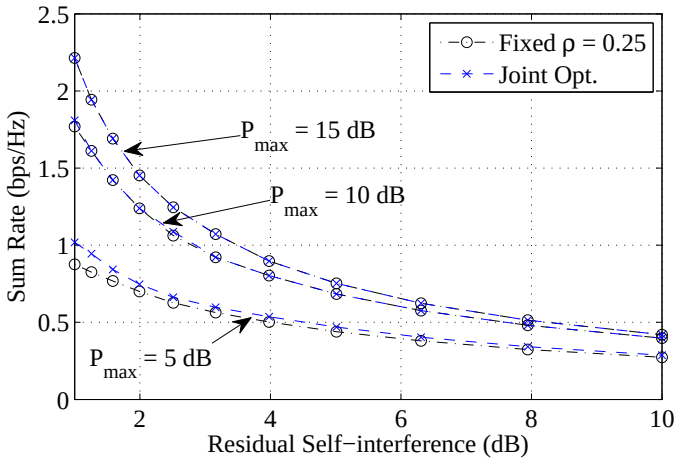

Figure 4.3: *Sum-rate versus residual self-interference above noise power.*

Also, the increased harvested energy constraints demand more power to be transmitted and hence yields higher sum-rate.

In Fig. 4.3, the impact of the residual self-interference on the sum-rate is investigated. Particularly, we investigate the performance of our proposed scheme for both fixed PS and joint optimization versus the residual self-interference (dB) above noise level for different values of transmit power constraint. Clearly, from Fig. 4.3, an increase in the residual self-interference results in a corresponding decrease in the achievable sum-rate. Also, it is observed that the sum-rate decreases faster at higher transmit power.

4.5 Conclusion

In this chapter, SWIPT in FD point-to-point communication systems has been investigated, and the transmit power and received power splitting ratio optimization algorithms which maximises the sum-rate subject to the transmit power and harvested energy constraints has been developed. Through computer simulation results, it is shown that the RSI, if not properly handled, inhibits system performance, thus reducing the achievable sum-rate.

Chapter 5

SWIPT in FD MIMO Two-Way Relay System

5.1 Two-way beamforming optimization for full-duplex SWIPT systems

In chapter 4, we investigated SWIPT in a point-to-point FD system. However, as wireless communication networks are subjected to fading, relay are often deployed to extend the network coverage, to increase throughput and to improve overall network performance. Thus, in this chapter, SWIPT in FD MIMO relay communication system is studied.

Conventionally, wireless communication nodes operate in HD mode under which they transmit and receive signals over orthogonal frequency or time resources. Recent advances, nevertheless, suggest that FD communications that allows simultaneous transmission and reception of signal over the same radio channel is possible [30], [75]. This brings a new opportunity for SWIPT [20], [76]. In addition to the immediate benefit of essentially doubling the bandwidth, FD communications also find applications in SWIPT. Much interest has turned to FD relaying in which information is sent from a source node to a destination node through an intermediate FD relaying node. In the literature, the studies on relay aided SWIPT largely consid-

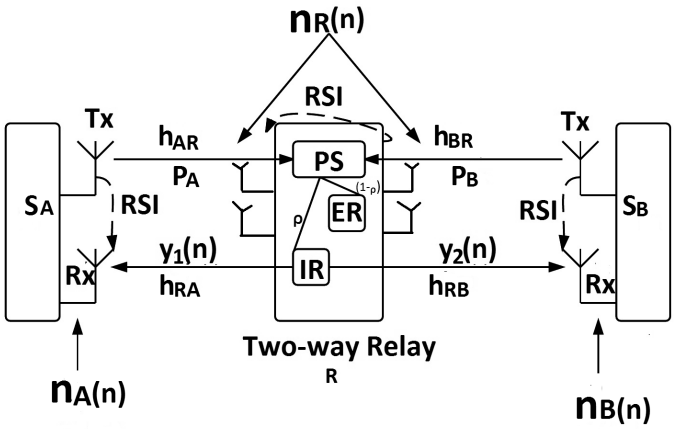

Figure 5.1: *The model of the two-way full-duplex SWIPT system.*

ered HD relaying and adopted a time-switched relaying (TSR) approach [77]- [79]. In contrast to the existing results, this thesis reports the joint optimization of two-way beamforming matrix for SWIPT in a MIMO amplify-and-forward full-duplex relay system employing a power splitter, where the sum-rate is maximized subject to the energy harvesting and total power constraints.

5.2 System model and problem formulation

Consider SWIPT in a three-node MIMO relay network consisting of two sources $\mathsf{S_A}$ and $\mathsf{S_B}$ wanting to exchange information with the aid of an AF relay R, as shown in Fig. 5.1. In our model, all the nodes are assumed to operate in FD mode, and it is also assumed that there is no direct link between $\mathsf{S_A}$ and $\mathsf{S_B}$ so communication between them must be done via R. Both $\mathsf{S_A}$ and $\mathsf{S_B}$ transmit their messages simultaneously to R with transmit power P_A and P_B, respectively. In the broadcast phase, the relay R employs linear processing with an amplification matrix $\mathbf{W}$ to process the received signal and broadcasts the processed signal to the nodes with the harvested power Q. It is assumed that each source node is equipped with a pair of transmitter-receiver antennas for signal transmission and reception respectively. M_T and M_R are used to denote the number of transmit and receive antennas at R, respectively. Also, $\mathbf{h}_{XR} \in \mathbb{C}^{M_R \times 1}$ and $\mathbf{h}_{RX} \in \mathbb{C}^{M_T \times 1}$ are used to, respectively, de-

note the directional channel vectors between the source node X's $\in (A,B)$ transmit antenna to R's receive antennas, and that between the relay's transmit antenna(s) to source node X's receive antenna. The concurrent transmission and reception of signals at the nodes produces SI which inhibits the performance of FD systems. We adopt existing SI cancellation mechanisms in the literature to mitigate the SI (e.g., antenna isolation, analog and digital cancellation, and etc.) [29].

Due to imperfect channel estimation, however, the SI cannot be cancelled completely [80]. Thus, h_{AA}, h_{BB} and $\mathbf{H}_{RR} \in \mathbb{C}^{M_R \times M_T}$ are then used to represent the RSI channels at the corresponding nodes. For simplicity, the RSI channel is modelled as a Gaussian distribution random variable with zero mean and variance σ_X^2, for $\mathsf{X} \in \{A,B,R\}$ [80]. It is further assumed that the relay is equipped with a PS device which splits the received signal power at the relay such that a $\rho \in (0,1)$ portion of the received signal power is fed to the information receiver (IR) and the remaining $(1-\rho)$ portion of the power is fed to the energy receiver (ER) at the relay.

When the source nodes transmit their signals to the relay, the AF relay employs a short delay to perform linear processing. It is assumed that the processing delay at the relay is given by a τ-symbol duration, which denotes the processing time required to implement the FD operation [43]. τ typically takes integer values. The delay is assumed short enough when compared to a time slot which has a large number of data symbols, and thus, its effect on the achievable rate is negligible. At time instant n, the received signal $\mathbf{y}_r[n]$ and the transmit signal $\mathbf{x}_R[n]$ at the relay can be written as

$$\mathbf{y}_R[n] = \mathbf{h}_{AR}s_A[n] + \mathbf{h}_{BR}s_B[n] + \mathbf{H}_{RR}\mathbf{x}_R[n] + \mathbf{n}_R[n], \tag{5.1}$$

$$\mathbf{x}_R[n] = \mathbf{W}\mathbf{y}_R^{IR}(n-\tau), \tag{5.2}$$

respectively, where $\mathbf{n}_R[n]$ is the AWGN and $\mathbf{y}_r^{\mathrm{IR}}[n]$ is the signal split to the IR at R given by

$$\mathbf{y}_R^{IR}[n] = \sqrt{\rho}\left(\mathbf{h}_{AR}s_A[n] + \mathbf{h}_{BR}s_B[n] + \mathbf{H}_{RR}\mathbf{x}_R[n] + \mathbf{n}_R[n]\right) + \mathbf{n}_p[n]. \tag{5.3}$$

Here $\mathbf{n}_p$ is the additional processing noise at the IR. Using (5.2) and (5.3) recursively, the overall relay output can be written as

$$\begin{aligned}\mathbf{x}_R[n] &= \mathbf{W}\left(\sqrt{\rho}\left(\mathbf{h}_{AR}s_A[n-\tau]+\mathbf{h}_{BR}s_B[n-\tau]\right.\right.\\ &+ \left.\left.\mathbf{H}_{RR}\mathbf{x}_R[n-\tau]+\mathbf{n}_R[n-\tau]\right)+\mathbf{n}_p[n-\tau]\right).\end{aligned} \tag{5.4}$$

The capacity of a relay network with delay depends only on the relative path delays from the sender to the receiver and not on absolute delays [81]. Thus, the relay output is given as

$$\begin{aligned}\mathbf{x}_R[n] &= \mathbf{W}\sum_{j=0}^{\infty}(\mathbf{H}_{RR}\mathbf{W})^j[\sqrt{\rho}(\mathbf{h}_{AR}s_A[n-j\tau-\tau]\\ &+ \mathbf{h}_{BR}s_B[n-j\tau-\tau]+\mathbf{n}_R[n-j\tau-\tau])\\ &+ \mathbf{n}_p[n-j\tau-\tau]],\end{aligned} \tag{5.5}$$

where j denotes the index of the delayed symbols.

To simplify the signal model and to keep the optimization problem tractable, we add the zero forcing (ZF) solution constraint such that the optimization of $\mathbf{W}$ nulls out the RSI from the relay output to the relay input [82]. To realise this, it is easy to check from (5.5) that the condition below is sufficient:

$$\mathbf{W}\mathbf{H}_{RR}\mathbf{W}=\mathbf{0}. \tag{5.6}$$

Consequently, (5.5) becomes

$$\begin{aligned}\mathbf{x}_R[n] &= \mathbf{W}\left(\sqrt{\rho}\left(\mathbf{h}_{AR}s_A[n-\tau]+\mathbf{h}_{BR}s_B[n-\tau]\right.\right.\\ &+ \left.\left.\mathbf{n}_R[n-\tau]\right)+\mathbf{n}_p[n-\tau]\right),\end{aligned} \tag{5.7}$$

with the covariance matrix

$$\mathbb{E}[\mathbf{x}_R\mathbf{x}_R^{\dagger}]=\rho P_A\mathbf{W}\mathbf{h}_{AR}\mathbf{h}_{AR}^{\dagger}\mathbf{W}^{\dagger}+\rho P_B\mathbf{W}\mathbf{h}_{BR}\mathbf{h}_{BR}^{\dagger}\mathbf{W}^{\dagger}+\rho\mathbf{W}\mathbf{W}^{\dagger}+\mathbf{W}\mathbf{W}^{\dagger}. \tag{5.8}$$

Thus, the relay output power can be written as

$$\begin{aligned} p_R = \text{trace}(\mathbb{E}[\mathbf{x}_R\mathbf{x}_R^\dagger]) &= \rho[P_A\|\mathbf{W}\mathbf{h}_{AR}\|^2 + P_B\|\mathbf{W}\mathbf{h}_{BR}\|^2 + \text{trace}(\mathbf{W}\mathbf{W}^\dagger)] \\ &+ \text{trace}(\mathbf{W}\mathbf{W}^\dagger). \end{aligned} \tag{5.9}$$

In the second time slot, the received signal at $\mathsf{S_A}$ is given by

$$\begin{aligned} y_{s_A}[n] &= \mathbf{h}_{RA}^\dagger\mathbf{x}_R[n] + h_{AA}s_A[n] + n_A[n] \\ &= \sqrt{\rho}(\mathbf{h}_{RA}^\dagger\mathbf{W}\mathbf{h}_{AR}s_A[n-\tau] \\ &+ \mathbf{h}_{RA}^\dagger\mathbf{W}\mathbf{h}_{BR}s_B[n-\tau] + \mathbf{h}_{RA}^\dagger\mathbf{W}\mathbf{n}_R[n]) \\ &+ \mathbf{h}_{RA}^\dagger\mathbf{W}n_p[n] + h_{AA}s_A[n] + n_A[n]. \end{aligned} \tag{5.10}$$

After cancelling its own signal $s_A[n-\tau]$, it becomes

$$\begin{aligned} y_{s_A}[n] &= \sqrt{\rho}(\mathbf{h}_{RA}^\dagger\mathbf{W}\mathbf{h}_{BR}s_B[n-\tau] + \mathbf{h}_{RA}^\dagger\mathbf{W}\mathbf{n}_R[n]) \\ &+ \mathbf{h}_{RA}^\dagger\mathbf{W}n_p[n] + h_{AA}s_A[n] + n_A[n]. \end{aligned} \tag{5.11}$$

The received signal-to-interference-plus-noise ratio at node $\mathsf{S_A}$, denoted as γ_A, can be expressed as

$$\gamma_A = \frac{\rho P_B|\mathbf{h}_{RA}^\dagger\mathbf{W}\mathbf{h}_{BR}|^2}{\rho\|\mathbf{h}_{RA}^\dagger\mathbf{W}\|^2 + \|\mathbf{h}_{RA}^\dagger\mathbf{W}\|^2 + P_A|h_{AA}|^2 + 1}. \tag{5.12}$$

Similarly, the received SINR at node $\mathsf{S_B}$ can be written as

$$\gamma_B = \frac{\rho P_A|\mathbf{h}_{RB}^\dagger\mathbf{W}\mathbf{h}_{AR}|^2}{\rho\|\mathbf{h}_{RB}^\dagger\mathbf{W}\|^2 + \|\mathbf{h}_{RB}^\dagger\mathbf{W}\|^2 + P_B|h_{BB}|^2 + 1}. \tag{5.13}$$

The achievable rates are then given by $R_A = \log_2(1+\gamma_A)$ and $R_B = \log_2(1+\gamma_B)$, at nodes A and B, respectively.

Now the signal split to ER at the relay node is given as

$$\mathbf{y}_R^{ER} = \sqrt{(1-\rho)}(\mathbf{h}_{AR}s_A[n] + \mathbf{h}_{BR}s_B[n] + \mathbf{H}_{RR}\mathbf{x}_R[n] + \mathbf{n}_R[n]).$$

Thus, the harvested energy at the relay is given by

$$Q = \alpha(1-\rho)\left(|\mathbf{h}_{AR}|^2 P_A + |\mathbf{h}_{BR}|^2 P_B + \bar{\mathrm{E}} + M_T\right), \tag{5.14}$$

where $\bar{\mathrm{E}} = \mathbb{E}[\mathbf{x}_R \mathbf{x}_R^\dagger]$, and α denotes the energy conversion efficiency of the ER at the relay which accounts for the loss in energy transducer for converting the RF energy to electrical energy to be stored. For simplicity, α is assumed to be unity.

Note that the conventional HD relay communication system requires two phases for $\mathsf{S_A}$ and $\mathsf{S_B}$ to exchange information [83]. FD relay systems on the other hand, reduce the whole operation to only one phase, hence increasing the spectrum efficiency. For simplicity, it is assumed that the transmit power at the source nodes are intelligently selected by the sources. Therefore, in this work, we do not consider optimization at the source nodes. To ensure a continuous information transfer between the two sources, the harvested energy at the relay should be above a given threshold so that a useful level of harvested energy is reached. As a result, we formulate the joint relay beamforming and receive PS ratio (ρ) optimization problem as a maximization problem of the sum-rate. Mathematically, this problem is formulated as

$$\begin{aligned} \max_{\mathbf{W},\rho\in(0,1)} \quad & R_A + R_B \\ \text{s.t.} \quad & Q \geq \bar{Q}, \quad p_R \leq P_R, \end{aligned} \tag{5.15}$$

where P_R is the maximum transmit power at the relay and $\bar{Q}$ is the minimum amount of harvested energy required to maintain the relay's operation.

5.3 Proposed solution

Considering the fact that each source only transmits a single data stream and the network coding principle encourages mixing rather than separating the data streams from the two sources, $\mathbf{W}$ can be decomposed as $\mathbf{W} = \mathbf{w}_t \mathbf{w}_r^\dagger$, where $\mathbf{w}_t$ is the transmit beam forming vector and $\mathbf{w}_r$ is the receive beam forming vector at the relay. Then, the ZF condition is simplified to $(\mathbf{w}_r^\dagger \mathbf{H}_{RR} \mathbf{w}_t)\mathbf{W} = 0$ or equivalently $(\mathbf{w}_r^\dagger \mathbf{H}_{RR} \mathbf{w}_t) = 0$

since in general $\mathbf{W} \neq 0$ [82]. It is further assumed without loss of optimality that $\|\mathbf{w}_r\| = 1$. Therefore, the optimization problem in (5.15) can be rewritten as (5.16)

$$\begin{aligned}
\max_{\mathbf{w}_r, \mathbf{w}_t \rho \in (0,1)} \quad & \log_2\left(1 + \frac{\rho P_B C_{rB} |\mathbf{h}_{RA}^\dagger \mathbf{w}_t|^2}{\rho \|\mathbf{h}_{RA}^\dagger \mathbf{w}_t\|^2 + \|\mathbf{h}_{RA}^\dagger \mathbf{w}_t\|^2 + P_A |h_{AA}|^2 + 1}\right) \\
& + \log_2\left(1 + \frac{\rho P_A C_{rA} |\mathbf{h}_{RB}^\dagger \mathbf{w}_t|^2}{\rho \|\mathbf{h}_{RB}^\dagger \mathbf{w}_t\|^2 + \|\mathbf{h}_{RB}^\dagger \mathbf{w}_t\|^2 + P_B |h_{BB}|^2 + 1}\right) \\
\text{s.t.} \quad & (1-\rho)(|\mathbf{h}_{AR}|^2 P_A + |\mathbf{h}_{BR}|^2 P_B + \bar{\mathrm{E}} + M_T) \geq \bar{Q}, \\
& \rho(P_A \|\mathbf{w}_t\|^2 C_{rA} + P_B \|\mathbf{w}_t\|^2 C_{rB} + \|\mathbf{w}_t\|^2) + \|\mathbf{w}_t\|^2 \leq P_R, \\
& \mathbf{w}_r^\dagger \mathbf{H}_{RR} \mathbf{w}_t = 0,
\end{aligned} \tag{5.16}$$

where $C_{rA} \triangleq |\mathbf{w}_r^\dagger \mathbf{h}_{AR}|^2$ and $C_{rB} \triangleq |\mathbf{w}_r^\dagger \mathbf{h}_{BR}|^2$.

5.3.1 Parametrization of the receive beamforming vector $\mathbf{w}_r$

Observe in (5.16) that $\mathbf{w}_r$ is mainly involved in $|\mathbf{w}_r^\dagger \mathbf{h}_{AR}|^2$ and $|\mathbf{w}_r^\dagger \mathbf{h}_{BR}|^2$, so it has to balance the signals received from the sources. According to the result obtained in [84], $\mathbf{w}_r$ can be parameterized by $0 \leq \beta \leq 1$ as

$$\mathbf{w}_r = \beta \frac{\Pi_{\mathbf{h}_{BR}} \mathbf{h}_{AR}}{\|\Pi_{\mathbf{h}_{BR}} \mathbf{h}_{AR}\|} + \sqrt{1-\beta} \frac{\Pi_{\mathbf{h}_{BR}}^\perp \mathbf{h}_{AR}}{\|\Pi_{\mathbf{h}_{BR}}^\perp \mathbf{h}_{AR}\|}, \tag{5.17}$$

where $\Pi_{\mathbf{X}} = \mathbf{X}(\mathbf{X}^\dagger \mathbf{X})^{-1} \mathbf{X}^\dagger$ denotes the orthogonal projection onto the column space of $\mathbf{X}$ and $\Pi_{\mathbf{X}}^\perp = \mathbf{I} - \Pi_{\mathbf{X}}$ denotes the orthogonal complement of the column space of $\mathbf{X}$.

It should be made clear that (5.17) is not the complete characterization of $\mathbf{w}_r$ because it is also involved in the ZF constraint $\mathbf{w}_r^\dagger \mathbf{H}_{RR} \mathbf{w}_t = 0$, but this parametrization makes the problem more tractable. Thus, given β, we can optimize $\mathbf{w}_t$ for fixed PS ratio ρ. Then perform a 1-D search to find the optimal β^*.

5.3.2 Optimization of the receive power splitter(ρ)

For given $\mathbf{w}_r$ and $\mathbf{w}_t$, the optimal receive PS ratio ρ can be determined. Firstly, using the monotonicity between SINR and the rate, (5.16) can be rewritten as

$$\begin{aligned}
\max_{\rho\in(0,1)} \quad & \frac{\rho P_B C_{rB}|\mathbf{h}_{RA}^{\dagger}\mathbf{w}_t|^2}{\rho\|\mathbf{h}_{RA}^{\dagger}\mathbf{w}_t\|^2+\|\mathbf{h}_{RA}^{\dagger}\mathbf{w}_t\|^2+P_A|h_{AA}|^2+1} \\
& + \frac{\rho P_A C_{rA}|\mathbf{h}_{RB}^{\dagger}\mathbf{w_t}|^2}{\rho\|\mathbf{h}_{RB}^{\dagger}\mathbf{w}_t\|^2+\|\mathbf{h}_{RB}^{\dagger}\mathbf{w}_t\|^2+P_B|h_{BB}|^2+1} && \text{(5.18a)} \\
\text{s.t.} \quad & (1-\rho)(|\mathbf{h}_{AR}|^2P_A+|\mathbf{h}_{BR}|^2P_B+\bar{\mathrm{E}}+M_T)\geq\bar{Q}, && \text{(5.18b)} \\
& \rho(P_A\|\mathbf{w}_t\|^2C_{rA}+P_B\|\mathbf{w}_t\|^2C_{rB}+\|\mathbf{w}_t\|^2)+\|\mathbf{w}_t\|^2\leq P_R. && \text{(5.18c)}
\end{aligned}$$

It is easy to verify that the objective of the problem (5.18) is an increasing function of ρ. Hence, the optimal receive power splitter ρ^* can be determined based on constraints (5.18b) and (5.18c) only. The optimal point will be the largest ρ satisfying both constraints. Note that the left-hand side of constraint (5.18b) is a decreasing function of ρ whereas that of constraint (5.18c) is an increasing function of ρ. Now the largest ρ satisfying constraint (5.18b) to equality is given by

$$\rho_l = 1-\frac{\bar{Q}}{|\mathbf{h}_{AR}|^2P_A+|\mathbf{h}_{BR}|^2P_B+\bar{\mathrm{E}}+M_T}. \tag{5.19}$$

On the other hand, the maximal ρ satisfying constraint (5.18c) to equality is given by

$$\rho_m = \frac{P_R-\|\mathbf{w}_t\|^2}{P_A\|\mathbf{w}_t\|^2C_{rA}+P_B\|\mathbf{w}_t\|^2C_{rB}+\|\mathbf{w}_t\|^2}. \tag{5.20}$$

We check whether ρ_l satisfies the constraint (5.18c). If it does, then it is the optimal solution ρ^*. Otherwise, we perform a one-dimensional search over ρ until ρ_m is reached. Obviously, if $\rho_m > \rho_l$, then the problem (5.18) turns to be infeasible.

5.3.3 Optimization of the transmit beamforming vector ($\mathbf{w}_t$)

In this subsection, we first study how to optimize $\mathbf{w}_t$ for given β and ρ. Then we perform a 1-D search on β to find optimal β^* which guarantees an optimal $\mathbf{w}_r^*$ as

defined in (5.17) for the given ρ. For convenience, we define a semidefinite matrix $\mathbf{W}_t \triangleq \mathbf{w}_t\mathbf{w}_t^\dagger$. Then the problem (5.16) becomes

$$\begin{aligned}
\max_{\mathbf{W}_t \succeq 0} \quad & F(\mathbf{W}_t) \\
\text{s.t.} \quad & \text{trace}(\mathbf{W}_t) \leq \frac{P_R}{\rho(P_A C_{rA} + P_B C_{rB} + 1) + 1}, \\
& (1-\rho)(|\mathbf{h}_{AR}|^2 P_A + |\mathbf{h}_{BR}|^2 P_B + \bar{\mathrm{E}} + 1) \geq \bar{Q}, \\
& \text{trace}(\mathbf{W}_t \mathbf{H}_{RR}^\dagger \mathbf{w}_r \mathbf{w}_r^\dagger \mathbf{H}_{RR}) = 0, \\
& \text{rank}(\mathbf{W}_t) = 1,
\end{aligned} \tag{5.21}$$

where $F(\mathbf{W}_t)$ is given as

$$\begin{aligned}
F(\mathbf{W}_t) \triangleq & \log_2\left(1 + \frac{\rho P_B C_{rB} \text{trace}(\mathbf{W}_t \mathbf{h}_{RA}\mathbf{h}_{RA}^\dagger)}{\rho \text{trace}(\mathbf{W}_t \mathbf{h}_{RA}\mathbf{h}_{RA}^\dagger) + \text{trace}(\mathbf{W}_t \mathbf{h}_{RA}\mathbf{h}_{RA}^\dagger) + P_A|h_{AA}|^2 + 1}\right) \\
& + \log_2\left(1 + \frac{\rho P_A C_{rA} \text{trace}(\mathbf{W}_t \mathbf{h}_{RB}\mathbf{h}_{RB}^\dagger)}{\rho \text{trace}(\mathbf{W}_t \mathbf{h}_{RB}\mathbf{h}_{RB}^\dagger) + \text{trace}\mathbf{W}_t(\mathbf{h}_{RB}\mathbf{h}_{RB}^\dagger) + P_B|h_{BB}|^2 + 1}\right).
\end{aligned} \tag{5.22}$$

Clearly, $F(\mathbf{W}_t)$ is not a concave function, making the problem challenging. To solve (5.22), we propose to use the difference of convex programming (DCP) to find a local optimum point. To this end, we express $F(\mathbf{W}_t)$ as a difference of two concave functions $f(\mathbf{W}_t)$ and $g(\mathbf{W}_t)$ i.e.,

$$\begin{aligned}
F(\mathbf{W}_t) \;=\; & \log_2((\rho P_B C_{rB} + \rho + 1)\text{trace}(\mathbf{W}_t \mathbf{h}_{RA}\mathbf{h}_{RA}^\dagger) \\
& +\; P_A|h_{AA}|^2 + 1) - \log_2(\rho \text{trace}(\mathbf{W}_t \mathbf{h}_{RA}\mathbf{h}_{RA}^\dagger) \\
& +\; \text{trace}(\mathbf{W}_t \mathbf{h}_{RA}\mathbf{h}_{RA}^\dagger) + P_A|h_{AA}|^2 + 1) \\
& +\; \log_2((\rho P_A C_{rA} + \rho + 1)\text{trace}(\mathbf{W}_t \mathbf{h}_{RB}\mathbf{h}_{RB}^\dagger) \\
& +\; P_B|h_{BB}|^2 + 1) - \log_2(\rho \text{trace}(\mathbf{W}_t \mathbf{h}_{RB}\mathbf{h}_{RB}^\dagger) \\
& +\; \text{trace}(\mathbf{W}_t \mathbf{h}_{RB}\mathbf{h}_{RB}^\dagger) + P_B|h_{BB}|^2 + 1) \\
=\; & f(\mathbf{W}_t) - g(\mathbf{W}_t),
\end{aligned} \tag{5.23}$$

where

$$
\begin{aligned}
f(\mathbf{W}_t) \triangleq\ & \log_2((\rho P_B C_{rB} + \rho + 1)\text{trace}(\mathbf{W}_t \mathbf{h}_{RA} \mathbf{h}_{RA}^{\dagger}) \\
+\ & P_A |h_{AA}|^2 + 1) + \log_2((\rho P_A C_{rA} + \rho + 1) \\
\times\ & \text{trace}(\mathbf{W}_t \mathbf{h}_{RB} \mathbf{h}_{RB}^{\dagger}) + P_B |h_{BB}|^2 + 1),
\end{aligned} \tag{5.24}
$$

$$
\begin{aligned}
g(\mathbf{W}_t) \triangleq\ & \log_2(\rho \text{trace}(\mathbf{W}_t \mathbf{h}_{RA} \mathbf{h}_{RA}^{\dagger}) + \text{trace}(\mathbf{W}_t \mathbf{h}_{RA} \mathbf{h}_{RA}^{\dagger}) \\
+\ & P_A |h_{AA}|^2 + 1) + \log_2(\rho \text{trace}(\mathbf{W}_t \mathbf{h}_{RB} \mathbf{h}_{RB}^{\dagger}) \\
+\ & \text{trace}(\mathbf{W}_t \mathbf{h}_{RB} \mathbf{h}_{RB}^{\dagger}) + P_B |h_{BB}|^2 + 1).
\end{aligned} \tag{5.25}
$$

Note that $f(\mathbf{W}_t)$ is a concave function while $g(\mathbf{W}_t)$ is a convex function. The main idea is to approximate $g(\mathbf{W}_t)$ by a linear function. The linearization (first-order approximation) of $g(\mathbf{W}_t)$ around the point $f(\mathbf{W}_{t,k})$ is given as

$$
\begin{aligned}
& g_L(\mathbf{W}_t; \mathbf{W}_{t,k}) = \\
& \frac{1}{\text{In}(2)} \frac{\rho \text{trace}((\mathbf{W}_t - \mathbf{W}_{t,k}) \mathbf{h}_{RA} \mathbf{h}^{\dagger}{}_{RA}) + \text{trace}((\mathbf{W}_t - \mathbf{W}_{t,k}) \mathbf{h}_{RA} \mathbf{h}^{\dagger}{}_{RA})}{\rho \text{trace}(\mathbf{W}_{t,k} \mathbf{h}_{RA} \mathbf{h}^{\dagger}{}_{RA}) + \text{trace}(\mathbf{W}_{t,k} \mathbf{h}_{RA} \mathbf{h}^{\dagger}{}_{RA}) + P_A |h_{AA}|^2 + 1} \\
& + \frac{1}{\text{In}(2)} \frac{\rho \text{trace}((\mathbf{W}_t - \mathbf{W}_{t,k}) \mathbf{h}_{RB} \mathbf{h}^{\dagger}{}_{RB}) + \text{trace}((\mathbf{W}_t - \mathbf{W}_{t,k}) \mathbf{h}_{RB} \mathbf{h}^{\dagger}{}_{RB})}{\rho \text{trace}(\mathbf{W}_{t,k} \mathbf{h}_{RB} \mathbf{h}^{\dagger}{}_{RB}) + \text{trace}(\mathbf{W}_{t,k} \mathbf{h}_{RB} \mathbf{h}^{\dagger}{}_{RB}) + P_B |h_{BB}|^2 + 1} \\
& + \log_2(\rho \text{trace}(\mathbf{W}_{t,k} \mathbf{h}_{RA} \mathbf{h}^{\dagger}{}_{RA}) + \text{trace}(\mathbf{W}_{t,k} \mathbf{h}_{RA} \mathbf{h}^{\dagger}{}_{RA}) + P_A |h_{AA}|^2 + 1) \\
& + \log_2(\rho \text{trace}(\mathbf{W}_{t,k} \mathbf{h}_{RB} \mathbf{h}^{\dagger}{}_{RB}) + \text{trace}(\mathbf{W}_{t,k} \mathbf{h}_{RB} \mathbf{h}^{\dagger}{}_{RB}) + P_B |h_{BB}|^2 + 1).
\end{aligned} \tag{5.26}
$$

Then, the DCP programming is applied to sequentially solve the following convex problem

$$
\begin{aligned}
\mathbf{W}_{t,k+1} =\ & \arg\max_{\mathbf{W_t}} f(\mathbf{W}_t) - g_L(\mathbf{W}_t; \mathbf{W}_{t,k}) \\
\text{s.t.} \quad & \text{trace}(\mathbf{W}_t) = \frac{P_R}{\rho(P_A C_{rA} + P_B C_{rB} + 1) + 1}, \\
& (1-\rho)(|\mathbf{h}_{AR}|^2 P_A + |\mathbf{h}_{BR}|^2 P_B + \bar{\text{E}} + 1), \geq \bar{Q}, \\
& \text{trace}(\mathbf{W}_t \mathbf{H}_{RR}^{\dagger} \mathbf{w}_r \mathbf{w}_r^{\dagger} \mathbf{H}_{RR}) = 0.
\end{aligned} \tag{5.27}
$$

Now the problem (5.21) can be solved by (i) Choosing an initial point $\mathbf{W}_t$ and ii) For $k = 0, 1, \cdots$, solving (5.27) until convergence. Notice that in (5.27), we have ignored the rank-1 constraint on $\mathbf{W}_t$. This constraint is guaranteed to be satisfied by the results in [85, Theorem 2] when $\mathrm{M}_T > 2$, therefore, the decomposition of $\mathbf{W}_t$ leads to the optimal solution $\mathbf{w}_t^{\dagger}$.

5.3.4 Optimization of the receive beamforming vector $(\mathbf{w}_r)$

Given $\mathbf{w}_t$, the value of the optimal receive beamforming vector $\mathbf{w}_r$ can be obtained by performing a 1-D search on β to find the maximum β^* which maximises $R_{\text{sum}}(\mathbf{w}_r)$ for a fixed value of $\rho \in (0,1)$. Algorithm 3 summarises this procedure. The bounds of the rate search interval are obtained as follows. The lower bound $(R_A + R_B)_{\text{low}}$ is obviously zero while the upper bound $(R_A + R_B)_{\max}$ is defined as the achievable sum-rate at zero RSI. With optimal β^*, optimal $\mathbf{w}_r^*$ can be obtained from (5.17).

Algorithm 3 Procedure for solving problem (5.21)

1: Set $0 \leq \beta \leq 1$ and $0 \leq \rho \leq 1$ as non-negative real-valued scaler and obtain $\mathbf{w}_r$ as given in (5.17).
2: At step k, set $\beta(k) = \beta(k-1) + \triangle\beta$ until $\beta(k) = 1$, where $\triangle\beta$ is the searching step size.
3: Initialise $(R_A + R_B)_{\text{low}} = 0$ and $(R_A + R_B)_{\text{up}} = (R_A + R_B)_{\max}$.
4: **Repeat**
a) Set $R \leftarrow \frac{1}{2}((R_A + R_B)_{\text{low}} + (R_A + R_B)_{\text{up}})$
b) Obtain the optimal relay transmit beamforming vector $\mathbf{w}_t$ by solving problem (5.27).
c) Update the value of R with the bisection search method: if (b) is feasible, set $(R_A + R_B)_{\text{low}} = R$; otherwise, $(R_A + R_B)_{\text{up}} = R$.
5: **Until** $(R_A + R_B)_{\text{up}} - (R_A + R_B)_{\text{low}} < \varepsilon$, where ε is a small positive number. Thus we get $R(\beta(k))$.
6: k = k+1
7: Find optimal β^* by comparing all $R(\beta(k))$ that yields maximal R. Corresponding $\mathbf{w}_t$ is the optimal one.
8: Obtain the optimal $\mathbf{w}_r^*$ from (5.17) using β^*.

5.3.5 Iterative update

Now, the original beamforming and receive power splitter optimization problem (5.16) can be solved by an iterative technique shown in Algorithm 4. Algorithm 4 continually updates the objective function in (5.16) until convergence.

Algorithm 4 Procedure for solving problem (5.16)

1: Initialise $0 \leq \rho \leq 1$.
2: **Repeat**
a) Obtain $\mathbf{w}_t^*$ and $\mathbf{w}_r^*$ using Algorithm 3
b) Obtain optimal ρ^* following the procedure in subsection 5.3.2
3: **Until** convergence.

5.4 Numerical examples

In this section, the performance of the proposed algorithm is evaluated through computer simulations. We simulate a flat Rayleigh fading environment where the channel fading coefficients are characterized as complex Gaussian numbers having entries with zero mean and are independent and identically distributed (i.d.d). In order to ensure that the relay harvests the maximum possible energy, it is assumed that the two source nodes transmit at their maximum power budget, i.e., $P_A = P_B =$ $\mathrm{P}_{\max}$ and $P_R = 4$ (dB). All simulations are averaged over 1000 independent channel realizations.

In Fig. 5.2, the sum-rate results is investigated against the transmit power budget $P_{\max}$ (dB) for various harvested energy constraint. The proposed scheme ('Joint Opt' in the figure) is compared with those of the fixed receive beamforming vector ($\mathbf{w}_r$) ('FRBV'= 0.583) at optimal PS coefficient (ρ^*). Remarkably, the proposed scheme yields higher sum-rate compared to the sum-rate of the FRBV scheme which essentially necessitates joint optimization. It can also be observed that as $P_{\max}$ increases, the sum-rate for both schemes increases. Also, as the harvested energy constraint decreases from 20 dBm to 10 dBm, the achievable sum-rate for both schemes increases but the joint optimization schemes achieves a higher sum rate

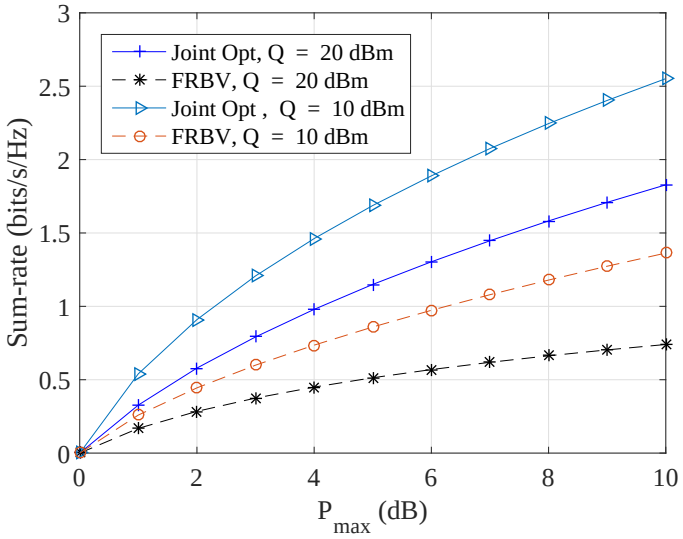

Figure 5.2: *Sum-rate versus* $P_{\max}$.

compared to the FRBV scheme. Thus, an increased energy harvesting constraint still necessitates joint optimization.

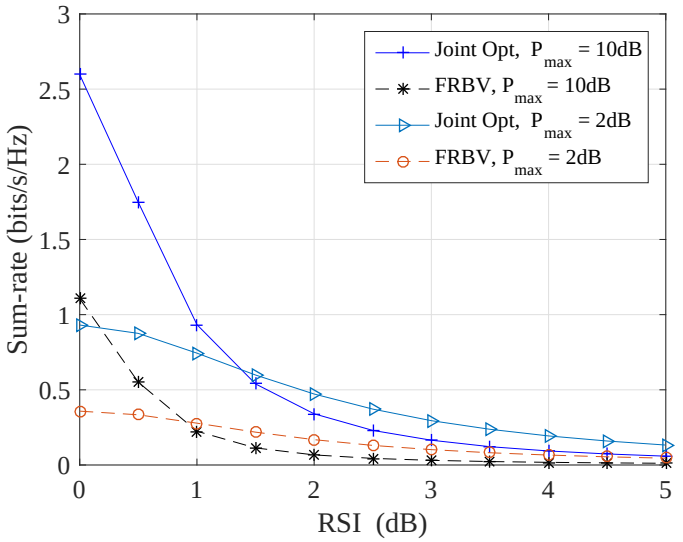

Figure 5.3: *Sum-rate versus residual self-interference.*

In the Fig.5.3, we analyze the impact of the residual self-interference on the sum-rate. Particularly, we investigate the performance in terms of the sum rate of our proposed scheme for both FRBV $\mathbf{w}_r$ and joint optimization versus the RSI (dB) above noise level for different values of transmit power constraint. We can observe from Fig. 5.3 that an increase in the residual self-interference results in a corre-

sponding decrease in the achievable sum- rate. Also, it is obvious that the sum-rate decreases faster at higher transmit power in the low RSI region.

5.5 Conclusion

In this chapter, the joint beamforming optimization for SWIPT in FD MIMO two-way AF relay channel has been investigated and an algorithm which maximizes the sum-rate subject to the relay transmit power and harvested energy constraints has been proposed. Using DCP and 1-D search, we jointly optimized the receive beamforming vector, the transmit beamforming vector, and receive PS ratio to maximize the sum-rate. Simulation results corroborates the importance of joint optimization.

Chapter 6

SWIPT in multiuser MIMO FD Communications Systems

6.1 SWIPT in Multiuser MIMO full-duplex systems

In this chapter, we investigate a multi-user multiple-input multiple-output full-duplex system for simultaneous wireless information and power transfer, in which a multi-antenna base station simultaneously sends wireless information and power to a set of single-antenna mobile stations using power splitters in the downlink and receives information in the uplink in full-duplex mode. In particular, we address the joint design of the PS ratio and the transmit power at the MSs, and the beamforming matrix at the BS under signal-to-interference-plus-noise ratio and harvested power constraints. Using semidefinite relaxation (SDR), we obtain the solution to the problem with imperfect channel state information of the self-interfering channels. Furthermore, we propose another suboptimal zero forcing based solution by separating the optimization of the transmit beamforming vector and the PS ratios. Numerical results are provided to evaluate the performance of the proposed beamforming designs. Under practically reasonable system settings, the proposed scheme achieves a near 1dB gain over the suboptimal ZF beamforming scheme.

6.2 System model and problem formulation

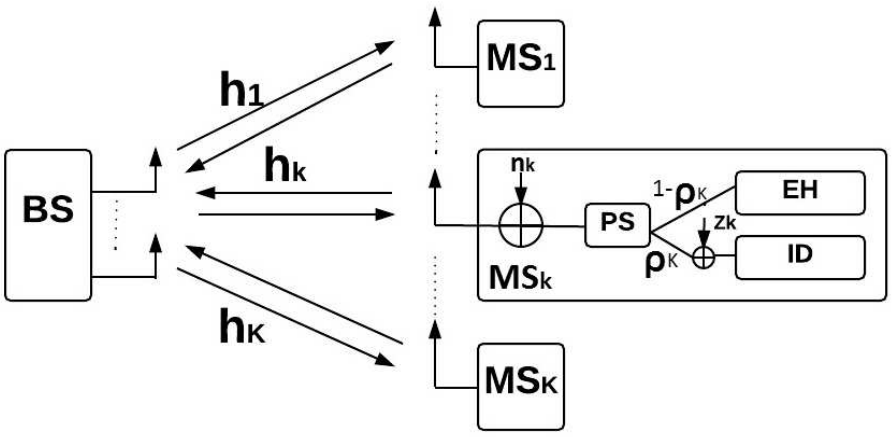

Figure 6.1: *Multiuser MIMO SWIPT FD system.*

We investigate the end-to-end transmit power minimization approach for a multi-user MIMO FD SWIPT system consisting of one BS and K MSs, denoted by $\text{MS}_1, \cdots, \text{MS}_k$, respectively, operating in FD mode as shown in Fig. 6.1. The BS simultaneously transmit wireless information and power to a set of single antenna MSs in the downlink and receives information in the uplink in full-duplex mode. We denote the number of transmit and receive antennas at the BS as N_t and N_r, and each MS uses identical pair of transmitter and receiver antennas for signal transmission and reception. In the first phase, the BS performs transmit beamforming to send information to the MSs in the downlink while in the next phase, the MSs use the harvested energy from its own reception to send feedback information to the BS in the reverse link with a transmit power $P_{\text{up,k}}$. The complex baseband transmitted signal at the BS can be expressed as

$$\mathbf{x}^{\text{BS}} = \sum_{k=1}^{K} \mathbf{v}_k s_k, \tag{6.1}$$

where $s_k \backsim CN(0,1)$ denotes the transmitted information symbol to MS_k, and $\mathbf{v}_k$ represents the corresponding transmit beamforming vector. It is assumed that s_k, $k = 1, \cdots, K$, are independent and identically distributed (i.i.d) circularly symmetric Gaussian (CSCG) random variables. We further assume quasi-static flat-fading

channel for all MSs and denote $\mathbf{h}_{\mathrm{dl},k}$ and $\mathbf{h}_{\mathrm{ul},k}$ as the conjugated complex channel vector from BS to $\mathrm{MS_k}$ and from $\mathrm{MS_k}$ to BS, respectively. The received signal at $\mathrm{MS_k}$ can be written as

$$y_k = \underbrace{\mathbf{h}_{\mathrm{dl},k}^H \mathbf{v}_k s_k}_{\text{desired signal}} + \underbrace{\sum_{j\neq k}^{K} \mathbf{h}_{\mathrm{dl},k}^H \mathbf{v}_j s_j}_{\text{interfering signal}} + \underbrace{h_{\mathrm{SI},k} m_k}_{\text{self-interference}} + n_k, \tag{6.2}$$

where m_k is the information carrying symbol of $\mathrm{MS_k}$ and $n_k \backsim CN(0,\sigma_k)$ denotes the antenna noise at the receiver of $\mathrm{MS_k}$. In this work, we assume that each $\mathrm{MS_k}$ is equipped with a PS device which coordinates the processes of information decoding and energy harvesting. In particular, we assume that the PS splits the received signal power such that a $\rho \in (0,1)$ portion of the signal power is fed to the ID and the remaining $(1-\rho)$ is fed to the EH. Accordingly, the signal split to the ID of $\mathrm{MS_k}$ can be written as

$$y_k^{\mathrm{ID}} = \sqrt{\rho_k} \left(\underbrace{\mathbf{h}_{\mathrm{dl},k}^H \mathbf{v}_k s_k}_{\text{desired signal}} + \underbrace{\sum_{j\neq k}^{K} \mathbf{h}_{\mathrm{dl},k}^H \mathbf{v}_j s_j}_{\text{interfering signal}} + \underbrace{h_{\mathrm{SI},k} m_k}_{\text{self interference}} + n_k, \right) + z_k, \tag{6.3}$$

where $z_k \backsim CN(0,\delta_k^2)$ denotes the additional processing noise introduced by the ID at $\mathrm{MS_k}$. The signal split to the EH of $\mathrm{MS_k}$ is given by

$$y_k^{\mathrm{EH}} = \sqrt{1-\rho_k} \left(\sum_{j=1}^{K} \mathbf{h}_{\mathrm{dl},j}^H \mathbf{v}_j s_j + h_{\mathrm{SI},k} m_k + n_k, \right). \tag{6.4}$$

Meanwhile, the signal received at the BS can be written as

$$\mathbf{y}^{\mathrm{BS}} = \underbrace{\sum_{k=1}^{K} \mathbf{h}_{\mathrm{ul},k} m_k}_{\text{desired signal}} + \underbrace{\sum_{j=1}^{K} \mathbf{H}_{\mathrm{SI,BS}} \mathbf{v}_j s_j}_{\text{self-interference}} + \mathbf{n}_{\mathrm{BS}}, \tag{6.5}$$

where $\mathbf{n}_{\mathrm{BS}} \backsim CN(\mathbf{0}, \sigma_{\mathrm{BS}}^2 \mathbf{I})$ is the AWGN noise vector at the BS. To decode the signal from $\mathrm{MS_k}$, the BS applies a receive beamformer $\mathbf{w}_k$ to equalise the received signal

from MS_k expressed as

$$\begin{aligned} s_k^{\mathrm{UL}} &= \mathbf{w}_k^H \mathbf{h}_{\mathrm{ul,k}} m_k + \mathbf{w}_k^H \sum_{j \neq k}^{K} \mathbf{h}_{\mathrm{ul,j}} m_j \\ &+ \mathbf{w}_k^H \sum_{j=1}^{K} \mathbf{H}_{\mathrm{SI,BS}} \mathbf{v}_j + \mathbf{w}_k^H \mathbf{n}_{\mathrm{BS}}. \end{aligned} \tag{6.6}$$

The SINR at the BS from MS_k is therefore given by

$$\gamma_k^{\mathrm{BS}} = \frac{P_{\mathrm{up},k} |\mathbf{w}_k^H \mathbf{h}_{\mathrm{ul},k}|^2}{\sum_{j \neq k}^{K} P_{\mathrm{up},j} |\mathbf{w}_k^H \mathbf{h}_{\mathrm{ul},j}|^2 + \sum_{j=1}^{K} |\mathbf{w}_k^H \mathbf{H}_{\mathrm{SI,BS}} \mathbf{v}_j|^2 + \sigma_{\mathrm{BS}}^2 \|\mathbf{w}_k\|^2}. \tag{6.7}$$

Accordingly, the SINR at the ID of MS_k is given by

$$\gamma_k^{\mathrm{MS}} = \frac{\rho_k |\mathbf{h}_{\mathrm{dl},k}^H \mathbf{v}_k|^2}{\rho_k (\sum_{j \neq k}^{K} |\mathbf{h}_{\mathrm{dl},k}^H \mathbf{v}_j|^2 + |h_{\mathrm{SI},k}|^2 P_{\mathrm{up,k}} + \sigma_k^2) + \delta_k^2}. \tag{6.8}$$

The harvested power by the EH of MS_k is given by

$$Q_k = \eta (1 - \rho_k) \left(\sum_{j=1}^{K} |\mathbf{h}_{\mathrm{dl},k}^H \mathbf{v}_j|^2 + |h_{\mathrm{SI},k}|^2 P_{\mathrm{up,k}} + \sigma_k^2 \right), \tag{6.9}$$

where η denotes the energy conversion efficiency at the EH of $\mathrm{MS_k}$ that accounts for the loss in energy transducer for converting the harvested energy to electrical energy to be stored. In practice, energy harvesting circuits are equipped at the energy harvesting receiver which are used to convert the received RF power into direct current power. The efficiency of a diode-based energy harvester is non-linear and largely depends on the input power level [71]. Hence, the conversion efficiency (η) should be included in the optimization expressions. However, for simplicity, this work assumes $\eta = 1$.

6.2.1 Modelling SI

Our aim is to minimize the end-to-end transmission power for SWIPT in a multiuser MIMO FD system while maintaining the QoS requirements for each MSs. It is worth pointing out that for the multiuser MIMO FD channel, we assume perfect

CSI for the uplink and downlink channels as this is an idealization of actual practical systems. Effectively, perfect CSI can be accomplished from fine measurements. In particular, via the transmission of dedicated training symbols at the receiver. In contrast, we assume an imperfect CSI for loop channels as a result of the fact that the distribution of self-interference channels are unknown. Thus, it becomes difficult to achieve perfect CSI for SI channels via measurements. Furthermore, SI channel measurements results obtained in [86] showed that the SI channel has a multipath nature. These multiple paths can have higher power compared to the line of sight (LOS) path. This behaviour necessitates the need of an adaptive cancellation technique whose measurement is used to cancel both the LOS path and the delayed version of the same, which is not the primary aim of this research work. However, it is a general practice to model the SI channels for simplicity as Gaussian channels [87]. Considering the fact that the residual SI cannot be eliminated completely due to the insufficient knowledge of the underlying channel, we consider a deterministic model for imperfect self-interfering channels. In particular, it is assumed that the SI channels $h_{\mathrm{SI},k}, \forall k$, and $\mathbf{H}_{\mathrm{SI,BS}}$ lie in the neighbourhood of the estimated channels $\hat{h}_{\mathrm{SI},k}, \forall k$, and $\hat{\mathbf{H}}_{\mathrm{SI,BS}}$, respectively, that are available at the nodes. Thus, the actual channels due to imperfect channel estimate can be modelled as

$$h_{\mathrm{SI},k} = \hat{h}_{\mathrm{SI},k} + \triangle h_{\mathrm{SI},k}, \tag{6.10a}$$

$$\mathbf{H}_{\mathrm{SI,BS}} = \hat{\mathbf{H}}_{\mathrm{SI,BS}} + \triangle \mathbf{H}_{\mathrm{SI,BS}}, \tag{6.10b}$$

where $\triangle h_{\mathrm{SI},k}$ and $\triangle \mathbf{H}_{\mathrm{SI,BS}}$ represent the channel uncertainties which are assumed to be bounded as

$$|\triangle h_{\mathrm{SI},k}| = |h_{\mathrm{SI},k} - \hat{h}_{\mathrm{SI},k}| \leq \varepsilon_1, \tag{6.11a}$$

$$\|\triangle \mathbf{H}_{\mathrm{SI,BS}}\| = \|\mathbf{H}_{\mathrm{SI,BS}} - \hat{\mathbf{H}}_{\mathrm{SI,BS}}\| \leq \varepsilon_2, \tag{6.11b}$$

for some $\varepsilon_1, \varepsilon_2 \geq 0$. The bounding values $\{\varepsilon_k\}$ depend on the accuracy of the CSI estimates. To efficiently define the worst-case SI level, we modify (6.10a) and (6.10b) using the triangle inequality and the Cauchy-Schwarz inequality, respectively [72].

It follows from (6.10a) and (6.10b) that

$$\begin{aligned} |h_{\mathrm{SI},k}|^2 &= |(\hat{h}_{\mathrm{SI},k} + \triangle h_{\mathrm{SI},k})|^2 \leq (|\hat{h}_{\mathrm{SI},k}| + |\triangle h_{\mathrm{SI},k}|)^2 \\ &\leq |\hat{h}_{\mathrm{SI},k}|^2 + \varepsilon_1^2 + 2\varepsilon_1 |\hat{h}_{\mathrm{SI},k}|, \qquad (6.12a) \\ \|\mathbf{H}_{\mathrm{SI,BS}}\mathbf{v}_k\|^2 &\leq \|\mathbf{H}_{\mathrm{SI,BS}}\|^2 \|\mathbf{v}_k\|^2 \\ &= \|\hat{\mathbf{H}}_{\mathrm{SI,BS}} + \triangle \mathbf{H}_{\mathrm{SI,BS}}\|^2 \|\mathbf{v}_k\|^2 \\ &\leq (\|\hat{\mathbf{H}}_{\mathrm{SI,BS}}\| + \|\triangle \mathbf{H}_{\mathrm{SI,BS}}\|)^2 \|\mathbf{v}_k\|^2 \\ &\leq (\|\hat{\mathbf{H}}_{\mathrm{SI,BS}}\|^2 + \varepsilon_2^2 + 2\|\hat{\mathbf{H}}_{\mathrm{SI,BS}}\|\varepsilon_2) \|\mathbf{v}_k\|^2. \end{aligned}$$

Note that ε_k is the minimal knowledge of the upper-bound of the channel error which is sufficient enough to describe the error in the absence of statistical information about the error. As a result, from (6.12a) and (6.12b), we obtain

$$\max_{|\triangle h_{\mathrm{SI}}| \leq \varepsilon_1} |h_{\mathrm{SI},k}|^2 \leq |\hat{h}_{\mathrm{SI},k}|^2 + \varepsilon_1^2 + 2\varepsilon_1 |\hat{h}_{\mathrm{SI},k}|, \qquad (6.13a)$$

$$\max_{\|\triangle \mathbf{H}_{\mathrm{SI,BS}}\mathbf{v}_k\| \leq \varepsilon_2} \|\mathbf{H}_{\mathrm{SI,BS}}\mathbf{v}_k\|^2 \leq (\|\hat{\mathbf{H}}_{\mathrm{SI,BS}}\|^2 + \varepsilon_2^2 + 2\|\hat{\mathbf{H}}_{\mathrm{SI,BS}}\|\varepsilon_2) \|\mathbf{v}_k\|^2. \qquad (6.13b)$$

On the other hand, it holds that

$$\begin{aligned} |(\hat{h}_{\mathrm{SI},k} + \triangle h_{\mathrm{SI},k})|^2 &\geq (|\hat{h}_{\mathrm{SI},k}| - |\triangle h_{\mathrm{SI},k}|)^2 \\ &\geq |\hat{h}_{\mathrm{SI},k}|^2 + \varepsilon_1^2 - 2|\hat{h}_{\mathrm{SI},k}|^2 \varepsilon_1. \qquad (6.14) \end{aligned}$$

Here, we assume that $|\hat{h}_{\mathrm{SI}}| \geq |\triangle h_{\mathrm{SI}}|$ which essentially means that the error $|\triangle h_{\mathrm{SI}}|$ is sufficiently small in comparison to the estimate or the estimate is meaningful. Accordingly,

$$\min_{|\triangle h_{\mathrm{SI},k}| \leq \varepsilon_1} |h_{\mathrm{SI},k}|^2 \geq |\hat{h}_{\mathrm{SI},k}|^2 + \varepsilon_1^2 - 2|\hat{h}_{\mathrm{SI},k}|\varepsilon_1. \qquad (6.15)$$

6.2.2 Problem formulation

We assume that each $\mathrm{MS_k}$ is characterized with strict QoS constraints. The QoS constraints require that the SINR for the downlink channel should be higher than

a given threshold denoted by γ_k^{DL}, at all times in order to ensure a continuous information transfer. Similarly, each $\mathrm{MS_k}$ also requires that its harvested power must be above certain useful level specified by a prescribed threshold denoted by $\bar{Q}_k$ in order to maintain its receiver's operation. Meanwhile, for the uplink channel, each $\mathrm{MS_k}$ is expected to send feedback to the BS, thus a strict QoS is required such that the SINR of the uplink channel for each $\mathrm{MS_k}$ is expected to be no less than a given threshold denoted γ_k^{UL}. It is worth noting that FD brings the SI to the BS and the $\mathrm{MS_k}$, and thus both the BS and the $\mathrm{MS_k}$ may not always use their maximum transmit power as it increases the level of RSI. The BS and $\mathrm{MS_k}$ must therefore carefully choose their transmit power. Considering the above constraints, our objective is to minimise the end-to-end transmit power for the multiser MIMO FD SWIPT system by jointly designing the transmit beamforming vector ($\mathbf{v}_k$) at the BS, the transmit power $P_{\mathrm{up,k}}$ and the receiver PS ratio, (ρ_k), at the $\mathrm{MS_k}$. Hence, the problem can be formulated as

$$
\begin{aligned}
&\min_{\mathbf{v}_k,\mathbf{w}_k,P_{\mathrm{up},k},\rho_k} \sum_{k=1}^{K} (\|\mathbf{v}_k\|^2 + P_{\mathrm{up},k}) \\
&\text{s.t.} \\
&\min_{\|\triangle \mathbf{H}_{\mathrm{SI,BS}}\| \le \varepsilon_2} \frac{P_{\mathrm{up},k} |\mathbf{w}_k^H \mathbf{h}_{\mathrm{ul},k}|^2}{\sum_{j\neq k}^{K} P_{\mathrm{up},j} |\mathbf{w}_k^H \mathbf{h}_{\mathrm{ul},j}|^2 + \sum_{j=1}^{K} \|\mathbf{H}_{\mathrm{SI,BS}} \mathbf{v}_j\|^2 \|\mathbf{w}_k\|^2 + \|\mathbf{w}_k\|^2} \ge \gamma_k^{\mathrm{UL}}, \quad \forall k, \\
&\min_{|\triangle h_{\mathrm{SI},k}| \le \varepsilon_1} \frac{\rho_k |\mathbf{h}_{\mathrm{dl},k}^H \mathbf{v}_k|^2}{\rho_k (\sum_{j\neq k} |\mathbf{h}_{\mathrm{dl},k}^H \mathbf{v}_j|^2 + |h_{\mathrm{SI},k}|^2 P_{\mathrm{up},k} + \sigma_k^2) + \delta_k^2} \ge \gamma_k^{\mathrm{DL}}, \forall k, \\
&\min_{|\triangle h_{\mathrm{SI},k}| \le \varepsilon_1} (1-\rho_k) \left(\sum_{j=1}^{K} |\mathbf{h}_k^H \mathbf{v}_j|^2 + |h_{\mathrm{SI},k}|^2 P_{\mathrm{up},k} + \sigma_k^2 \right) \ge \bar{Q}_k, \forall k, \\
&0 < P_{\mathrm{up},k} \le \min(\bar{Q}_k, P_{\max}), \quad 0 < \|\mathbf{v}_k\|^2 \le P_{\max}, \quad \forall k, \\
&0 < \rho_k < 1, \forall k.
\end{aligned} \tag{6.16}
$$

Substituting the result obtained in (6.13a), (6.13b) and (6.15) into (6.16), the optimization problem in (6.16) can now be upper-bounded as given in (6.17)

$$
\begin{aligned}
&\min_{\mathbf{v}_k,\mathbf{w}_k,P_{\mathrm{up},k},\rho_k} \sum_{k=1}^{K} (\|\mathbf{v}_k\|^2 + P_{\mathrm{up},k}) \\
&\text{s.t.} \\
&\frac{\sum_{k=1}^{K} |\mathbf{w}_k^H \mathbf{h}_{\mathrm{ul},k}|^2 P_{\mathrm{up},k}}{\sum_{j\neq k}^{K} P_{\mathrm{up},j} |\mathbf{w}_k^H \mathbf{h}_{\mathrm{ul},j}|^2 + (\|\hat{\mathbf{H}}_{\mathrm{SI,BS}}\|^2 + \varepsilon_2^2 + 2\|\hat{\mathbf{H}}_{\mathrm{SI,BS}}\|^2 \varepsilon_2) K P_{\max} \|\mathbf{w}_k\|^2 + \|\mathbf{w}_k\|^2} \geq \gamma_k^{\mathrm{UL}}, \quad \forall k, \\
&\frac{\rho_k |\mathbf{h}_{\mathrm{dl},k}^H \mathbf{v}_k|^2}{\rho_k (\sum_{j\neq k} |\mathbf{h}_{\mathrm{dl},k}^H \mathbf{v}_j|^2 + (|\hat{h}_{\mathrm{SI},k}|^2 + \varepsilon_1^2 + 2\varepsilon_1 |\hat{h}_{\mathrm{SI},k}|^2) P_{\max} + \sigma_k^2) + \delta_k^2} \geq \gamma_k^{\mathrm{DL}}, \forall k, \\
&(1-\rho_k) \left(\sum_{j=1}^{K} |\mathbf{h}_k^H \mathbf{v}_j|^2 + (|\hat{h}_{\mathrm{SI},k}|^2 + \varepsilon_1^2 - 2|\hat{h}_{\mathrm{SI},k}|^2 \varepsilon_1) P_{\max} + \sigma_k^2 \right) \geq \bar{Q}_k, \forall k, \\
&0 < P_{\mathrm{up},k} \leq \min(\bar{Q}_k, P_{\max}), \quad 0 < \|\mathbf{v}_k\|^2 \leq P_{\max}, \quad \forall_k, \\
&0 < \rho_k < 1, \quad \forall k.
\end{aligned} \tag{6.17}
$$

Note that the upper bound of the SI at the BS and MS_k is obtained when the source nodes transmits at maximum available power, i.e., when $P_{\mathrm{up},k} = \|\mathbf{v}_k\|^2 = P_{\max}$ [88]. As such, we denote the upper-bound of the SI power at the BS and MS_k as $\bar{E}$ and $\bar{G}$, respectively. Therefore, (6.17) is rewritten as

$$
\begin{aligned}
&\min_{\mathbf{v}_k,\mathbf{w}_k,P_{\mathrm{up},k},\rho_k} \sum_{k=1}^{K} (\|\mathbf{v}_k\|^2 + P_{\mathrm{up},k}) \\
&\text{s.t.} \\
&\frac{P_{\mathrm{up},k} |\mathbf{w}_k^H \mathbf{h}_{\mathrm{ul},k}|^2}{\sum_{j\neq k}^{K} P_{\mathrm{up},j} |\mathbf{w}_k^H \mathbf{h}_{\mathrm{ul},j}|^2 + \bar{E} \|\mathbf{w}_k\|^2 + \|\mathbf{w}_k\|^2} \geq \gamma_k^{\mathrm{UL}}, \quad \forall k, \\
&\frac{\rho_k |\mathbf{h}_{\mathrm{dl},k}^H \mathbf{v}_k|^2}{\rho_k (\sum_{j\neq k} |\mathbf{h}_{\mathrm{dl},k}^H \mathbf{v}_j|^2 + \bar{G}_k + \sigma_k^2) + \delta_k^2} \geq \gamma_k^{\mathrm{DL}}, \forall k, \\
&(1-\rho_k) \left(\sum_{j=1}^{K} |\mathbf{h}_k^H \mathbf{v}_j|^2 + \tilde{G}_k + \sigma_k^2 \right) \geq \bar{Q}_k, \forall k, \\
&0 < P_{\mathrm{up},k} \leq \min(\bar{Q}_k, P_{\max}), \;\; 0 < \|\mathbf{v}_k\|^2 \leq P_{\max}, \; \forall k, \\
&0 < \rho_k < 1,
\end{aligned} \tag{6.18}
$$

where $\bar{E} \triangleq (\|\hat{\mathbf{H}}_{\mathrm{SI,BS}}\|^2 + \varepsilon_2^2 + 2\|\hat{\mathbf{H}}_{\mathrm{SI,BS}}\|^2 \varepsilon_2) K P_{\max}$, $\bar{G}_k \triangleq (|\hat{h}_{\mathrm{SI},k}|^2 + \varepsilon_1^2 + 2\varepsilon_1 |\hat{h}_{\mathrm{SI},k}|^2) P_{\max}$ and $\tilde{G}_k \triangleq (|\hat{h}_{\mathrm{SI},k}|^2 + \varepsilon_1^2 - 2|\hat{h}_{\mathrm{SI},k}|^2 \varepsilon_1) P_{\max}$ is the maximum SI power

associated with the energy harvesting constraint at MS_k.

We investigate the general case where all MSs are characterised as having a non-zero SINR and harvested power targets, i.e., γ_k^{DL}, γ_k^{UL}, $\bar{Q}_k, > 0$ $\forall k$. As such, the receive PS ratio at all MSs should satisfy $0 < \rho_k < 1$, as given by the PS ratio constraint. It is easy to see that formulation (6.18) is non-convex and very challenging to solve. Thus, we solve this problem in a two step process. Firstly, we observe that the QoS uplink constraint (γ_k^{UL}) does not have the PS coefficient and this is because in our model, the BS is not designed to harvest energy. Hence, we can decompose problem (6.18) into two sub-problems. The resulting sub-problems can be written as

$$\begin{aligned}
&\min_{\mathbf{w}_k, P_{\text{up},k}} \sum_{k=1}^{K} P_{\text{up},k} \\
&\text{s.t.} \\
&\frac{P_{\text{up},k} |\mathbf{w}_k^H \mathbf{h}_{\text{ul},k}|^2}{\sum_{j\neq k}^{K} P_{\text{up},j} |\mathbf{w}_k^H \mathbf{h}_{\text{ul},j}|^2 + \bar{E}\|\mathbf{w}_k\|^2 + \|\mathbf{w}_k\|^2} \geq \gamma_k^{\text{UL}}, \quad \forall k, \\
&0 < P_{\text{up},k} \leq \min(\bar{Q}_k, P_{\max}), \quad \forall k,
\end{aligned} \tag{6.19}$$

and

$$\begin{aligned}
&\min_{\mathbf{v}_k, \rho_k} \sum_{k=1}^{K} \|\mathbf{v}_k\|^2 \\
&\text{s.t.} \\
&\frac{\rho_k |\mathbf{h}_{\text{dl},k}^H \mathbf{v}_k|^2}{\rho_k (\sum_{j\neq k} |\mathbf{h}_{\text{dl},k}^H \mathbf{v}_j|^2 + \bar{G}_k + \sigma_k^2) + \delta_k^2} \geq \gamma_k^{\text{DL}}, \forall k, \\
&(1-\rho_k) \left(\sum_{j=1}^{K} |\mathbf{h}_k^H \mathbf{v}_j|^2 + \tilde{G}_k + \sigma_k^2 \right) \geq \bar{Q}_k, \forall k, \\
&0 < \|\mathbf{v}_k\|^2 \leq P_{\max}, \quad \forall k, \\
&0 < \rho_k < 1, \forall k.
\end{aligned} \tag{6.20}$$

Note that (6.19) corresponds to optimizing the variables involved in the uplink, and (6.20) involves those in the downlink. Next, we apply SDR to the relevant sub-problems as discussed below.

6.3 Solutions

In this section, we will focus on how to solve problem (6.19) and (6.20) optimally. Let us proceed first by solving problem (6.19) to determine the optimal value $P^*_{\text{up,k}}$ and $\mathbf{w}^*_k$. For given $\mathbf{w}_k$, the optimal $P^*_{\text{up},k}$ can be determined. Problem (6.19) is thus reformulated as

$$\min_{P_{\text{up},k}} \sum_{k=1}^{K} P_{\text{up},k} \tag{6.21a}$$

s.t.

$$\frac{P_{\text{up},k}|\mathbf{w}_k^H \mathbf{h}_{\text{ul},k}|^2}{\sum_{j\neq k}^{K} P_{\text{up},j}|\mathbf{w}_k^H \mathbf{h}_{\text{ul},j}|^2 + \bar{E}\|\mathbf{w}_k\|^2 + \|\mathbf{w}_k\|^2} \geq \gamma_k^{\text{UL}}, \tag{6.21b}$$

$$0 < P_{\text{up},k} \leq \min(\bar{Q}_k, P_{\max}), \quad \forall k. \tag{6.21c}$$

The optimal $P^*_{\text{up},k}$ is the minimum $P_{\text{up},k}$ which satisfies (6.21b) to equality. As a result, the optimal $P_{\text{up},k}$ is given by

$$P^*_{\text{up}} = \frac{\gamma_k^{\text{UL}}(\bar{E}\|\mathbf{w}_k\|^2 + \|\mathbf{w}_k\|^2)}{|\mathbf{w}_k^H \mathbf{h}_{\text{ul},k}|^2 - \gamma_k^{\text{UL}}(\sum_{j\neq k}^{K} |\mathbf{w}_k^H \mathbf{h}_{\text{ul},j}|^2)}. \tag{6.22}$$

The optimal receiver can be defined as the Wiener filter [88]

$$\mathbf{w}^*_k = \left(\sum_{j=1}^{K} P_{\text{up},j} \mathbf{h}_{\text{ul},j} \mathbf{h}_{\text{ul},j}^H + \left[\sigma_j^2 + \sum_{j=1}^{K} \|\mathbf{v}_j\|^2 \right] \mathbf{I} \right)^{-1} \times \sqrt{P_{\text{up},j}} \mathbf{h}_{\text{ul},j}. \tag{6.23}$$

Secondly, we investigate problem (6.20) to determine the optimal value of the receive PS ratio and the transmit beamforming vector at the BS. It is worth pointing out that the feasibility of problem (6.20) has been proved in [89].

Accordingly, by applying semidefinite programming (SDP) technique to solve problem (6.20), we define $\mathbf{Z}_k = \mathbf{v}_k \mathbf{v}_k^H, \forall k$. Thus, it follows that $\text{Rank}(\mathbf{Z}_k) \leq 1, \forall k$. If we ignore the rank-one constraint for all $\mathbf{Z}_k$'s, the SDR of problem (6.20) can be written

as

$$\begin{aligned}
&\min_{\mathbf{Z}_k,\rho_k} \sum_{k=1}^{K} \mathrm{Tr}(\mathbf{Z}_k) \\
&\text{s.t.} \\
&\frac{\rho_k \mathbf{h}_{\mathrm{dl},k}^H \mathbf{Z}_k \mathbf{h}_{\mathrm{dl},k}}{\rho_k(\sum_{j\neq k} \mathbf{h}_{\mathrm{dl},k}^H \mathbf{Z}_j \mathbf{h}_k + \bar{G}_k + \sigma_k^2) + \delta_k^2} \geq \gamma_k^{\mathrm{DL}}, \forall k, \\
&(1-\rho_k)\left(\sum_{j=1}^{K} \mathbf{h}_{\mathrm{dl},k}^H \mathbf{Z}_j \mathbf{h}_{\mathrm{dl},k} + \tilde{G}_k + \sigma_k^2\right) \geq \bar{Q}_k, \ \forall k, \\
&0 < \rho_k < 1, \forall k \\
&\mathbf{Z}_k \succeq 0, \quad \forall k.
\end{aligned} \tag{6.24}$$

Problem (6.24) is non-convex since both the SINR and harvested power constraints involve coupled $\mathbf{Z}_k$ and ρ_k's. Nonetheless, problem (6.24) can be reformulated as the following problem:

$$\begin{aligned}
&\min_{\{\mathbf{Z}_k,\rho_k\}} \sum_{k=1}^{K} \mathrm{Tr}(\mathbf{Z}_k) \\
&\frac{1}{\gamma_k^{\mathrm{DL}}} \mathbf{h}_{\mathrm{dl},k}^H \mathbf{Z}_k \mathbf{h}_{\mathrm{dl},k} - \sum_{j\neq k} \mathbf{h}_{\mathrm{dl},k}^H \mathbf{Z}_j \mathbf{h}_{\mathrm{dl},k} + \bar{G}_k \geq \sigma_k^2 + \frac{\delta_k^2}{\rho_k}, \forall k, \\
&\sum_{j=1}^{K} \mathbf{h}_{\mathrm{dl},k}^H \mathbf{Z}_j \mathbf{h}_{\mathrm{dl},k} + \tilde{G}_k \geq \frac{\bar{Q}_k}{(1-\rho_k)} - \sigma_k^2, \forall k, \\
&0 < \rho_k < 1, \forall k, \\
&\mathbf{Z}_k \succeq 0, \quad \forall k.
\end{aligned} \tag{6.25}$$

As shown in (6.25), both $\frac{1}{\rho_k}$ and $\frac{1}{1-\rho_k}$ are convex functions over ρ_k, thus problem (6.25) is convex and can be solved using disciplined convex programming. To proceed, let $\mathbf{Z}_k^*$ denote the optimal solution to problem (6.25).

Accordingly, it follows that if $\mathbf{Z}_k^*$ satisfies the $\mathrm{Rank}(\mathbf{Z}_k^*) = 1, \forall k$, then the optimal beamforming solution $\mathbf{v}_k^*$ to problem (6.20) can be obtained from the eigenvalue decomposition of $\mathbf{Z}_k^*$, $k = 1, \ldots, K$ and the optimal PS solution of problem (6.20) is given by the associated ρ_k^*'s. However, in the case that there exists any k such

that $\text{Rank}(\mathbf{Z}_k^*) > 1$, then in general the solution $\mathbf{Z}_k^*$ and ρ_k^* of problem (6.25) is not always optimal for problem (6.20). We show in the appendix that it is indeed true that for problem (6.20), the solution satisfies $\text{Rank}(\mathbf{Z}_k^*) = 1, \forall k$.

Proposition 1. *Given $\gamma_k^{\text{DL}} > 0$ and $\bar{Q}_k > 0, \forall k$, for problem (6.25), we have*
1) $\{\mathbf{Z}_k^*\}$ and $\{\rho_k\}$ satisfy the first two sets of constraints of (6.25) with equality;
2) $\{\mathbf{Z}_k^*\}$ satisfies $\text{Rank}(\mathbf{Z}_k^*) = 1$, $\forall k$.

Proof. Please refer to Appendix A. □

6.4 Suboptimal Solution

To effectively make meaningful comparison based on the performance analysis for SWIPT in a multiuser MIMO FD system, in this section, we investigate a suboptimal solution based on ZF by jointly designing the beamforming vector and PS ratios.

6.4.1 ZF Beamforming

To simplify the beamforming design, we add the ZF constraint. As such, by restricting $\mathbf{v}_k$ in problem (6.20) to satisfy $\mathbf{h}_{\text{dl},i}^H \mathbf{v}_k = 0, \forall i \neq k$, ZF can be used to eliminate multiuser interference. Applying the ZF transmit beamforming constraint, problem (6.20) can be reformulated as the following problem:

$$
\begin{aligned}
&\min_{\{\mathbf{v}_k, \rho_k\}} \sum_{k=1}^{K} \|\mathbf{v}_k\|^2 \\
&\text{s.t.} \\
&\frac{\rho_k |\mathbf{h}_{\text{dl},k}^H \mathbf{v}_k|^2}{\rho_k(\bar{G}_k + \sigma_k^2) + \delta_k^2} \geq \gamma_k^{\text{DL}}, \forall k, \\
&(1-\rho_k)\left(|\mathbf{h}_{\text{dl},k}^H \mathbf{v}_k|^2 + \tilde{G}_k + \sigma_k^2\right) \geq \bar{Q}_k, \forall k, \\
&\mathbf{H}_{\text{dl},k}^H \mathbf{v}_k = 0, \quad \|\mathbf{v}_k\|^2 \leq P_{\max}, \quad \forall k, \\
&0 < \rho_k < 1, \forall k,
\end{aligned} \tag{6.26}
$$

where $\mathbf{H}_{\mathrm{dl},k} \triangleq [\mathbf{h}_{\mathrm{dl},1} \cdots \mathbf{h}_{\mathrm{dl},k-1}, \mathbf{h}_{dl,k+1} \cdots \mathbf{h}_{\mathrm{dl},K}] \in \mathbb{C}^{N_t \times (K-1)}$. Clearly, problem (6.17) must be visible if $N_t \geq K$ due to the ZF transmit beamforming [89]. Proposition 2 gives the optimal solution to problem (6.26).

Proposition 2. *From the result obtained in [89], let* $\mathbf{U}_k$ *denote the orthogonal basis of the null space of* $\mathbf{H}_{\mathrm{dl},k}^H, k = 1, \ldots, K$.

The optimal solution to problem (6.26) is thus given by

$$\tilde{\rho}_k^* = \frac{+\beta_k \pm \sqrt{\beta_k^2 + 4\alpha_k C_k}}{2\alpha_k} \quad \forall_k, \tag{6.27}$$

$$\tilde{\mathbf{v}}_k^* = \sqrt{\gamma_k^{\mathrm{DL}} \left(\bar{G}_k + \sigma_k^2 + \frac{\delta_k^2}{\rho_k} \right)} \frac{\mathbf{U}_k \mathbf{U}_k^H \mathbf{h}_{\mathrm{dl},k}}{\| \mathbf{U}_k \mathbf{U}_k^H \mathbf{h}_{\mathrm{dl},k} \|^2} \quad \forall_k. \tag{6.28}$$

Proof. Please refer to Appendix B. □

6.5 Numerical examples

Here, we investigate the performance of the proposed joint beamforming and received power splitting (JBPS) optimization design for SWIPT in Multiuser MIMO FD systems through computer simulations. We simulated a flat Rayleigh fading environment in which the channel fading coefficients are characterized as complex Gaussian numbers with zero mean and are i.i.d. and we assume there are $K = 2$ MSs and all MSs have the same set of parameters i.e., $\sigma_k^2 = \sigma^2$, $\delta_k^2 = \delta^2$, $\bar{Q}_k = Q$, and $\gamma_k^{\mathrm{DL}} = \gamma^{\mathrm{DL}}$. We also assume that 60% of the SI power has been cancelled using existing SIC techniques [29]. All simulations are averaged over 500 independent channel realizations.

In Fig. 6.2, we investigate the minimum end-to-end transmission power for SWIPT in multiuser MIMO FD systems versus the SINR target for all MSs, γ^{UL}, for fixed harvested power threshold $Q = 20$ dBm. It is assumed that the BS is equipped with $N_t = 2$ transmit antennas. Fig. 6.2 shows the performance comparison in terms of end-to-end sum transmit power, between the optimal JBPS solution to (6.18) and the suboptimal solution based on ZF beamforming. As can be observed, the

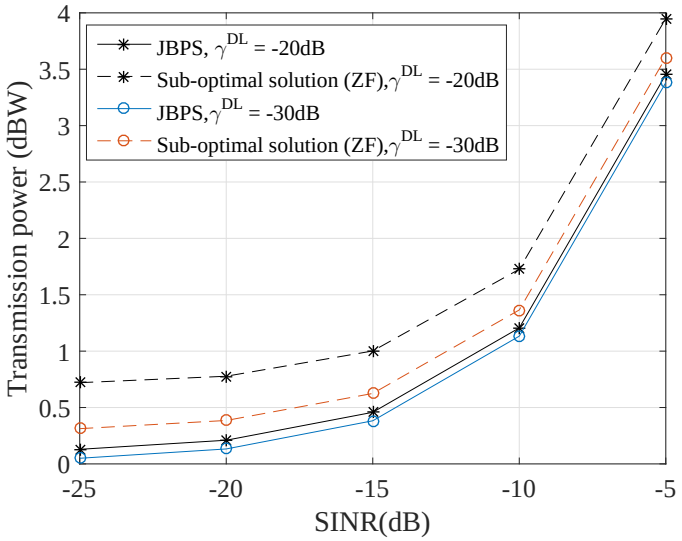

Figure 6.2: *Transmission power versus SINR,* γ^{UL}.

minimum end-to-end sum transmit power rises with the increase in γ^{UL}. However, for different values of γ^{DL}, the optimal JBPS scheme outperforms the optimization scheme based on ZF beamforming. For example, at $\gamma^{\mathrm{UL}} = -20$dB, the optimal JBPS scheme achieves a near 1dB gain over the suboptimal ZF beamforming scheme. It is also observed that for both cases of $\gamma^{\mathrm{DL}} = -20$dB and $\gamma^{\mathrm{DL}} = -30$dB, the minimum end-to end-transmission power is achieved by optimal JBPS solution for all values of γ^{UL}. Thus, with an increase in SINR uplink threshold, γ^{UL}, the optimal JBPS scheme achieves a transmit power gain over the suboptimal ZF beamforming scheme.

In Fig. 6.3, we study the impact of the number of transmit antennas at the BS, N_t, on the minimum end-to-end transmission power for the proposed solutions for fixed harvested power threshold, $Q = 20$dBm. As can be observed, the minimum end-to-end sum transmit power decreases with the increase in the number of the transmit antennas at the BS. However, the optimal JBPS scheme outperforms the optimization scheme based on ZF beamforming. For example, for $N_t = 2$, $\gamma^{\mathrm{DL}} = -20$dB and $\gamma^{\mathrm{UL}} = -20$dB, the optimal JBPS achieves 1dB gain over the suboptimal ZF beamforming scheme. Thus, we can conclude that more transmit antennas at the BS which adopts beamforming allow it to focus more power to MS_k.

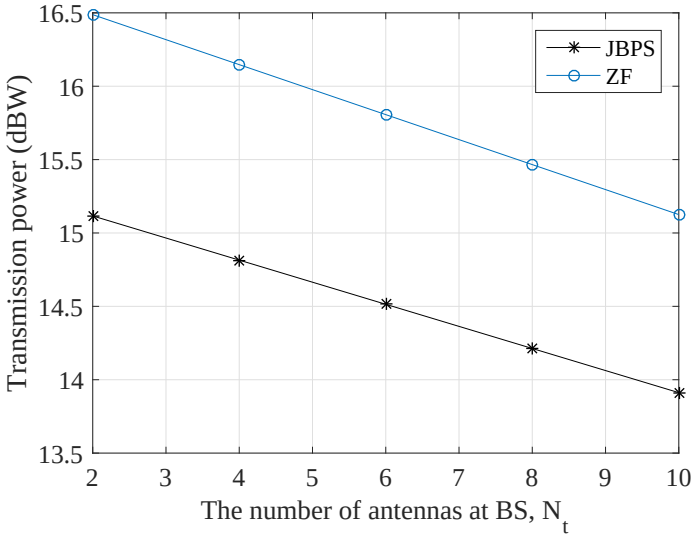

Figure 6.3: *Transmission power versus number of transmit antenna at BS, N_t.*

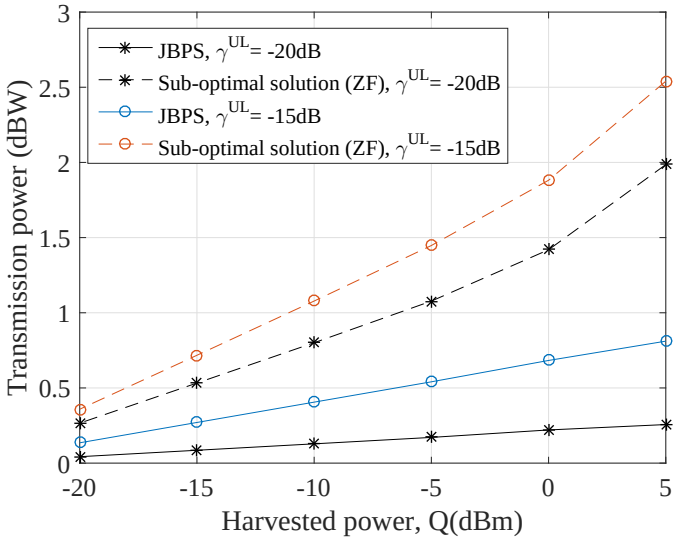

Figure 6.4: *Transmission power versus harvested energy.*

In Fig. 6.4, we illustrate the minimum transmission power achieved by JBPS and ZF for a downlink SINR, $\gamma^{\mathrm{DL}} = -20$dB, for different threshold of the harvested power. As observed in Fig. 6.4, the optimal JBPS schemes achieves the minimum transmission power for all values of the harvested power threshold. Also, the increased harvested energy threshold demands more transmit power. We also see that for increasing values of the harvested power threshold, JBPS achieves an increasing transmit power gain over the ZF scheme.

6.6 Conclusion

In this chapter, the joint transmit beamforming and receive PS design for SWIPT in a multiuser MIMO FD system is investigated. The end-to-end sum transmit power has been minimized subject to the given SINR and harvested power constraints for each MSs by jointly optimising the transmit beamforming vector at the BS, the PS ratio and the transmit power at the MSs. A suboptimal scheme based on ZF was also presented. We showed through simulation results that the proposed optimal scheme achieves a transmit power gain over the suboptimal ZF scheme.

Chapter 7

Secure FD SWIPT systems

7.1 Secure Full-duplex Two-way Relaying for SWIPT

This chapter studies bi-directional secure information exchange in a SWIPT system enabled by a FD MIMO AF relay. The AF relay injects artificial noise (AN) in order to confuse the eavesdropper. Specifically, we assume a zeroforcing solution constraint to cancel the RSI. Thus, we address the optimal joint design of the ZF matrix and the AN covariance matrix at the relay node as well as the transmit power at the sources. We propose an alternating algorithm based on SDP technique and one-dimensional searching to achieve the optimal solution. Simulation results are provided to demonstrate the effectiveness of the proposed algorithm.

Recently, the possibility of the simultaneous transfer of wireless information and power has attracted an upsurge of interest from industrial and academic communities [5, 87, 90]. On the other hand, bi-directional wireless communications exploiting full-duplex technology has also been demonstrated possible [29], [91]- [94], despite the tricky issue of SI. Combining FD bi-directional communications with SWIPT is hence a timely problem, and deserves further investigation.
On the other hand, wireless channels are exposed to security threats. Physical-layer (PHY) security is an attractive means of securing communications at the PHY layer complementing the high-layer encryption and decryption. To achieve security at

the PHY layer, it is often required that the legitimate users have better reception quality than potential eavesdroppers. As a result, AN is intentionally used to jam the eavesdropper's reception. Cooperative jamming has also been considered to improve secrecy rate performance [95].

Of particular relevance to this work, secrecy in FD systems has been studied in [96–98]. In [96], the weighted sum of downlink and uplink secrecy rates was maximized by jointly optimizing the information covariance matrix, AN covariance matrix, and the receiver vector. In [97], optimal and suboptimal FD secure beamforming designs for MISO two-way communications were studied. Authors in [98], studied a novel multi-antenna wireless powered communication system and proposed a partial Lagrange dual method and a two-stage optimization method that jointly optimizes the energy and information beamforming vectors under the transmit power and energy source constraints.

In contrast to the existing works, this thesis investigates the joint optimization of the transmit power at the sources, the AN covariance and two-way relay beamforming matrix to maximize the secrecy sum-rate for SWIPT with a FD MIMO AF relay employing power splitter. Specifically, the total transmit power is minimized while guaranteeing the end-to-end SINR at the two legitimate users as well as the eavesdropper and the energy harvesting constraint at the relay.

7.2 System Model

This chapter considers SWIPT in a three-node MIMO relay network with sources $\mathsf{S_A}$ and $\mathsf{S_B}$, consisting of one transmit and receive antenna for information transmission and reception, respectively, exchanging confidential information with the aid of an AF relay R, in the presence of a single antenna eavesdropper E, capable of wiretapping the information exchange. In our model, we assume that: i) $\mathsf{S_A}$, $\mathsf{S_B}$ and R all operate in FD mode, ii) there is no direct link between $\mathsf{S_A}$ and $\mathsf{S_B}$, thus information exchange between the source nodes must be done via R, and iii) the source nodes are not aware of any eavesdropper thus, no direct link exist between

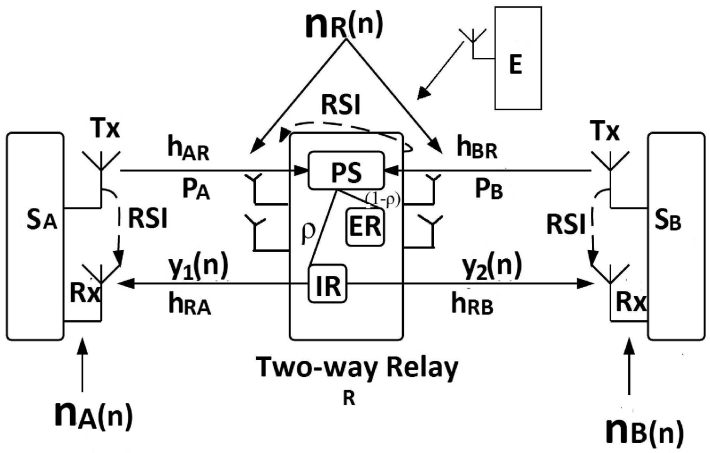

Figure 7.1: *The model of the two-way full-duplex SWIPT system with a friendly jammer.*

the source nodes and the eavesdropper [99]. The relay however, is aware of the eavesdropper. As a result, the relay injects AN signals to confuse the eavesdropper. Specifically, we consider that the FD AF relay receives confidential information from $\mathsf{S_A}$ and $\mathsf{S_B}$ in the first phase. In the next phase, R amplifies and forwards the processed information to both sources with the AN signal being superimposed with the received signal to jam the eavesdropper [99]. The harvested energy at the relay is used to complete the bi-directional information exchange between the source nodes. Using the transmit power P_A and P_B, respectively, sources $\mathsf{S_A}$ and $\mathsf{S_B}$ transmit their confidential messages simultaneously to R. On the other hand, relay R employs linear processing with amplification matrix $\mathbf{W}$ to process the received signal and broadcasts the processed signal to the nodes with harvested power Q.

The number of transmit and receive antennas at R are represented as M_T and M_R, respectively. Furthermore, we denote $\mathbf{h}_{XR} \in \mathbb{C}^{M_R \times 1}$ and $\mathbf{h}_{RX} \in \mathbb{C}^{M_T \times 1}$ to, respectively, represent the directional channel vectors between the source node X's $\in (A, B)$ transmit antenna to R's receive antennas, and that between R's transmit antenna(s) to the node X's receiver antenna. Accordingly, we use $\mathbf{h}_{RE}$ to denote the channel between E and R.

To achieve FD communication, SI must be significantly suppressed, as total cancellation is not possible as a result of imperfect channel estimation [87]. Thus, we

adopt the use of existing SI cancellation mechanisms (e.g., antenna isolation, digital and analog cancellation, etc.), to reduce the effect of SI. For convenience, we denote h_{AA}, h_{BB}, and $\mathbf{H}_{RR} \in \mathbb{C}^{M_R \times M_T}$ as the RSI channels at the respective nodes. Also, the RSI channel is represented as a Gaussian distribution random variable with zero mean and variance σ_X^2, for $\mathsf{X} \in \{A, B, R\}$ [87]. Furthermore, the relay, assumed to be equipped with a PS device, coordinates information decoding and energy harvesting. Specifically, the relay splits the received signal power such that a $\rho \in (0,1)$ portion of the received signal power is fed to the IR and the remaining $(1-\rho)$ portion of the power is fed to the ER at the relay.

7.3 Signal Model

Consider a system with only one intermediate relay and we assume that no direct link exist between the two legitimate sources. Thus, this sole relay is necessary for information exchange between the two nodes. The eavesdropper, in contrast, is a legitimate but not an intended receiver. Due to FD operation, the received signal $\mathbf{y}_r[n]$ and the transmit signal $\mathbf{x}_R[n]$ at the relay node at time instant n, can be written, respectively, as

$$\mathbf{y}_r[n] = \mathbf{h}_{AR} s_A[n] + \mathbf{h}_{BR} s_B[n] + \mathbf{H}_{RR}\mathbf{x}_R[n] + \mathbf{n}_R[n], \tag{7.1}$$

$$\mathbf{x}_R[n] = \mathbf{W}\mathbf{y}_R^{IR}[n-\tau] + \mathbf{z}[n], \tag{7.2}$$

where τ is the processing delay to implement FD operation and assumed short enough to be neglected as far as the achievable rate computation is concerned, $\mathbf{n}_R \backsim \mathrm{CN}(\mathbf{0}, \sigma_R^2\mathbf{I})$ denotes AWGN, $\mathbf{z}[n] \backsim \mathrm{CN}(\mathbf{0}, \mathbf{Q})$, with $\mathbf{Q} \succeq \mathbf{0}$, is the AN used for interfering E, and $\mathbf{y}_R^{IR}[n]$ is the signal split to the IR at R given by

$$\mathbf{y}_R^{IR}[n] = \sqrt{\rho}\Big(\mathbf{h}_{AR} s_A[n] + \mathbf{h}_{BR} s_B[n] + \mathbf{H}_{RR}\mathbf{x}_R[n] + \mathbf{n}_R[n]\Big). \tag{7.3}$$

Accordingly, the signal transmitted by the relay can then be expressed as

$$\mathbf{x}_R[n] = \sqrt{\rho}\mathbf{W}\Big(\mathbf{h}_{AR}s_A[n-\tau] + \mathbf{h}_{BR}s_B[n-\tau] + \mathbf{H}_{RR}\mathbf{x}_R[n-\tau] + \mathbf{n}_R[n-\tau]\Big) + \mathbf{z}[n-\tau]. \quad (7.4)$$

As shown in [81], the capacity of relay networks with delay is dependent only on the relative path delays from the source to the destination and not on absolute delays. Consequently, the relay output can be written as [81]

$$\mathbf{x}_R[n] = \mathbf{W}\sum_{j=0}^{\infty}(\mathbf{H}_{RR}\mathbf{W})^j\Big[\sqrt{\rho}(\mathbf{h}_{AR}s_A[n-j\tau-\tau] + \mathbf{h}_{BR}s_B[n-j\tau-\tau] + \mathbf{n}_R[n-j\tau-\tau])\Big] + \mathbf{z}[n-j\tau-\tau], \quad (7.5)$$

where j denotes the index of the delayed symbols. We define the covariance matrix of (7.5) as

$$\mathbb{E}[\mathbf{x}_R\mathbf{x}_R^\dagger] = \rho\Big[P_A\mathbf{W}\sum_{j=0}^{\infty}(\mathbf{H}_{RR}\mathbf{W})^j\mathbf{h}_{AR}\mathbf{h}_{AR}^\dagger((\mathbf{H}_{RR}\mathbf{W})^j)^\dagger\mathbf{W}^\dagger + P_B\mathbf{W}\sum_{j=0}^{\infty}(\mathbf{H}_{RR}\mathbf{W})^j\mathbf{h}_{BR}\mathbf{h}_{BR}^\dagger((\mathbf{H}_{RR}\mathbf{W})^j)^\dagger\mathbf{W}^\dagger + \mathbf{W}\sum_{j=0}^{\infty}(\mathbf{H}_{RR}\mathbf{W}\mathbf{W}^\dagger\mathbf{H}_{RR}^\dagger)^j\mathbf{W}^\dagger\Big] + \mathbf{Q}. \quad (7.6)$$

Clearly, the relay's transmit covariance is indeed a complicated function of $\mathbf{W}$. Thus, we assume the ZF solution constraint to cancel the RSI from the relay output to the relay input via the optimization of $\mathbf{W}$ [90]. In particular, depending on the relationship between M_T and M_R, the ZF constraints may take the following form defined as [99]

$$1) \quad M_R > M_T : \text{ZF} \triangleq \mathbf{W}\mathbf{H}_{RR} = \mathbf{0}, \quad (7.7)$$

$$2) \quad M_T > M_R : \text{ZF} \triangleq \mathbf{H}_{RR}\mathbf{W} = \mathbf{0}. \quad (7.8)$$

We consider the case where $M_T > M_R$. The other case can also be handled in a similar manner. Consequently, (7.5) becomes

$$\mathbf{x}_R[n] = \sqrt{\rho}\mathbf{W}\Big[\mathbf{h}_{AR}s_A[n-\tau] + \mathbf{h}_{BR}s_B[n-\tau] + \mathbf{n}_R[n-\tau]\Big] + \mathbf{z}[n],$$

with the relay output power expressed as

$$\begin{aligned} P_R &= \text{trace}(\mathbb{E}[\mathbf{x}_R\mathbf{x}_R^\dagger]) \\ &= \rho\left[P_A\|\mathbf{W}\mathbf{h}_{AR}\|^2 + P_B\|\mathbf{W}\mathbf{h}_{BR}\|^2 + \text{trace}(\mathbf{W}\mathbf{W}^\dagger)\right] \\ &\quad + \text{trace}(\mathbf{Q}). \end{aligned} \tag{7.9}$$

In the second time slot, the received signal at $\mathsf{S_A}$ (after cancelling the SI signal $s_A[n-\tau]$) is given as

$$\begin{aligned} y_{sA}[n] &= \sqrt{\rho}\left(\mathbf{h}_{RA}^\dagger\mathbf{W}\mathbf{h}_{BR}s_B[n-\tau] + \mathbf{h}_{RA}^\dagger\mathbf{W}\mathbf{n}_R[n]\right) \\ &\quad + \mathbf{h}_{RA}^\dagger\mathbf{z}[n] + h_{AA}s_A[n] + n_A[n], \end{aligned} \tag{7.10}$$

where $n_A[n]$ is the AWGN at node A. From this, we can work out the rates at $\mathsf{S_A}$ and $\mathsf{S_B}$ as

$$R_A = \log_2(1+\Gamma_A), \tag{7.11}$$

$$R_B = \log_2(1+\Gamma_B), \tag{7.12}$$

where

$$\Gamma_A = \frac{\rho P_B|\mathbf{h}_{RA}^\dagger\mathbf{W}\mathbf{h}_{BR}|^2}{\rho\sigma_R^2\|\mathbf{h}_{RA}^\dagger\mathbf{W}\|^2 + P_A|h_{AA}|^2 + \mathbf{h}_{RA}^\dagger\mathbf{Q}\mathbf{h}_{RA} + 1}, \tag{7.13}$$

$$\Gamma_B = \frac{\rho P_A|\mathbf{h}_{RB}^\dagger\mathbf{W}\mathbf{h}_{AR}|^2}{\rho\sigma_R^2\|\mathbf{h}_{RB}^\dagger\mathbf{W}\|^2 + P_B|h_{BB}|^2 + \mathbf{h}_{RB}^\dagger\mathbf{Q}\mathbf{h}_{RB} + 1}. \tag{7.14}$$

The signal received at E can be expressed as

$$\gamma_E[n] = \sqrt{\rho}\left(\mathbf{h}_{RE}^{\dagger}\mathbf{W}\mathbf{h}_{AR}s_A[n-\tau] + \mathbf{h}_{RE}^{\dagger}\mathbf{W}\mathbf{h}_{BR}s_B[n-\tau] + \mathbf{h}_{RE}^{\dagger}\mathbf{W}\mathbf{n}_R\right) + \mathbf{h}_{RE}^{\dagger}\mathbf{z}[n] + n_E, \tag{7.15}$$

where n_E is the AWGN at E. Also, the achievable sum-rate at E is upper bounded as [99]

$$R_E = \log_2(1+\Gamma_E), \tag{7.16}$$

where

$$\Gamma_E = \frac{\rho P_A|\mathbf{h}_{RE}^{\dagger}\mathbf{W}\mathbf{h}_{AR}|^2 + \rho P_B|\mathbf{h}_{RE}^{\dagger}\mathbf{W}\mathbf{h}_{BR}|^2}{\rho\sigma_R^2\|\mathbf{h}_{RE}^{\dagger}\mathbf{W}\|^2 + \mathbf{h}_{RE}^{\dagger}\mathbf{Q}\mathbf{h}_{RE} + 1}. \tag{7.17}$$

The achievable secrecy sum-rate is then defined as [99]

$$R_{sec} = [R_A + R_B - R_E]^+, \tag{7.18}$$

where $[x]^+$ represents $\max(x,0)$. Meanwhile, the signal split to the ER at R is given by

$$\mathbf{y}_R^{ER}[n] = \sqrt{1-\rho}\left(\mathbf{h}_{AR}s_A[n] + \mathbf{h}_{BR}s_B[n] + \mathbf{H}_{RR}\mathbf{x}_R[n] + \mathbf{n}_R[n]\right).$$

The harvested energy at the relay is thus given as [87]

$$Q = \beta(1-\rho)(|\mathbf{h}_{AR}|^2P_A + |\mathbf{h}_{BR}|^2P_B + \bar{\mathrm{E}} + \sigma_R^2M_R), \tag{7.19}$$

where $\bar{\mathrm{E}} = \mathbb{E}[\mathbf{x}_R\mathbf{x}_R^{\dagger}]$ and β, which denotes the energy conversion efficiency of the ER at the relay is assumed throughout this paper to be unity for notational simplicity.

7.4 Problem Statement

Due to the inherent SI generated at each FD node, the transmitting nodes often do not always use the maximum available transmit power as this has the potential to increase the level of SI. To this end, it is important that the transmitters use their optimal transmit power during the communication process. Furthermore, it

is known that optimal values of system parameters guarantees that the secrecy rate is as large as possible [99]. We study in general, the case where the source nodes $(\mathsf{S_A}, \mathsf{S_B})$ and the eavesdropper E, have a non-zero SINR thresholds denoted by γ_A, γ_B and γ_E, respectively. Consequently, our aim is to maximize the secrecy sum-rate for SWIPT by ensuring system parameters are optimal. We achieve this by jointly optimizing the transmit power at the source nodes (P_A, P_B), the relaying matrix $(\mathbf{W})$ and the AN covariance matrix $(\mathbf{Q})$ at the relay. Thus, the problem can be formulated as

$$\min_{\substack{\rho\in(0,1),\mathbf{W},\mathbf{Q}\succeq\mathbf{0}\\ 0<P_A\leq P_{\max},0<P_B\leq P_{\max}}} P_A+P_B+P_R \ \text{ s.t.}$$
$$\begin{cases} \Gamma_A \geq \gamma_A, \\ \Gamma_B \geq \gamma_B, \\ \Gamma_E \leq \gamma_E, \\ (1-\rho)(|\mathbf{h}_{AR}|^2 P_A + |\mathbf{h}_{BR}|^2 P_B + \bar{\mathrm{E}} + \sigma_R^2 M_R) \geq \bar{Q}, \\ \mathbf{H}_{RR}\mathbf{W} = \mathbf{0}. \end{cases} \tag{7.20}$$

7.5 Proposed Scheme

In this section, we address the optimal design of the PS coefficient (ρ), ZF relaying matrix $(\mathbf{W})$, the AN covariance $(\mathbf{Q})$ and the transmit power at the sources (P_A, P_B). As (7.20) is nonconvex, obtaining a closed-form solution to optimize jointly $\rho, \mathbf{W}, \mathbf{Q}, P_A$ and P_B is extremely difficult. As a consequence, we propose to solve (7.20) in an alternating fashion.

7.5.1 Optimization of W and Q at the Relay

Here, we study the optimal beamforming matrix and the AN covariance matrix assuming the source power (P_A, P_B) and the PS ratio (ρ) all being fixed. For convenience, we define $\mathbf{W} = \mathbf{N}_t\mathbf{V}$, where $\mathbf{N}_t \in \mathbb{C}^{\mathrm{M}_T \times \mathrm{M}_T}$ represents the null space of $\mathbf{H}_{RR}$, and $\mathbf{V} \in \mathbb{C}^{\mathrm{M}_T \times \mathrm{M}_T}$ is the new optimization variable. Subsequently, the optimization of $\mathbf{W}$ reduces to optimizing matrix $\mathbf{V}$ [82]. Accordingly, we remove the

ZF constraint in (7.20) and obtain the equivalent optimization problem:

$$\min_{\mathbf{V},\mathbf{Q}\succeq\mathbf{0}} P_R \ \text{ s.t.}$$
$$\begin{cases} \Gamma_A \geq \gamma_A, \\ \Gamma_B \geq \gamma_B, \\ \Gamma_E \leq \gamma_E, \\ (1-\rho)(|\mathbf{h}_{AR}|^2 P_A + |\mathbf{h}_{BR}|^2 P_B + \bar{\mathrm{E}} + \sigma_R^2 M_R) \geq \bar{Q}. \end{cases} \tag{7.21}$$

Problem (7.21) is a nonconvex problem due to the coupled optimization variables in the constraints. However, by rearranging the terms in the constraints, (7.21) can be re-expressed as

$$\min_{\Sigma,\mathbf{Q}\succeq\mathbf{0}} P_R \ \text{ s.t.} \tag{7.22a}$$
$$\frac{1}{\gamma_A} P_B C_{rA} \mathbf{h}_{BR}^\dagger \Sigma \mathbf{h}_{BR} - \sigma_R^2 C_{Nt} \mathbf{h}_{RA}^\dagger \Sigma \mathbf{h}_{RA} \geq \frac{1}{\rho}(P_A |h_{AA}|^2 + \mathbf{h}_{RA}^\dagger \mathbf{Q} \mathbf{h}_{RA} + 1), \tag{7.22b}$$
$$\frac{1}{\gamma_B} P_A C_{rB} \mathbf{h}_{AR}^\dagger \Sigma \mathbf{h}_{AR} - \sigma_R^2 C_{Nt} \mathbf{h}_{RB}^\dagger \Sigma \mathbf{h}_{RB} \geq \frac{1}{\rho}(P_B |h_{BB}|^2 + \mathbf{h}_{RB}^\dagger \mathbf{Q} \mathbf{h}_{RB} + 1), \tag{7.22c}$$
$$\frac{1}{\gamma_E}\left[P_A C_{rE} \mathbf{h}_{AR}^\dagger \Sigma \mathbf{h}_{AR} + P_B C_{rE} \mathbf{h}_{BR}^\dagger \Sigma \mathbf{h}_{BR}\right] - \sigma_R^2 C_{Nt} \mathbf{h}_{RE}^\dagger \Sigma \mathbf{h}_{RE} \leq \frac{1}{\rho}\left(\mathbf{h}_{RE}^\dagger \mathbf{Q} \mathbf{h}_{RE} + 1\right), \tag{7.22d}$$
$$|\mathbf{h}_{AR}|^2 P_A + |\mathbf{h}_{BR}|^2 P_B + \bar{\mathrm{E}} \geq \frac{Q}{(1-\rho)} - \sigma_R^2 M_R, \tag{7.22e}$$

where $\Sigma = \mathbf{V}\mathbf{V}^\dagger, C_{rA} = \|\mathbf{N}_t \mathbf{h}_{RA}\|^2, C_{Nt} = \mathrm{trace}(\mathbf{N}_t \mathbf{N}_t^\dagger), C_{rB} = \|\mathbf{N}_t \mathbf{h}_{RB}\|^2$ and $C_{rE} = \|\mathbf{N}_t \mathbf{h}_{RE}\|^2$. Problem (7.22) can be efficiently solved by existing solvers such as CVX [72]. Once the optimal Σ is obtained, optimal $\mathbf{V}$ can be constructed through matrix decomposition.

7.5.2 Optimization of the PS Coefficient (ρ)

For fixed values of the relay beamforming matrix ($\mathbf{W}$), AN covariance ($\mathbf{Q}$) and for given values of the transmit power (P_A, P_B) at the sources, problem (7.20) can be reformulated as

$$\min_{\rho\in(0,1)} \quad P_A + P_B + P_R \qquad \text{s.t.} \tag{7.23a}$$

$$\frac{\rho P_B |\mathbf{h}_{RA}^{\dagger}\mathbf{W}\mathbf{h}_{BR}|^2}{\rho\sigma_R^2\|\mathbf{h}_{RA}^{\dagger}\mathbf{W}\|^2+P_A|h_{AA}|^2+\mathbf{h}_{RA}^{\dagger}\mathbf{Q}\mathbf{h}_{RA}+1} \geq \gamma_A, \tag{7.23b}$$

$$\frac{\rho P_A |\mathbf{h}_{RB}^{\dagger}\mathbf{W}\mathbf{h}_{AR}|^2}{\rho\sigma_R^2\|\mathbf{h}_{RB}^{\dagger}\mathbf{W}\|^2+P_B|h_{BB}|^2+\mathbf{h}_{RB}^{\dagger}\mathbf{Q}\mathbf{h}_{RB}+1} \geq \gamma_B, \tag{7.23c}$$

$$\frac{\rho P_A |\mathbf{h}_{RE}^{\dagger}\mathbf{W}\mathbf{h}_{AR}|^2 + \rho P_B |\mathbf{h}_{RE}^{\dagger}\mathbf{W}\mathbf{h}_{BR}|^2}{\rho\sigma_R^2\|\mathbf{h}_{RE}^{\dagger}\mathbf{W}\|^2 + \mathbf{h}_{RE}^{\dagger}\mathbf{Q}\mathbf{h}_{RE}+1} \leq \gamma_E, \tag{7.23d}$$

$$(1-\rho)(|\mathbf{h}_{AR}|^2 P_A + |\mathbf{h}_{BR}|^2 P_B + \bar{\mathrm{E}} + \sigma_R^2 M_R) \geq \bar{Q}. \tag{7.23e}$$

Problem (7.23) can be expressed in a convenient form to be solved using existing solvers by rearranging the terms in the constraints as

$$\min_{\rho\in\{0,1\}} \; P_A + P_B + P_R \qquad \text{s.t.} \tag{7.24a}$$

$$\frac{1}{\gamma_A}\rho P_B C_{rA}\mathbf{h}_{BR}^{\dagger}\Sigma\mathbf{h}_{BR} - \rho\sigma_R^2 C_{Nt}\mathbf{h}_{RA}^{\dagger}\Sigma\mathbf{h}_{RA} \geq P_A|h_{AA}|^2 + \mathbf{h}_{RA}^{\dagger}\mathbf{Q}\mathbf{h}_{RA} + 1, \tag{7.24b}$$

$$\frac{1}{\gamma_B}\rho P_A C_{rB}\mathbf{h}_{AR}^{\dagger}\Sigma\mathbf{h}_{AR} - \rho\sigma_R^2 C_{Nt}\mathbf{h}_{RB}^{\dagger}\Sigma\mathbf{h}_{RB} \geq P_B|h_{BB}|^2 + \mathbf{h}_{RB}^{\dagger}\mathbf{Q}\mathbf{h}_{RB} + 1, \tag{7.24c}$$

$$\frac{1}{\gamma_E}\left[P_A C_{rE}\mathbf{h}_{AR}^{\dagger}\Sigma\mathbf{h}_{AR} + P_B C_{rE}\mathbf{h}_{BR}^{\dagger}\Sigma\mathbf{h}_{BR}\right] - \sigma_R^2 C_{Nt}\mathbf{h}_{RE}^{\dagger}\Sigma\mathbf{h}_{RE} \leq \frac{1}{\rho}\left(\mathbf{h}_{RE}^{\dagger}\mathbf{Q}\mathbf{h}_{RE}+1\right), \tag{7.24d}$$

$$(1-\rho)(|\mathbf{h}_{AR}|^2 P_A + |\mathbf{h}_{BR}|^2 P_B + \bar{\mathrm{E}} + \sigma_R^2 M_R) \geq \bar{Q}. \tag{7.24e}$$

Problem (7.24) can be efficiently solved by existing solvers such as CVX [72].

7.5.3 Optimization of the Source Power (P_A, P_B)

For given values of the relay beamforming matrix ($\mathbf{W}$), AN covariance matrix ($\mathbf{Q}$) and the relay PS ratio, problem (7.20) can be written as

$$\min_{P_A,P_B} \quad P_A + P_B + P_R \qquad \text{s.t.}$$

$$\frac{\rho P_B |\mathbf{h}_{RA}^{\dagger}\mathbf{W}\mathbf{h}_{BR}|^2}{\rho\sigma_R^2\|\mathbf{h}_{RA}^{\dagger}\mathbf{W}\|^2 + P_A|h_{AA}|^2 + \mathbf{h}_{RA}^{\dagger}\mathbf{Q}\mathbf{h}_{RA} + 1} \geq \gamma_A, \tag{7.25a}$$

$$\frac{\rho P_A |\mathbf{h}_{RB}^{\dagger}\mathbf{W}\mathbf{h}_{AR}|^2}{\rho\sigma_R^2\|\mathbf{h}_{RB}^{\dagger}\mathbf{W}\|^2 + P_B|h_{BB}|^2 + \mathbf{h}_{RB}^{\dagger}\mathbf{Q}\mathbf{h}_{RB} + 1} \geq \gamma_B, \tag{7.25b}$$

$$\frac{\rho P_A |\mathbf{h}_{RE}^{\dagger}\mathbf{W}\mathbf{h}_{AR}|^2 + \rho P_B |\mathbf{h}_{RE}^{\dagger}\mathbf{W}\mathbf{h}_{BR}|^2}{\rho\sigma_R^2\|\mathbf{h}_{RE}^{\dagger}\mathbf{W}\|^2 + \mathbf{h}_{RE}^{\dagger}\mathbf{Q}\mathbf{h}_{RE} + 1} \leq \gamma_E, \tag{7.25c}$$

$$(1-\rho)(|\mathbf{h}_{AR}|^2 P_A + |\mathbf{h}_{BR}|^2 P_B + \bar{\mathrm{E}} + \sigma_R^2 M_R) \geq \bar{Q}, \tag{7.25d}$$

$$0 < P_A \leq P_{\max}, \quad 0 < P_B \leq P_{\max}. \tag{7.25e}$$

It is worth noting that full-duplexity in communication systems is preceded by successful SIC. In our model, the source nodes are equipped with a single transmitter-receiver pair for signal transmission and reception, respectively. As a result, it is impossible to cancel the SI in the spatial domain [87]. The relay, in contrast, equipped with at least two transmitter-receiver pairs, can cancel the generated SI in the spatial domain. We proceed to investigate the optimal power solution (P_A, P_B) at sources $\mathrm{S_A}$ and $\mathrm{S_B}$, respectively, assuming $\mathbf{W}$, $\mathbf{Q}$ and ρ all being fixed. Evidently, it is easy to check that at optimum, at least one source will be transmitting with maximum power [87] i.e., $P_A = P_{\max}$ or $P_B = P_{\max}$. As a consequence, we can relax (7.25) into two sub-problems with: (i) $P_A = P_{\max}$, (ii) $P_B = P_{\max}$. Considering the symmetric nature of case (i) and case (ii), we study case (i) as an example and solve problem

(7.25) analytically. Problem (7.25) is thus reformulated as

$$\min_{P_B} \quad P_B + \bar{P}_R \qquad \text{s.t.} \tag{7.26a}$$

$$\frac{\rho P_B |\mathbf{h}_{RA}^{\dagger}\mathbf{W}\mathbf{h}_{BR}|^2}{\rho\sigma_R^2\|\mathbf{h}_{RA}^{\dagger}\mathbf{W}\|^2 + P_{\max}|h_{AA}|^2 + \mathbf{h}_{RA}^{\dagger}\mathbf{Q}\mathbf{h}_{RA} + 1} \geq \gamma_A, \tag{7.26b}$$

$$\frac{\rho P_{\max} |\mathbf{h}_{RB}^{\dagger}\mathbf{W}\mathbf{h}_{AR}|^2}{\rho\sigma_R^2\|\mathbf{h}_{RB}^{\dagger}\mathbf{W}\|^2 + P_B|h_{BB}|^2 + \mathbf{h}_{RB}^{\dagger}\mathbf{Q}\mathbf{h}_{RB} + 1} \geq \gamma_B, \tag{7.26c}$$

$$\frac{\rho P_{\max} |\mathbf{h}_{RE}^{\dagger}\mathbf{W}\mathbf{h}_{AR}|^2 + \rho P_B |\mathbf{h}_{RE}^{\dagger}\mathbf{W}\mathbf{h}_{BR}|^2}{\rho\sigma_R^2\|\mathbf{h}_{RE}^{\dagger}\mathbf{W}\|^2 + \mathbf{h}_{RE}^{\dagger}\mathbf{Q}\mathbf{h}_{RE} + 1} \leq \gamma_E, \tag{7.26d}$$

$$(1-\rho)(|\mathbf{h}_{AR}|^2 P_{\max} + |\mathbf{h}_{BR}|^2 P_B + \bar{\mathrm{E}} + \sigma_R^2 M_R) \geq \bar{Q}, \tag{7.26e}$$

$$0 < P_B \leq P_{\max}, \tag{7.26f}$$

where $\bar{P}_R = \rho\left[P_{\max}\|\mathbf{W}\mathbf{h}_{AR}\|^2 + P_B\|\mathbf{W}\mathbf{h}_{BR}\|^2 + \mathrm{trace}(\mathbf{W}\mathbf{W}^{\dagger})\right] + \mathrm{trace}(\mathbf{Q})$. Theoretically, since $0 < P_B \leq P_{\max}$, we can obtain the feasible range $[P_B^{\min}, P_B^{\max}]$ for P_B. With regards to its special structure, the constraints in (7.26) can be analysed with respect to P_B :

1) A continuous increase in the value of P_B should guarantee that (7.26b) remains satisfied. Thus, we can define the minimum P_B that satisfies (7.26b) to equality as $P_B^{\min} = \frac{\gamma_A(\rho\sigma_R^2\|\mathbf{h}_{RA}^{\dagger}\mathbf{W}\|^2 + P_A|h_{AA}|^2 + \mathbf{h}_{RA}^{\dagger}\mathbf{Q}\mathbf{h}_{RA} + 1)}{\rho|\mathbf{h}_{RA}^{\dagger}\mathbf{W}\mathbf{h}_{BR}|^2}$.

2) Constraint (7.26c) is a decreasing function of P_B. Thus, the maximum P_B satisfying (7.26c) to equality is defined as $P_B^{\max} = \frac{\rho P_A|\mathbf{h}_{RB}^{\dagger}\mathbf{W}\mathbf{h}_{AR}|^2 - \gamma_B(\rho\sigma_R^2\|\mathbf{h}_{RB}^{\dagger}\mathbf{W}\|^2 + \mathbf{h}_{RB}^{\dagger}\mathbf{Q}\mathbf{h}_{RB} + 1)}{\gamma_B|h_{BB}|^2}$.

3) An upper bound of the eavesdropping constraint in (7.26d) is satisfied when $P_B \leq P_B^{\max}$.

4) A lower bound of the energy harvesting constraint in (7.26e) is guaranteed to be satisfied when $P_B \geq P_B^{\min}$.

The optimal P_B^* is chosen between $P_B^{\min}$ and $P_B^{\max}$ which satisfies (7.26b)-(7.26e). Accordingly, to obtain the optimal P_B, we perform a 1-D search over P_B starting from $P_B^{\min}$ until $P_B^{\max}$ is reached to find a feasible solution to problem (7.26). Clearly, if $P_B^{\min} > P_B^{\max}$ then (7.26) becomes infeasible. In a similar fashion, the optimal P_A can be obtained for case (ii).

7.6 Numerical example

In this section, we present numerical results to investigate the performance of the proposed scheme through computer simulations. In particular, we consider a flat fading communication channel where the coefficients are described as complex Gaussian numbers with zero mean and which are independent and identically distributed. The simulation is averaged over 1000 independent channel realizations and SINR at node A, node B and the eavesdropper is given, respectively, as γ_A = -5 (dB), γ_B = -5 (dB), γ_E = -15 (dB). We also assume that 60% of the SI at node A and node B has been eliminated through digital cancellation [87].

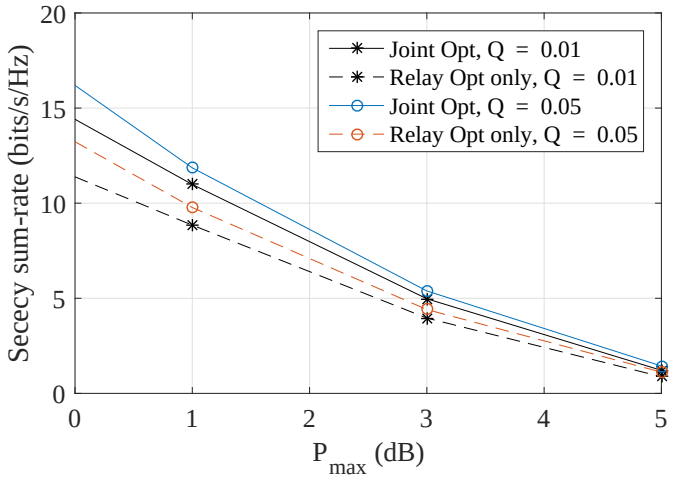

Figure 7.2: *Secrecy sum-rate vs P_{max}*

In Fig. 7.2, we investigate the secrecy sum-rate for SWIPT in FD systems versus the transmit power budget P_{max} (dB) for different values of the harvested power constraint. In particular, we study the performance of the proposed scheme (denoted 'Joint Opt.' in the figure) in comparison with the relay-only optimization scheme (denoted 'Relay Only Opt.' in the figure). Upon investigation, the proposed scheme yields a higher secrecy sum-rate compared to the achievable secrecy sum-rate of the relay-only optimization scheme. However, the secrecy sum-rate decreases with a continuous increase in P_{max}. This is because the residual SI increases with an increase in P_{max} thereby compensating any SINR gains as a result of transmit optimization [100].

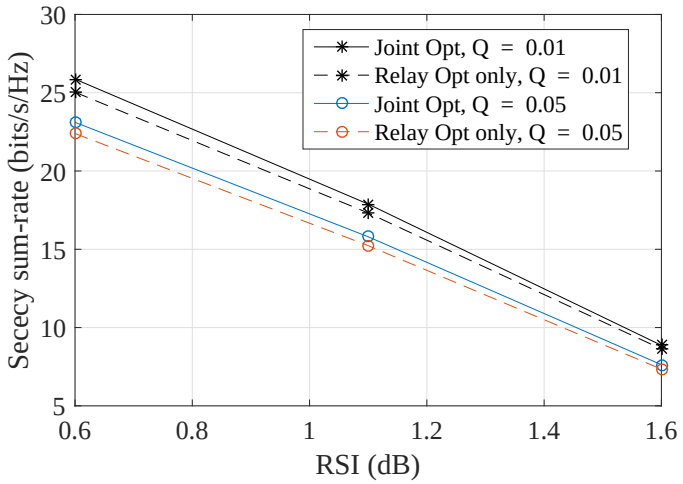

Figure 7.3: *Secrecy sum-rate vs Residual self-interference*

In Fig. 7.3, we investigate further, the secrecy sum-rate performance against the RSI for different values of the harvested power constraints. Evidently, as RSI increases, a corresponding decrease in the secrecy sum-rate is observed. However, the proposed scheme ('Joint Opt') yields higher secrecy sum-rate compared to the secrecy sum-rate of the relay-only optimization scheme. Hence, the need for joint optimization is justified.

7.7 Conclusion

In this chapter, the joint optimization of the source transmit power, AN covariance matrix and the relay beamforming matrix for SWIPT in FD AF relaying system in the presence of an eavesdropper is investigated. Specifically, using SDP and 1-D searching, we proposed an algorithm that minimises the total transmit power for secure SWIPT in a FD MIMO AF relay system. Computer simulations corroborates the effectiveness of the proposed approach.

Chapter 8

Conclusion

Integrating energy harvesting technology into wireless communication networks is essential as it provides an effective way to implement green communications and to extend the lifetime of battery constrained systems thus, eliminates the traditional over dependence of wireless devices on the grid power supply which invariably reduces the cost of operating wireless communication systems. In addition, integrating SWIPT in FD systems guarantees the provision of information and energy to users as well as the efficient use of the radio spectrum. Furthermore, as bi-directional wireless communications are exposed to security threat, integrating physical layer security with SWIPT in FD systems is necessary. Accordingly, this thesis has proposed and developed a number of strategies to maximize the sum-rate for SWIPT in FD systems and also to the maximize secrecy sum-rate for secure SWIPT in FD systems.

8.1 Result Summary

In this section, we proceed to summarise the results in this thesis and the consideration of future work. We provide a general overview of full-duplex systems in chapter 2. As full-duplex communication is preceded by successful SI cancellation, we provide an overview of the conventional SI cancellation method. Due to imperfect channel estimation for the SI channel, the SI can not be completely cancelled.

Thus, the RSI if not properly manage, affects the overall system performance. As a result, we show in this thesis, how RSI can be managed to ensure optimal utilization of full-duplexity in wireless communications. Furthermore, integrating SWIPT in FD systems necessitates the need to study existing FD network architectures. For this reason, we provide in chapter 2, a review of FD point-to-point, FD point-to-many, FD MIMO relay and secrecy in wireless communication networks.

In chapter 3, we present a review of energy harvesting technology. Energy harvesting systems have the capability to capture free energy, available without cost from the environment. Thus, we provide an overview of energy harvesting systems with emphasis on radio frequency energy harvesting technology as this is most relevant to this research. Since RF signals can simultaneously transmit wireless information and power, we also provide a review of the RF receiver architecture design with energy harvesting capabilities.

In chapter 4, we proposed a novel algorithm which maximises the sum-rate for FD point-to-point energy harvesting system. A typical scenario application is a wireless sensor network. Altogether, from this chapter, we observed the following key points:

- For a point-to-point FD SWIPT system, for fixed PS ratio, the optimal transmit power can be obtained by introducing the rate-split scheme between the two nodes, whereas for given transmit power at the nodes, closed-form expressions for the receive PS ratios can be obtained.

- For a point-to-point FD SWIPT system, as SI is a function of transmitted power, a continuous increase in the transmit power corresponds to an increase in the RSI, which degrades the overall system performance. Hence, to maximally exploit FD in SWIPT systems, system parameters such as transmit power at both nodes and receiver power splitter coefficient must be optimal. To achieve optimal system performance as well as maximal spectral efficiency for SWIPT in FD point-to-point system, using the rate split method and 1-dimensional search technique, we proposed an iterative algorithm which max-

imises the sum-rate.

- We investigated the aforementioned system assuming the receiver power splitter is fixed. We observed that the system performance in terms of achievable sum-rate was lower, an observation that corroborated the need for the joint optimization of system parameters.

Cooperative communications in general, enables efficient utilization of communication resources. Specifically, cooperative communications allow nodes in a communication network to collaborate with each other to ensure efficient information transmission. To be more specific, cooperative communications using relay enables wider coverage, increased throughput and increases overall network performance. For this reason, in chapter 5, we investigated SWIPT in FD MIMO two-way relay system, where all the nodes are assumed to operate in FD. The relay in particular, is motivated to take part in the communication process by the energy it can harvest from the received signal. We considered practical communication system architecture where two nodes operating in FD with the desire to exchange information from each other, require the services of a MIMO two-way relay to complete the information exchange. As before, successful SI cancellation is necessary to achieve FD communication. Hence, a key technique adopted in this work is to assume ZF solution constraints such that the optimization of the relay beamforming matrix cancels the RSI from the relay output to the relay input. From this chapter, we observed the following key points:

- We consider the fact that each source transmits single data stream only and that network coding principles encourages mixing rather than separating the data streams from the sources. Thus, the beamforming matrix $\mathbf{W}$ was decomposed as $\mathbf{W} = \mathbf{w_r}\mathbf{w_t}^{\dagger}$, which resulted into a simplified ZF matrix expression. Accordingly, if we assume that the nodes transmit at maximum power, using the difference of convex programming and 1-Dimensional search technique, we developed iterative algorithm which maximises the sum-rate for SWIPT in FD MIMO two-way relay system.

- We consider the case where the receive beamforming vector is fixed, we observed a decrease in overall system performance, an observation which necessitated the need for joint optimization of system parameters.

Multipath induced errors and interference have the potential to degrade the performance of wireless communication systems. To tackle this challenge, digital communication systems adopts the use of multiple antenna array. For this reason, in chapter 6, we consider a virtual MIMO set-up where a multiple antenna BS in the first phase, simultaneously transmits wireless information and power in the downlink to a set of single antenna mobile users. In the next phase, the MS transmits feedback information to the BS using the energy harvested from the received signal. Using SDP, we developed algorithm which minimises the sum-transmit power for SWIPT in a multiuser MIMO FD system subject to transmit power, harvested energy constraints, uplink and downlink SINR constraints. Results obtained in chapter 6 showed that the proposed scheme achieves a transmit power gain over the suboptimal ZF scheme.

To conclude this thesis, in chapter 7, we focus on the integration of physical layer security and SWIPT in FD systems. As wireless communication systems are constantly faced with the challenge of secrecy in information exchange, this thesis documents a novel integration of SWIPT, FD technology and physical layer security to jointly maximise the secrecy sum-rate of SWIPT in FD MIMO two-way relay system. The proposed scheme show that given the transmit power, harvested energy and SINR constraints for secure SWIPT in FD MIMO two-way relay systems, an increase in the transmit power corresponds to a decrease in the secrecy sum-rate due to an increase in RSI.

8.2 Future Work

This thesis studies the potentials of simultaneous wireless information and power transfer in full-duplex communication systems. Specifically, throughout this work, we developed algorithms that aims to maximise the sum-rate for SWIPT in FD

systems as well as to maximize secrecy sum-rate for SWIPT in FD systems under specific communication system architecture as detailed in the report. The work in this thesis therefore motivates further investigation in some research areas which are identified and summarized below:

Secure SWIPT in multiuser MIMO FD systems: As an extension to the work done in chapter 6, we consider a scenario where secure bidirectional information exchange is required in a multiuser MIMO SWIPT system. Specifically, we propose the end-to-end sum-transmit power minimization approach for secure SWIPT in a multiuser MIMO FD system where the BS simultaneously transmits K independent confidential messages to K-single-antenna receivers in the downlink, in the presence of external l-single-antenna eavesdroppers, and receives information in the uplink in FD mode. In addition to external eavesdroppers, each receiver attempts to eavesdrops messages intended for other receivers. Thus, to ensure secure information transmission, AN is added in the transmitted signal to confuse these potential and external eavesdroppers. As an increase in transmit power causes a corresponding increase in SI, it is important for communication nodes to transmit at optimality. To this end, we propose a study which aims to minimize the sum-transmit power for secure SWIPT in multiuser MIMO FD system while maintaining the achievable secrecy rate and energy harvesting constraints at each receiver as well as the non-zero uplink SINR ($\gamma^{\mathrm{BS}} > 0$).

SWIPT in FD device-to-device communications in heterogeneous networks: FD heterogeneous networks in general, can accommodate the coexistence of device-to-device communications. As a result, user equipment in close proximity are able to communicate directly without routing through BS. Furthermore, D2D communication, characterised as having low transmit power within a shorter link, is known to have a weaker SI. Thus, it is interesting to investigate SWIPT in FD D2D heterogeneous network. Specifically, user equipments exchange bidirectional information using the harvested energy from nearby BS. To optimise system performance, we propose a joint investigation of the SI in FD communications and D2D under-

lay through power control, beamforming and link adaptation subject to harvested power, transmit power and SINR constraints.

Overall, this thesis has presented key results in the study of SWIPT in FD systems. It is hoped that the results and conclusions derived in this thesis will help explore the potentials for future designs of SWIPT in FD system.

Appendix A

Proof of Proposition 1

Firstly, let us proceed to prove the first part of proposition 1. Problem (6.25) is convex and satisfies the Slater's condition, and therefore its duality gap is zero [72]. We denote $\{\lambda_k\}$ and $\{\mu_k\}$ as the dual variables associated with the SINR constraints and harvested power constraints of problem (6.25), respectively. The partial Lagrangian of problem (6.25) is thus given as shown in (A.1).

$$\begin{aligned} L(\{\mathbf{Z}_k, \rho_k, \lambda_k, \mu_k\}) \triangleq & \sum_{k=1}^{K} \mathrm{Tr}(\mathbf{Z}_k) \\ & - \sum_{k=1}^{K} \lambda_k \left(\frac{1}{\gamma_k^{\mathrm{DL}}} \mathbf{h}_{\mathrm{dl},k}^H \mathbf{Z}_k \mathbf{h}_{\mathrm{dl},k} - \sum_{j \neq k} \mathbf{h}_{\mathrm{dl},k}^H \mathbf{Z}_j \mathbf{h}_{\mathrm{dl},k} + \bar{G}_k - \sigma_k^2 - \frac{\delta_k^2}{\rho_k} \right) \\ & - \sum_{k=1}^{K} \mu_k \left(\sum_{j=1}^{K} \mathbf{h}_{\mathrm{dl},k}^H \mathbf{Z}_j \mathbf{h}_{\mathrm{dl},k} + \tilde{G}_k - \frac{\bar{Q}_k}{(1-\rho_k)} + \sigma_k^2 \right). \end{aligned} \tag{A.1}$$

Given the Lagrangian function, the dual function of problem (6.25) as given by [72, Sec.5.7.3]

$$\min_{\mathbf{Z}_k \succeq 0, 0 < \rho_k < 1, \forall k} L(\{\mathbf{Z}_k, \rho_k, \lambda_k, \mu_k\}). \tag{A.2}$$

Equation (A.2) can explicitly be written as shown in (A.3)

$$\min_{\mathbf{Z}_k \succeq 0, 0<\rho_k<1, \forall k} \Bigg[\sum_{k=1}^{K} \mathrm{Tr}(\mathbf{A}_k \mathbf{Z}_k) + \sum_{k=1}^{K} (-\lambda_k(\bar{G}_k - \sigma_k^2) - \mu_k(\tilde{G}_k + \sigma_k^2)) + \sum_{k=1}^{K} \left(\frac{\lambda_k \delta_k^2}{\rho_k} + \frac{\mu_k \bar{Q}_k}{(1-\rho_k)}\right) \Bigg], \tag{A.3}$$

where

$$\mathbf{A}_k = \mathbf{I}_{N_t} + \sum_{j=1}^{K} (\lambda_j - \mu_j) \mathbf{h}_{\mathrm{dl},j} \mathbf{h}_{\mathrm{dl},j}^H - \left(\frac{\lambda_k}{\gamma_k^{\mathrm{DL}}} + \lambda_k \right) \mathbf{h}_{\mathrm{dl},k} \mathbf{h}_{\mathrm{dl},k}^H. \tag{A.4}$$

Denote $\{\lambda_k^*\}$ and $\{\mu_k^*\}$ as the optimal dual solution to problem (6.25). As a result, we define

$$\mathbf{A}_k^* = \mathbf{I}_{N_t} + \sum_{j=1}^{K} (\lambda_j^* - \mu_j^*) \mathbf{h}_{\mathrm{dl},j} \mathbf{h}_{\mathrm{dl},j}^H - \left(\frac{\lambda_k^*}{\gamma_k^{\mathrm{DL}}} + \lambda_k^* \right) \mathbf{h}_{\mathrm{dl},k} \mathbf{h}_{\mathrm{dl},k}^H. \tag{A.5}$$

We observe from (A.3) that for any given k, $\mathbf{Z}_k^*$ must be a solution to the following problem

$$\min_{\mathbf{Z}_k \succeq 0} \mathrm{Tr}(\mathbf{A}_k^* \mathbf{Z}_k). \tag{A.6}$$

To guarantee a bounded dual optimal value, we must have

$$\mathbf{A}_k^* \succeq 0, \text{for } \; k = 1, 2, \ldots, K. \tag{A.7}$$

Consequently, the optimal value for problem (A.6) is zero, i.e., $\mathrm{Tr}(\mathbf{A}_k^* \mathbf{Z}_k) = 0, k = 1, 2, \ldots, K$, which in conjunction with $\mathbf{A}_k^* \succeq 0$ and $\mathbf{Z}_k^* \succeq 0, k = 1, 2, \ldots, K$, implies that

$$\mathbf{A}_k^* \mathbf{Z}_k^* = 0, \text{for } \; k = 1, 2, \ldots, K. \tag{A.8}$$

Nonetheless, from (A.3) it is observed that the optimal PS solution ρ_k^* for any given $k \in \{1, \ldots, K\}$ must be a solution of the following problem:

$$\min_{\rho_k} \frac{\lambda_k^* \delta_k^2}{\rho_k} + \frac{\mu_k^* \bar{Q}_k}{(1-\rho_k)} \;\; \text{s.t. } \; 0 < \rho_k < 1. \tag{A.9}$$

Note that we observe from problem (A.9) that for the case when $\lambda_k^* = 0$ and $\mu_k^* > 0$, the optimal solution will be $\rho_k^* \to 0$. Similarly, for the case when $\mu_k^* = 0$ and $\lambda_k^* > 0$, the optimal solution is $\rho_k^* \to 1$. Since $\bar{Q}_k > 0$ and $\gamma_k^{\mathrm{DL}} > 0, \forall k, 0 < \rho_k < 1$ must hold for all k's in problem (6.25), the above two cases cannot be true. Consequently, we prove that $\lambda_k^* = 0$ and $\mu_k^* = 0$ cannot be true for any k by contradiction. Let us assume there exist some k's such that $\lambda_k^* = \mu_k^* = 0$. We therefore define a set

$$\Theta \triangleq \{k | \lambda_k^* = 0, \mu_k^* = 0, 1 \leq k \leq K\}, \text{ where } \Theta \neq \Phi. \tag{A.10}$$

We also define

$$\mathbf{B}^* \triangleq \mathbf{I}_{N_t} + \sum_{j \notin \Theta} (\lambda_j^* - \mu_j^*) \mathbf{h}_{\mathrm{dl},j} \mathbf{h}_{\mathrm{dl},j}^H. \tag{A.11}$$

Then $\mathbf{A}_k^*$ can be written as

$$\mathbf{A}_k^* = \begin{cases} \mathbf{B}^*, & \text{if } k \in \Theta; \\ \mathbf{B}^* - \left(\frac{\lambda_k^*}{\gamma_k^{\mathrm{DL}}} + \lambda_k^* \right) \mathbf{h}_{\mathrm{dl},k} \mathbf{h}_{\mathrm{dl},k}^H, & \text{otherwise.} \end{cases} \tag{A.12}$$

Since $\mathbf{A}_k^* \succeq 0$ and $-\left(\frac{\lambda_k^*}{\gamma_k^{\mathrm{DL}}} + \lambda_k^* \right) \mathbf{h}_{\mathrm{dl},k} \mathbf{h}_{\mathrm{dl},k}^H \preceq 0$, consequently, $\mathbf{B}^* \succeq 0$. Let us proceed to show that $\mathbf{B}^* \succ 0$ by contradiction. Assuming the minimum eigenvalue of $\mathbf{B}^*$ is zero, consequently, there exists at least an $\mathbf{x} \neq 0$ such that $\mathbf{x}^H \mathbf{B}^* \mathbf{x} = 0$. From equation (A.12), it follows that

$$\mathbf{x}^H \mathbf{A}_k^* \mathbf{x} = -\left(\frac{\lambda_k^*}{\gamma_k^{\mathrm{DL}}} + \lambda_k^* \right) \mathbf{x}^H \mathbf{h}_{\mathrm{dl},k} \mathbf{h}_{\mathrm{dl},k}^H \mathbf{x} \geq 0, k \notin \Theta. \tag{A.13}$$

Notice that we have $\lambda_k^* > 0$ if $k \notin \Theta$. Accordingly, from (A.13) we obtain $|\mathbf{h}_{\mathrm{dl},k}^H \mathbf{x}|^2 \leq 0$, $k \notin \Theta$. It follows that

$$\mathbf{h}_{\mathrm{dl},k}^H \mathbf{x} = 0, k \notin \Theta. \tag{A.14}$$

Conclusively, we have

$$\begin{aligned} \mathbf{x}^H \mathbf{B}^* \mathbf{x} &= \mathbf{x}^H \left(\mathbf{I}_{N_t} + \sum_{j \notin \Theta} (\lambda_j^* - \mu_j^*) \mathbf{h}_{\mathrm{dl},j} \mathbf{h}_{\mathrm{dl},j}^H \right) \mathbf{x} \\ &= \mathbf{x}^H \mathbf{x} > 0, \end{aligned} \tag{A.15}$$

which contradicts to $\mathbf{x}^H\mathbf{B}^*\mathbf{x} = 0$. Thus, we have $\mathbf{B}^* \succ 0$, i.e., $\text{Rank}(\mathbf{B}^*) = N_t$. We can therefore deduce from (A.12) that $\text{Rank}(\mathbf{A}_k^*) = N_t$ if $k \in \Theta$. From (A.8), we have $\mathbf{Z}_k^* = 0$ if $k \in \Theta$. However, we can easily verify that $\mathbf{Z}_k^* = 0$ cannot be optimal for problem (6.25). Appropriately, it must follow that $\Theta = \Phi$, i.e., $\lambda_k = 0$ and $\mu_k = 0$ cannot be true for any k. Interestingly, as we have previously shown that both cases of $\lambda_k^* = 0, \mu_k^* = 0$ and $\lambda_k^* > 0, \mu_k^* = 0$ cannot be true for any k, it follows that $\lambda_k^* > 0, \mu_k^* > 0, \forall k$. In agreement to complementary slakeness [72], the first part of of Proposition 1 is thus proved. Secondly, we proceed to prove the second part of Proposition 1. Since $\Theta = \Phi$, it follows that (A.11) and (A.12) reduces to

$$\mathbf{A}_k^* = \mathbf{B}^* - \left(\frac{\lambda_k^*}{\gamma_k^{\text{DL}}} + \lambda_k^* \right) \mathbf{h}_{\text{dl},k} \mathbf{h}_{\text{dl},k}^H, k = 1, \ldots, K. \tag{A.16}$$

On account of the fact that we have shown from the first part of the proof that $\text{Rank}(\mathbf{B}^*) = N_t$, it follows that $\text{Rank}(\mathbf{A}_k^*) \geq N_t - 1$, $k = 1, \ldots, K$. Notice that if $\mathbf{A}_k^*$ is characterized as having a full rank, then we have $\mathbf{Z}^* = 0$, which cannot be the optimal solution to (6.25). Thus, it follows that $\text{Rank}(\mathbf{A}_k^*) = N_t - 1, \forall k$. According to (A.8), we have $\text{Rank}(\mathbf{Z})^* = 1, k = 1, \ldots, K$. We thus proved the second part of Proposition 1. By combining the proofs for both parts, we have thus completed the proof of Proposition 1 [89].

Appendix B

Proof of Proposition 2

From problem (6.26), we see that the ZF transmit beamforming constraints make it possible for us to decouple the SINR and the harvested power constraints over k because the objective function in problem (6.26) is separable over k. Therefore, problem (6.26) can be decomposed into K subproblems, $k = 1, \ldots, K$, with the kth subproblem expressed as

$$\begin{aligned}
&\min_{\mathbf{v}_k, \rho_k} \|\mathbf{v}_k\|^2 \\
&\text{s.t.} \\
&\frac{\rho_k |\mathbf{h}_{\mathrm{dl},k}^H \mathbf{v}_k|^2}{\rho_k(\bar{G}_k + \sigma_k^2) + \delta_k^2} \geq \gamma_k^{\mathrm{DL}}, \\
&(1-\rho_k)\left(|\mathbf{h}_{\mathrm{dl},k}^H \mathbf{v}_k|^2 + \tilde{G}_k + \sigma_k^2\right) \geq \bar{Q}_k, \\
&\mathbf{H}_{\mathrm{dl},k}^H \mathbf{v}_k = 0, \quad \|\mathbf{v}_k\|^2 \leq P_{\max}, \\
&0 < \rho_k < 1.
\end{aligned} \tag{B.1}$$

We remark that for problem (B.1), with the optimal ZF beamforming solution $\tilde{\mathbf{v}}_k^*$, and PS solution $\tilde{\rho}_k^*$, the SINR constraint and the harvested power constraint should both hold with equality by contradiction. Notice the following:

(i) Suppose that both the SINR and harvested power constraint are not tight given $\tilde{\rho}_k^*$ and $\tilde{\mathbf{v}}_k^*$, this implies that there must be an α_k, $0 < \alpha_k < 1$ such that with the new solution $\mathbf{v}_k^* = \alpha_k \tilde{\mathbf{v}}_k^*$, and $\rho_k^* = \tilde{\rho}_k^*$, either the SINR or harvested power

constraint is tight. This new solution gives rise to a reduction in the transmission power which contradicts the fact that $\tilde{\mathbf{v}}_k^*$, and $\tilde{\rho}_k^*$ is optimal for problem (B.1). Therefore, the case that both the SINR and harvested power constraints are not tight cannot be true [89].

(ii) Also, the scenario where the SINR constraint is tight but the harvested energy constraint is not tight cannot be true as $\tilde{\rho}_k^*$ can be increased slightly such that both the SINR and harvested power constraints become not tight anymore.

(iii) Similarly, the conclusions drawn in [89] also verify that the case where the harvested power constraint is tight but the SINR constraint is not tight cannot be true.

To summarize, with the optimal solution using the ZF transmit beamforming constraint, for problem (B.1), the SINR and harvested power constraints must both hold with equality. Accordingly, problem (B.1) is equivalent to

$$\begin{aligned}
&\min_{\mathbf{v}_k,\rho_k} \|\mathbf{v}_k\|^2 \\
&\text{s.t.} \\
&\frac{\rho_k|\mathbf{h}_{\mathrm{dl},k}^H\mathbf{v}_k|^2}{\rho_k(\bar{G}_k+\sigma_k^2)+\delta_k^2} = \gamma_k^{\mathrm{DL}}, \\
&(1-\rho_k)\left(|\mathbf{h}_{\mathrm{dl},k}^H\mathbf{v}_k|^2+\tilde{G}_k+\sigma_k^2\right) = \bar{Q}_k, \\
&\mathbf{H}_{\mathrm{dl},k}^H\mathbf{v}_k = 0, \quad \|\mathbf{v}_k\|^2 \le P_{\max}, \\
&0<\rho_k<1.
\end{aligned} \tag{B.2}$$

Notice from problem (B.2) that the first two equality constraints can be rearranged to give the following equation

$$\gamma_k^{\mathrm{DL}}\left(\bar{G}_k+\sigma_k^2+\frac{\delta_k^2}{\rho_k}\right) = \frac{\bar{Q}_k}{(1-\rho_k)} - \tilde{G}_k - \sigma_k^2. \tag{B.3}$$

After some mathematical manipulations, (B.3) can be written as

$$\alpha_k\rho_k^2 - \beta_k\rho_k - C_k = 0, \tag{B.4}$$

where

$$\alpha_k = \gamma_k^{\mathrm{DL}}(\bar{G}_k + \sigma_k^2) + \tilde{G}_k + \sigma_k^2, \tag{B.5}$$

$$\beta_k = \gamma_k^{\mathrm{DL}}(\bar{G}_k + \sigma_k^2) + \tilde{G}_k + \sigma_k^2 - \bar{Q}_k - \gamma_k^{\mathrm{DL}}\delta_k^2, \tag{B.6}$$

$$C_k = -\gamma_k^{\mathrm{DL}}\delta_k^2. \tag{B.7}$$

The optimal solution satisfying $0 < \rho_k < 1$ is given by

$$\tilde{\rho}_k^* = \frac{+\beta_k \pm \sqrt{\beta_k^2 + 4\alpha_k C_k}}{2\alpha_k}. \tag{B.8}$$

Next, we define $\mathbf{v}_k = \sqrt{p_k}\tilde{\mathbf{v}}_k$ with $\|\tilde{\mathbf{v}}_k\| = 1, \forall k$. Then problem (B.2) is equivalent to:

$$\begin{aligned} &\min_{p_k, \tilde{\mathbf{v}}_k} \ p_k \\ &\text{s.t.} \\ &p_k |\mathbf{h}_{\mathrm{dl},k}^H \tilde{\mathbf{v}}_k|^2 = \tau_k, \\ &\mathbf{H}_{\mathrm{dl},k}^H \tilde{\mathbf{v}}_k = 0, \\ &\|\tilde{\mathbf{v}}_k\| = 1, \end{aligned} \tag{B.9}$$

where $\tau_k \triangleq \gamma_k^{\mathrm{DL}} \left(\bar{G}_k + \sigma_k^2 + \frac{\delta_k^2}{\rho_k} \right)$. It is evident from the first constraint of (B.9) that to achieve the minimum p_k, the optimal $\tilde{\mathbf{v}}_k$ should be the optimal solution to the following problem:

$$\begin{aligned} &\max_{\tilde{\mathbf{v}}_k} \ |\mathbf{h}_{\mathrm{dl},k}^H \tilde{\mathbf{v}}_k|^2 \\ &\text{s.t.} \\ &\mathbf{H}_{\mathrm{dl},k}^H \tilde{\mathbf{v}}_k = 0, \\ &\|\tilde{\mathbf{v}}_k\| = 1. \end{aligned} \tag{B.10}$$

Result obtained in [89] shows that the unique (up to phase rotation) optimal solution to problem (B.10) is given by

$$\tilde{\mathbf{v}}_k = \frac{\mathbf{U}_k \mathbf{U}_k^H \mathbf{h}_{\mathrm{dl},k}}{\|\mathbf{U}_k \mathbf{U}_k^H \mathbf{h}_{\mathrm{dl},k}\|}, \tag{B.11}$$

where $\mathbf{U}_k$ denotes the orthogonal basis for the null space of $\mathbf{H}_k^H$. Accordingly, the optimal power solution as given in [89] is given by

$$p_k = \frac{\tau_k}{|\mathbf{h}_{\mathrm{dl},k}^H \tilde{\mathbf{v}}_k|^2} = \frac{\tau_k}{\|\mathbf{U}_k \mathbf{U}_k^H \mathbf{h}_{\mathrm{dl},k}\|^2}. \tag{B.12}$$

Thus, it follows that $\tilde{\mathbf{v}}_k$ for problem (B.2) is given by

$$\tilde{\mathbf{v}}_k^* = \sqrt{\gamma_k^{\mathrm{DL}} \left(\bar{G}_k + \sigma_k^2 + \frac{\delta_k^2}{\rho_k} \right)} \frac{\mathbf{U}_k \mathbf{U}_k^H \mathbf{h}_{\mathrm{dl},k}}{\|\mathbf{U}_k \mathbf{U}_k^H \mathbf{h}_{\mathrm{dl},k}\|^2}. \tag{B.13}$$

Bibliography

[1] L. R. Varshney, "Transporting information and energy simultaneously," in *Proc. IEEE Int. Symp. Inf. Theory (ISIT)*, pp. 1612-1616, Jul. 2008, Toronto, ON, Canada.

[2] P. Grover, and A. Sahai, "Shannon meets Tesla: wireless information and power transfer," in *Proc. IEEE Int. Symp. Inf. Theory*, pp. 2363-2367, Jun. 2010, Austin, TX, USA.

[3] H. Nishimoto, Y. Kawahara, and T. Asami, "Prototype implementation of ambient RF energy harvesting wireless sensor networks," in *Proc. IEEE Sensors,* Nov. 2010, kona, HI.

[4] X. Zhang, H. Jiang, L. Zhang, Z. Wang, and Z. Chen, "An energy-efficient ASIC for wireless body sensor networks in medical applications," *IEEE Trans. biomedical circuits and Sys.,* vol. 4, no. 1, pp. 11-18, Feb. 2010.

[5] R. Zhang, and C. K. Ho, "MIMO broadcasting for simultaneously wireless information and power transfer," *IEEE Trans. Wireless Commun.*, vol. 12, no. 5, pp. 1989-2001, May 2013.

[6] X. Zhou, R. Zhang, and C. Keong, "Wireless information and power transfer: Architecture design and rate-energy trade-off," *IEEE Trans. Wireless Commun.*, vol. 61, no.11, Nov. 2013.

[7] L. Liu, R. Zhang, and K. C. Chua, "Wireless information transfer with opportunistic energy harvesting," *IEEE Trans. Wireless Commun.*, vol. 12, no. 1, pp.

228–300, Jan. 2013.

[8] X. Huang, Q. Li, Q. Zhang, and J. Qin, "Power allocation for secure OFDMA systems with wireless information and power transfer," *IET Electronics Letters*, vol. 50, no. 3, pp. 229-230, Jan. 2014.

[9] D. W. K. Ng, and R. Schober, "Resource allocation for coordinated multipoint networks with wireless information and power transfer," in *Proc. IEEE Global communications conference (Globecom)*, Dec. 2014, Austin, TX, USA.

[10] X. Li, Y. Sun, F. Richard Yu, and N. Zhao, "Antenna selection and power splitting for simultaneous wireless information and power transfer in interference alignment networks," in *Proc. IEEE Global communications conference (Globecom)*, Dec. 2014, Austin, TX, USA.

[11] B. Fang, W. Zhong, Z. Qian, S. Jin, J. Wang, and W. Shao, "Optimal precoding for simultaneous information and power transfer in MIMO relay networks," in *Proc. 9th International conference on communications and networking*, pp. 462-467, Aug. 2014, Maoming, China.

[12] S. Guo, Y. Yang, and Y. Yang, "Wireless energy harvesting and information processing in cooperative wireless sensors networks," in *Proc. IEEE International conference on communication, (ICC)*, pp. 5392-5397, Jun. 2015, London, UK.

[13] M. Chynonova, R. Morsi, D. W. K. Ng, and R. Schober, "Optimal multiuser scheduling schemes for simultaneous wireless information and power transfer," in *Proc. European signal processing conference (EUSIPCO)*, pp. 1989-1993, Sep. 2015, Nice, France.

[14] I. Krikidis, S. Timotheou, S. Nikolaou, G. Zheng, D. W. K. Ng, and R. Schober, "Simultaneous wireless information and power transfer in modern communication systems," *IEEE Commun. Letts.*, vol. 52, no. 11, pp. 104-110, Nov. 2014.

[15] Q. Sun, L. Li, and J. Mao, "Simultaneous information and power transfer scheme for energy efficient MIMO systems," *IEEE Commun. Letts.*, vol. 18, no. 4, pp. 600-603, Apr. 2014.

[16] K. Huang, and E. Larsson, "Simultaneous information and power transfer for broadband wireless systems," *IEEE Trans. Signal Process.*, vol. 61, no. 23, pp. 5972-5986, Dec. 2013.

[17] C. Yuen, M. Elkashlan, Y. Qian, T. Q. Duong, L. Shu, and F. Schmidt, "Energy harvesting communications: Part III [Guest Editorial]," *IEEE Communications magazine*, Vol. 53, no. 8, pp. 90-91, Aug. 2015.

[18] B. K. Chalise, Y. D. Zhang, and M. G. Amin, "Energy harvesting in an OSTBC based amplify-and-forward MIMO relay system," in *Proc. IEEE ICASSP,* pp. 3201–3204, Mar. 2012.

[19] A. M. Fouladgar, and O. Simeone, "On the transfer of information and energy in multi-user systems," *IEEE Commun. Lett.,* vol. 16, no. 11, pp. 1733-1736, Nov. 2012.

[20] M. R. A. Khandaker, and K-K. Wong, "SWIPT in MISO multicasting systems," *IEEE Wireless Commun. Letts.*, vol. 3, no. 3, Jun. 2014.

[21] S. Leng, D. W. K. Ng, N. Zlatanov, and R. Schober, "Multi-objective resource allocation in full-duplex SWIPT systems," in *Proc. IEEE International conference on communications (ICC)*, pp. 1-7, May. 2016, Kuala Lumpur, Malaysia.

[22] D. Wang, R. Zhang, X. Cheng, and L. Yang, "Capacity-enhancing full-duplex relay networks based on power-splitting (PS) SWIPT," *IEEE Trans. Veh. Tech.*, vol. 66, no. 6. pp. 5445-5450, Oct. 2016.

[23] Z. Hu, C. Yuan, F. Zhu, and F. Gao, "Weighted sum transmit power minimization for full-duplex system with SWIPT and self-energy recycling," *IEEE Early access*, vol. 4, pp. 4874-4881, Jul. 2016.

[24] Z. Wen, X. Liu, Y. Chen, R. Wang, and Z. Xie, "Joint transceiver designs for full-duplex MIMO SWIPT systems based on MSE criterion," *China communications*, vol. 13, no. 10, pp. 79-85, Nov. 2016.

[25] Z. Chen, P. Xu, Z. Ding, and X. Dai, "The application of SWIPT to a cooperative full-duplex node," in *Proc. International symposium on wireless communications (ISWCS)*, pp. 426-430, Aug. 2015, Brussels, Belgium.

[26] Z. Wen, X. Liu, N. C. Beaulieu, R. Wang, and S. Wang, "Joint source and relay beamforming design for full-duplex MIMO AF relay SWIPT systems," *IEEE Commun. Letts.*, vol. 20, no. 2, pp. 320-323, Jan. 2016.

[27] J. H. Moon, J. J. Park, and D. I. Kim, "Energy signal design and decoding procedure for full-duplex two-way wireless powered relay," in *Proc. URSI Asia-Pacific radio science conference (URSI AP-RASC)*, pp. 442-445, Aug. 2016, Seoul, South Korea.

[28] M. E. Knox, "Single antenna full-duplex communication using a common carrier" in *Proc. Asilomar Conf. Signal Syst. Comput.,* Nov, 2013, Pacific Grove, CA, USA.

[29] M. Duarte, and A. Sabharwal, "Full-duplex wireless communication using off-the-shelf radios: Feasibility and first result," in *Proc. 44th Asilomar conference on signals, systems and computers*, pp. 1558-1562, Nov. 2010, CA, USA.

[30] M. Duarte, C. Dick, and A. Sabharwal, "Experiment-driven characterization of full-duplex wireless systems," *IEEE Trans. Wireless Commun.*, vol. 11, no. 12, pp. 4296-4307, Dec. 2012.

[31] E. Ahmed, A. M. Eltawil, and A. Sabharwal "Self-interference cancellation with nonlinear distortion suppression for full-duplex" in *Proc. Asilomar Conf. Signals Syst. Comput.,* pp. 1199-1203, Nov. 2013, Pacific Grove, CA, USA.

[32] A. Sabharwal, P. Schniter, D. Guo, D. Bliss, S. Rangarajan, and R. Wichman, "In-band full-duplex wireless: Challenges and opportunities," *IEEE Journal on*

Selected Areas In Communications, vol. 32, no. 9, pp. 1637-1652, Oct. 2014.

[33] E. Everett, A. Sahai, and A. Sabharwal , "Passive self-interference suppression for full-duplex infrastructure nodes," *IEEE Trans.Wireless Commun.*, vol. 13, no. 2, pp. 680-694, Feb. 2014.

[34] D. Bharadia, E. Mcmilin, and S. Katti, "Full-duplex radios," in *Proc. Sigcomm*, Aug. 2013, Hong Kong, China.

[35] B. Day, A. Margetts, D. Bliss, and P. Schniter, "Full-duplex bidirectional MIMO: Achievable rates under limited dynamic range," *IEEE Trans. Signal Process.*, vol. 60, no. 7, pp. 3702-3713, Jul. 2012.

[36] M. Jain, J. I. Choi, T. Kim, D. Bharadia, S. Seth, K. Srinivasan, P. Levis, S. Katti, and P. Sinha, "Practical, real-time, full-duplex wireless" in *Proc. 17th Annual International Conf. on mobile computing and networking*, pp. 301-312, Sep. 2011, Las Vegas, Nevada, USA.

[37] D. Korpi, T. Riihonen, V. Syrjala, L. Anttila, M. Valkama, and R. Wichman, "Full-duplex transceiver system calculations: Analysis of ADC and linearity challenges," *IEEE Trans. Wireless Commun.*, vol. 13, no. 7, pp. 3821-3836, Jul. 2014.

[38] A. S. Arifin, and T. Ohtsuki, "Outage probability analysis in bidirectional full-duplex SISO system with self-interference," in *Proc. 20th Asia-Pacific conference on communications APCC2014*, pp. 6-8, Oct. 2014, Thailand.

[39] J. N. Laneman, D. N. C. Tse, and G. W. Wornell, "Cooperative diversity in wireless networks: efficient protocols and outage behaviour," *IEEE Trans. Inf. Theory,* vol. 50, no. 12, pp. 3062-3080, Dec. 2004.

[40] T. M. Cover, and A. A. El Gamal, "Capacity theorems for the relay channel," *IEEE Trans. Inf. Theory,* vol. 25, no. 5, pp. 572-584, Sep. 1979.

[41] J. N. Laneman, and G. W. Wornell, "Distributed space-time-coded protocols for exploiting diversity in wireless network," *IEEE Trans. Inf. Theory,* vol. 49, no. 10, pp. 2415-2425, Oct. 2013.

[42] T. Riihonen, S. Werner, and R. Wichman, "Hybrid full-duplex / half-duplex relaying with transmit power adaptation," *IEEE Trans. Wireless Commun.*, vol. 10, no. 9, pp. 3074–3085, Sep. 2011.

[43] T. Riihonen, S. Werner, and R. Wichman, "Mitigation of loopback self-interference in full-duplex MIMO relays," *IEEE Trans. Signal Process.*, vol. 59, no. 12, pp. 5983-5993, Dec. 2011.

[44] A. L. Moustakas, and S. H. Simon, "Optimising multiple-input single-output (MISO) communication systems with general gaussian channels: Nontrivial covariance and nonzero mean," *IEEE Trans. Info. Theory*, vol. 49, no. 10, pp. 2770-2780, Oct. 2003.

[45] A. D. Wyner, "The wiretap channel," *Bell Sys. Tech.*, vol. 54, no. 8, pp. 1355-1387, May 1975.

[46] S. Geol, and R. Negi, "Guaranteering secrecy using artificial noise," *IEEE Trans. Wireless. Commun*, vol. 7, no. 6, pp. 2180-2189, Jun. 2008.

[47] A. L. Swindlehurst, "Fixed SINR solutions for the MIMO wiretap channel," in *Proc. IEEE Int. Conf. Acoust., Speech, Signal Process. (ICASSP)*, pp. 2437-2440, Apr. 2009, Taiwan.

[48] Q. Li, W. Ma, and A. So, "Safe convex approximation to outage-based MISO secrecy rate optimization under imperfect CSI and with artificial noise," in *Proc. Asilomar Conf. Signal, Syst. Comput.*, pp. 207-211, Nov. 2011, CA, USA.

[49] L. Dong, Z. Han, A. P. Petropulu, and H. V. Poor, "Improving wireless physical layer security via cooperating relays," *IEEE Trans. Signal Process.*, vol. 58, no. 3, pp. 1857-1888, Mar. 2010.

[50] G. Zheng, L.-C. Choo, and K. K. Wong, "Optimal cooperative jamming to enhance physical layer security using relays," *IEEE Trans. Signal Process.*, vol. 59, no. 3, pp. 1317-1322, Mar. 2011.

[51] I. Krikidis, J. S. Thompson, and S. McLaughlin, "Relay selection for secure cooperative networks with jamming," *IEEE Trans. Wireless Commun.*, vol. 8, pp. 5003-5011, Oct. 2009.

[52] J. Vilela, M. Bloch, J. Barros, and S. W. McLaughlin, "Wireless secrecy regions with friendly jamming," *IEEE Trans. Inf. Forensics Security*, vol. 6, no. 2, pp. 256-266, Jun. 2011.

[53] Z. Ding, M. Peng, and H.-H. Chen, "A general relaying transmission protocol for MIMO secrecy communications," *IEEE Trans. Commun.*, vol. 60, no. 11, pp. 3461-3471, Nov. 2012.

[54] G. Zheng, I. Krikidis, J. Li, A. P. Petropulu, and B. Ottersten, "Improving physical layer secrecy using full-duplex jamming receivers," *IEEE Trans. Signal Process.*, vol. 61, no. 20, pp. 4962-4874, Oct. 2013.

[55] S. Gollakota, and D. Katabi, "Physical layer wireless security made fast and channel independent," in *Proc. IEEE Int. Conf. Comput. Commun.*, pp. 1125-1133, Apr. 2011, Shanghai, China.

[56] E. Ahmed, and A. M. Eltawil, "All-digital self-interference cancellation technique for full-duplex systems," *IEEE Trans. Wireless Commun.*, vol. 14, no.7, July 2015.

[57] J. Yang, and S. Ulukus, "Optimal packet scheduling in an energy harvesting communication system," *IEEE Trans. Commun.,* vol. 60, no. 1, pp. 220-230, Jan. 2012.

[58] C. K. Ho, and R. Zhang, "Optimal energy allocation for wireless communications with energy harvesting constraints," *IEEE Trans. Signal Process.,* vol. 60, no. 9, pp. 4808-4818, Sep. 2012.

[59] Y. Cui, K. N. Lau, and Y. Wu, "Delay-aware BS discontinuous transmission control and user scheduling for energy harvesting downlink coordinated MIMO systems," *IEEE Trans. Signal Process.,* vol. 60, no. 7, Jul. 2012.

[60] K. Tutuncuoglu, and A. Yener, "Optimum transmission policies for battery limited energy harvesting nodes," *IEEE Trans. Wireless Commun.,* vol. 11, no. 3, Mar. 2012.

[61] K. Tutuncuoglu, and A. Yener, "Transmission with energy harvesting nodes in fading wireless channels: Optimal policies," *IEEE Journal on selected areas in communications,* vol. 29, no. 8, Sep. 2011.

[62] D. Niyato, E. Hossain, M. M. Rashid, and V. Bhargava, "Wireless sensor networks with energy harvesting technologies: A game-theoretic approach to optimal energy management," *IEEE Wireless Commun.*, vol. 14, no. 4, pp. 90-96, Aug. 2007.

[63] V. Raghunathan, A. Kansal, J. Hsu, J. Friedman, and M. Srivastava, "Design considerations for solar energy harvesting wireless embedded systems," in *Proc. IEEE Int. Conf. Inf. Process. Sensor Netw.,* pp. 457-462, Apr. 2000 Boise, ID, USA.

[64] S. L. Kok, M. F. Rahman, D. F. Weng, and Y. H. Ho, "Bandwidth widening strategy for piezoelectric based energy harvesting from ambient vibration sources,"in *Proc. International conference on computer applications and industrial electronics (ICCAIE)*, Dec. 2011, Penang, Malaysia.

[65] H. M. G. ElAnzeery, M. E. ElBagouri, and R. Guindi "Novel radio frequency energy harvesting model," in *Proc. IEEE International power engineering and optimization conference (PEOCO)*, Jun. 2012, Melaka, Malaysia.

[66] C. Mikeka, and H. Arai, "Design issues in radio frequency energy harvesting systems," *Sustainable energy harvesting- past, present and future,* Dec. 2011.

[67] Product Datasheet, P2110-915MHz RF Powerharvester Receiver, Powercast Corporation.

[68] J. Zhang, O. Taghizadeh, and M. Haardt: "Transmit strategies for full-duplex point-to-point systems with residual self-interference," in *Proc. Smart Antennas (WSA), 17th Int. ITG. Workshop*, Mar. 2013, Stuttgart, Germany.

[69] H. Ju, and R. Zhang, "Optimal resource allocation in full-duplex wireless-powered communication network," *IEEE Trans. Commun.*, Vol. 62, pp. 3528–3540, Oct. 2014.

[70] Y. Zeng, and R. Zhang, "Full-duplex wireless powered relay with self-energy recycling," *IEEE Wireless Commun. Letters*, vol. 4, no.2, Apr. 2015.

[71] C. Valenta, and G. Durgin, "Harvesting wireless power: Survey of energy-harvester conversion efficiency in far field, wireless power transfer systems," *IEEE Microw. Mag.*, vol. 15, pp. 108–120, Jun. 2014.

[72] S. Boyd, and L. Vandenberghe, Convex optimization, 2004.

[73] H. Wang, M. Luo, Q. Yin, and X. Xia, "Hybrid cooperative beam-forming and jamming for physical-layer security of two-way relay networks," *IEEE Trans. Inf. Forensics and Security*, vol. 8, no. 12, Dec. 2013.

[74] M. Grant, and S. Boyd, "CVX: Matlab Software for disciplined convex programming (online)", http://cvxr.com/cvx, Apr. 2010.

[75] Y. Hua, P. Liang, Y. Ma, A. C. Cirik, and Q. Gao, "A method for broadband full-duplex MIMO radio," *IEEE Signal Process. Lett.*, vol. 19, pp. 793-796. Dec. 2012.

[76] M. R. A. Khandaker, and K-K. Wong, "Masked beamforming in the presence of energy-harvesting eavesdroppers," *IEEE Trans. Inf. Forensics and Security*, vol. 10, pp. 4054, Jan. 2015.

[77] I. Krikidis, S. Timotheou, and S. Sasaki, "RF energy transfer for cooperative networks: Data relaying or energy harvesting ?," *IEEE Commun. Lett.* , vol. 16, pp. 1772-1775. Nov. 2012.

[78] H. Ju, and R. Zhang, "User cooperation in wireless powered communication networks," in *Proc. IEEE Global communications conference (GLOBECOM)*, Dec. 2014, Austin, Texas, USA.

[79] A. A. Nasir, X. Zhou, S. Durrani, and R. A. Kennedy, "Relaying protocols for wireless energy harvesting and information processing," *IEEE Trans. Wireless Commun.*, vol. 12, no. 7, pp. 3622-3636, Jul. 2013.

[80] J. I. Choi, M. Jain, K. Srinivasan, P. Lewis, and S. Katti, "Achieving single channel, full-duplex wireless communication," in *Proc. ACM Mobicom*, pp. 1-12, Sept. 2010, Illinois, Chicago, USA.

[81] A. E. Gamal, N. Hassanpour, and J. Mammen, "Relay networks with delay," *IEEE Trans. on Info. Theory.*, vol. 53, no. 10, Oct. 2007.

[82] G. Zheng, "Joint beamforming optimization and power control for full-duplex MIMO two-way relay channel," *IEEE Trans. signal process.*, vol. 63, no. 3, feb. 2015.

[83] X. Ji, B. Zheng, Y. Cai, and L. Zou, "On the study of half-duplex asymmetric two-way relay transmission using an amplify-and-forward relay," *IEEE Trans. vehicular technology*, vol. 61, no. 4, pp. 1649-1664, May. 2012.

[84] E. A. Jorswieck, and E. Larsson, "Complete characterization of the pareto boundary for the MISO interference channel," *IEEE Trans. Signal Process.*, vol. 56, no. 10, pp. 5292-5296, Oct. 2008

[85] W. Ai, Y. Huang, and S. Zhang, "New results on Hermitian matrix rank-one decomposition," *Math. Program. Ser. A*, vol. 128, no. 1-2, pp. 253-283, Jun. 2011.

[86] A. Sethi, V. Tapio, and M. Junti, "Self-interference channel for full duplex Transceiver" in *Proc. IEEE WCNC*, Apr. 2014, Istanbul, Turkey.

[87] A. A. Okandeji, M. R. A. Khandaker, K-K. Wong, and Z. Zheng, "Joint transmit power and relay two-way beamforming optimization for energy harvesting full-duplex communications," in *Proc. IEEE Globecom Int. workshop on full-duplex wireless Commun.*, Dec. 2016, Washington DC, USA.

[88] D. H. N. Nguyen, L. B. Le, and Z. Han, "Optimal uplink and downlink channel assignment in a full-duplex multiuser system" in *Proc. IEEE ICC*, Kuala Lumpur, May, 2016.

[89] Q. Shi, L. Liu, W. Xu, and R. Zhang, "Joint transmit beamforming and receive power splitting for MISO SWIPT systems," *IEEE Trans. Wireless Commun.*, vol. 13, no. 6, Jun. 2014.

[90] A. A. Okandeji, M. R. A. Khandaker, and K-K. Wong, "Two-way beamforming optimization for full-duplex SWIPT systems," in *Proc. EUSIPCO*, Budapest, Hungary. Aug. 2016.

[91] B. A. Harvey, "LPI, full-duplex voice communication using adaptive rate delta modulation," *MILCOM proceedings, communications for network-centric operations: Creating the information force*, vol. 2. pp. 1190-1194, Oct. 2001, VA, USA.

[92] K. S. Subramanyam, and A. K. Gogoi, "Full-duplex voice communication handsets over single carrier frequency," in *Proc. IEEE International conference on personal wireless communications*, pp. 307-309, Dec. 2000, Hyderabad, India.

[93] G. H. Smith, D. Novak, C. Lim, and K. Wu, "Full-duplex broadband millimeter-wave optical transport system for fibre wireless access," *IET Electronics Letters*, vol.33, no. 13, pp. 1159-1160, Jun. 1997.

[94] H-H. Lu, S-J. Tzeng, and Y-L. Liu, "Intermodulation distortion suppression in a full-duplex radio-on-fibre ring network," *IEEE Photonics letters*, vol. 16, no. 2. pp. 602-604, Feb, 2004.

[95] L. Lai, and H. E. Gamal, "The relay-eavesdropper channel: Cooperation for secrecy," *IEEE Trans. Inf. Theory*, vol. 54, no. 9, pp. 4005-4019, Sep. 2008.

[96] Y. Wang, R. Sun, and X. Wang, "Transceiver design to maximise the weighted sum secrecy rate in full-duplex SWIPT systems," *IEEE Signal Process. Lett.*, vol. 23, no. 6, Jun. 2016.

[97] Y. Wan, Q. Li, Q. Zhang, and J. Qin, "Optimal and suboptimal full-duplex secure beamforming designs for MISO two-way communications," *IEEE Wireless Commun. Lett.*, vol. 4, no. 5, Oct. 2015.

[98] Hongjun Kim, J. Kang, S. Jeong, K. E. Lee, and J. Kang, "Secure beamforming and self-energy recycling with full-duplex wireless-powered relay," 13th *IEEE Annual Consumer Communications and Networking Conference (CCNC)*, Las Vegas, NV, 2016, pp. 662-667.

[99] Q. Li, and D. Han, "Sum secrecy rate maximization for full-duplex two-way relay networks," in *Proc. IEEE Int. Conf. Acous., Speech and Sig. Process.*, pp. 3641-3645, Mar. 2016.

[100] Q. Li, W.K. Ma, and D. Han, "Sum secrecy rate maximization for full-duplex two-way relay networks using Alamouti-Based rank-two beamforming," *IEEE J. Sel. Topics Signal Process.,* vol. 10, pp. 1359-1374, 2016, ISSN 1932-4553.